

**Gravity regulated differential auxin transport in Arabidopsis roots
and the search for interaction partners of AtPIN1**

Inaugural-Dissertation
zur
Erlangung des Doktorgrades
der Mathematisch-Naturwissenschaftlichen Fakultät
der Universität zu Köln

vorgelegt von
Iris Ottenschläger
aus Linz an der Donau

Köln 2002

Berichterstatter:

Herr Priv. Doz. Dr. Klaus Theres

Herr Prof. Dr. Martin Hülskamp

Herr Prof. Dr. Klaus Palme

Herr Prof. Dr. Börries Kemper

Tag der mündlichen Prüfung:

11. Juni 2002

Für meine Eltern Ilse und Erich Ottenschläger

Table of contents

1	INTRODUCTION	1
1.1	ROOT GRAVITROPISM	1
1.2	AUXIN TRANSPORT IN ROOTS	6
1.3	AIM OF THE WORK	13
2	MATERIALS AND METHODS	14
2.1	MATERIALS	14
2.1.1	<i>Plants</i>	14
2.1.2	<i>Bacteria</i>	14
2.1.3	<i>Yeasts</i>	14
2.1.4	<i>Plasmids</i>	15
2.1.5	<i>Synthetic oligonucleotides</i>	16
2.1.6	<i>Antibodies</i>	17
2.1.7	<i>Enzymes</i>	17
2.1.8	<i>Chemicals and radiochemicals</i>	17
2.1.9	<i>Other materials</i>	17
2.1.10	<i>Media for plants</i>	18
2.1.11	<i>Media for bacteria</i>	18
2.1.12	<i>Media for yeasts</i>	19
2.1.13	<i>Microscopes</i>	19
2.1.14	<i>Computer programs</i>	20
2.2	METHODS	20
2.2.1	<i>Cloning strategies</i>	20
2.2.2	<i>Construction and cloning of a cDNA library in pN_{ub}m</i>	23
2.2.3	<i>Methods for the analysis of nucleic acids</i>	26
2.2.4	<i>Methods for the analysis of proteins</i>	29
2.2.5	<i>Methods for the cultivation and transformation of bacteria</i>	31
2.2.6	<i>Methods for the cultivation and transformation of yeasts</i>	33
2.2.7	<i>Methods for the cultivation and transformation of plants</i>	34
3	RESULTS	36
3.1	GENERATION OF TRANSGENIC DR5-GFP ARABIDOPSIS PLANTS	36
3.1.1	<i>The pDR5-GFP construct</i>	36
3.1.2	<i>Analysis of Arabidopsis DR5-GFP plants</i>	37
3.2	DR5-GFP EXPRESSION DURING ROOT GRAVITROPISM	41
3.3	THE EFFECT OF EXOGENOUS AUXIN APPLICATION ON DR5-GFP EXPRESSION DURING ROOT GRAVITROPISM	43
3.3.1	<i>Effect of IAA</i>	44
3.3.2	<i>Effect of I-NAA</i>	44

3.3.3	<i>Effect of 2,4-D</i>	44
3.4	THE EFFECT OF EXOGENOUS AUXIN APPLICATION ON GRAVITY INDUCED ROOT CURVATURE	46
3.5	THE EFFECT OF AUXIN TRANSPORT INHIBITORS ON <i>DR5-GFP</i> EXPRESSION DURING ROOT GRAVITROPISM	47
3.5.1	<i>Effect of NPA and TIBA</i>	48
3.5.2	<i>Effect of BFA</i>	48
3.5.3	<i>Effect of 1-NOA</i>	48
3.6	THE EFFECT OF AUXIN TRANSPORT INHIBITORS ON GRAVITY INDUCED ROOT CURVATURE.....	51
3.7	<i>DR5-GFP</i> EXPRESSION IN THE ROOT TIP OF THE <i>EIR1-1</i> MUTANT	51
3.8	IDENTIFICATION OF AtPIN1 INTERACTION PARTNERS WITH THE SPLIT-UBIQUITIN-SYSTEM	53
3.8.1	<i>The use of USPS to detect the interaction of plant proteins</i>	54
3.8.2	<i>The establishment of AtPIN1-C_{ub} as a bait in USPS</i>	58
3.8.3	<i>The construction and cloning of a plant cDNA library for USPS</i>	63
3.8.4	<i>A small scale screen for interaction partners of AtPIN1</i>	63
4	DISCUSSION	65
4.1	<i>DR5-GFP</i> AS AN AUXIN BIOSENSOR	66
4.2	GRAVITY INDUCED ASYMMETRIC AUXIN ACCUMULATION IN THE LRC	69
4.3	THE ROLE OF POLAR AUXIN TRANSPORT IN GRAVITY INDUCED ASYMMETRIC AUXIN ACCUMULATION ...	71
4.4	A PRELIMINARY MODEL FOR ARABIDOPSIS ROOT GRAVITROPISM AND ITS REGULATION.....	75
4.5	THE SPLIT-UBIQUITIN-SYSTEM AS A METHOD TO FIND INTERACTION PARTNERS OF AtPIN1	78
4.6	PERSPECTIVES	82
5	BIBLIOGRAPHY	84
6	DANKSAGUNG	94
7	ERKLÄRUNG	95
8	ABSTRACT	96
9	ZUSAMMENFASSUNG	97
10	AUSFÜHRLICHE ZUSAMMENFASSUNG	98
11	LEBENS LAUF	100

Abbreviations and symbols

A	Absorbance
Aa	Amino acids
Amp	Ampicillin
AP	Alkaline phosphatase
APS	Ammoniumperoxodisulfate
<i>A. tumefaciens</i>	<i>Agrobacterium tumefaciens</i>
ATP	Adenosine-5'-triphosphate
bp	Basepair
BSA	Bovine serum albumin
cDNA	Complementary DANN
Ci	Curie
Col0	<i>Arabidopsis thaliana</i> L., ecotype Columbia 0
C-terminal	Carboxy-terminal
Da	Dalton
DMF	Dimethylformamide
DMSO	Dimethylsulfoxide
DNA	Deoxyribonucleic acid
<i>E.coli</i>	<i>Escherichia coli</i>
EDTA	Ethylendiaminetetraacetate
Etbr	Ethidiumbromide
EtOH	Ethanol
FITC	Fluorescein-Isothiocyanate
g	Gram
Gm	Gentamycin
GUS	β -Glucuronidase
HAc	Acetic acid
h	Hour
hrs	Hours
HEPES	N-(2-Hydroxyethyl)piperazine-N'-(2-ethansulfonic acid)
HPLC	High-performance liquid chromatography
KAc	Potassiumacetate
kb	Kilobase
kDa	Kilodalton
l	Liter
M	Molar
mA	Milliampere
MeOH	Methanol
Mes	2-(N-Morpholino)ethansulfonic acid
mg	Milligram
min	Minute
ml	Milliliter
mM	Millimolar
mRNA	Messenger RNA
MOPS	3'-(Morpholino)propanesulfonic acid
NaAc	Sodiumacetate
Nr	Number
N-terminal	Amino-terminal
o/n	Over night

PAA	Polyacrylamide
PAGE	Polyacrylamide gel electrophoresis
pBSK	pBluescript
PCR	Polymerase chain reaction
PEG	Polyethylene glycol
Rif	Rifampicin
RNA	Ribonucleic acid
RNase	Ribonuclease
RT	Room temperature
SDS	Sodium dodecylsulfate
TEMED	N,N,N',N'-Tetramethylethylenediamine
TIBA	2,3,5-Triiodobenzoic acid
Tris	Tris(hydroxymethyl)aminoethane
U	Unit of enzyme activity
V	Volt
WT	Wildtype
μg	Microgram
μl	Microliter
Ω	Ohm

Amino acids

A	Alanine
C	Cysteine
D	Aspartic acid
E	Glutamic acid
F	Phenylalanine
G	Glycine
H	Histidine
I	Isoleucine
K	Lysine
L	Leucine
M	Methionine
N	Asparagine
P	Proline
Q	Glutamine
R	Arginine
S	Serine
T	Threonine
V	Valine
W	Tryptophane
Y	Tyrosine

Nucleotides

A	Adenine
C	Cytosine
G	Guanine
T	Thymine

1 Introduction

In the course of their development, higher plants constantly coordinate the formation and growth of organs in response to environmental cues. By definition, the directional bending during growth of organs with respect to a bending inducing stimulus, is termed tropic growth or plant tropism. Multiple environmental parameters direct tropic growth of organs. Depending on the nature of the stimulus, one speaks of phototropism (bending in response to light), hydrotropism (bending in response to water), thigmotropism (bending in response to touch), gravitropism (bending in response to gravity) and several more. While most of these stimuli vary during a plant life, the gravitational force on earth remains normally constant.

Gravity directs the growth of shoots upward (negative gravitropism), where light can be used for photosynthesis, and the growth of main roots downward (positive gravitropism), where the plant is anchored in soil for uptake of water and mineral ions needed for growth and development. In the natural environment, root growth in response to gravity can often not be retained. Thus, main roots, growing towards the center of the earth, may deviate from their direction of growth in response to water and nutrient supply, or encountering an obstacle. In that case, other tropic stimuli would cause the root to bend away from its perceived gravity vector until nutrient and water supply are reached or the object is bypassed. Subsequently roots would bend and again resume growth along the gravity vector. Plants therefore have to remain capable of perceiving the gravity stimulus and responding to it throughout their lifetime.

1.1 Root gravitropism

Growth along the gravity vector or bending in response to the gravity stimulus involves the perception of the gravity vector orientation, the formation of a signal at the site of perception and the transmission of the signal to the site of root bending, where differential growth is induced.

Roots grow by cell division in the apical root meristem and cell elongation in the elongation zone basal to the root meristem (Fig. 1). Growth by elongation occurs in spiral movements (circumnutations) and is responsible for directing the growth of roots along the

gravity vector (Buer *et al.*, 2000; Johnsson, 1997; Simmons *et al.*, 1995). In vertically growing roots, the maximum rate of cell elongation is found in a zone, termed the central elongation zone (CEZ) with a growth rate of three times more than in the region apical to the CEZ, defined as the distal elongation zone (DEZ) (Ishikawa and Evans, 1993).

When *in vitro* grown roots are gravistimulated, by rotating the agar plates to a certain angle from the vertical, root curvature is initiated and roots start to bend until the root tip is again aligned towards the gravitational vector, *i.e.* center of the earth. Bending commences in the DEZ and is the result of inhibition of elongation in DEZ and CEZ on the lower half, as well as initiation of cell elongation in the DEZ on the upper half of the gravistimulated root (Mullen *et al.*, 1998). As root bending proceeds, the region of curvature shifts towards the root base. Before reaching the vertical, root growth often slightly overshoots and requires transient backward bending for vertical alignment (Barlow and Rathfelder, 1985; Pilet and Ney, 1981).

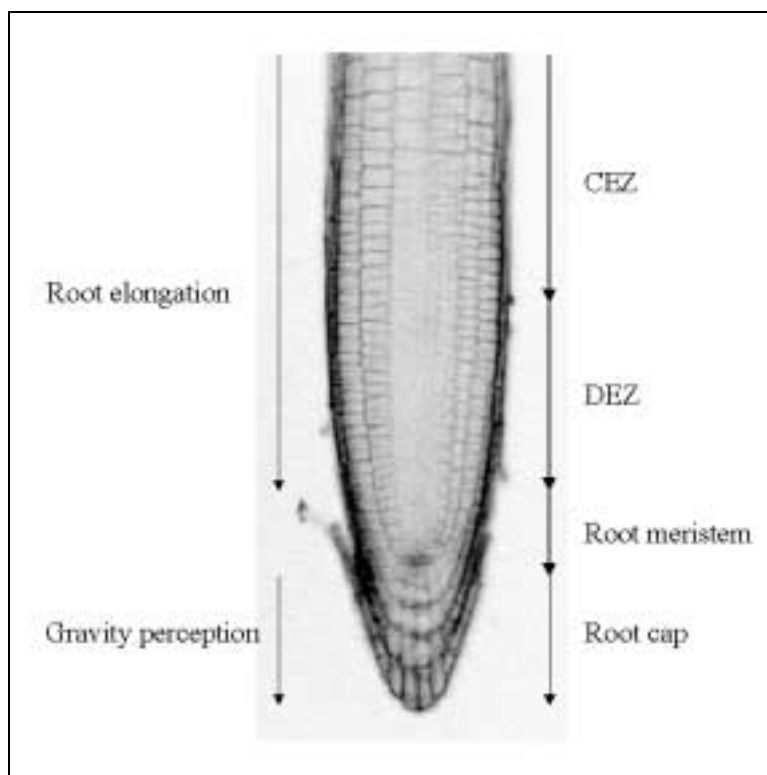


Fig. 1: Different sites in the root are responsible for gravity perception and root bending. Roots grow by cell division in the root meristem and cell elongation in the elongation zone (EZ). Changes in gravity vector orientation are perceived in columella cells of the root cap. Gravity induced root curvature occurs by differential cell elongation in the distal and central elongation zone (DEZ and CEZ, respectively).

Perception of the gravity stimulus

Perception of the gravity stimulus is generally attributed to the root cap (Sack, 1991). Removal of the whole cap (Juniper *et al.*, 1966) or small portions of the cap (Blancaflor *et al.*, 1998; Koderá and Sato, 2001; Konings, 1968; Tsugeki and Fedoroff, 1999; Younis, 1954) lead to complete or partial loss of the gravitropic response. Specific elimination of single cells or groups of cells of the Arabidopsis root cap by laser ablation revealed that gravity perception occurs only in a part of the root cap, the columella cells (Fig. 1) (Blancaflor *et al.*, 1998). Characteristically, the columella tissue of the Arabidopsis root tip consists of a single story of columella initial cells, followed by three horizontal stories (S1, S2 and S3) and four vertical files of columella cells (see also Fig. 5) (according to Blancaflor *et al.*, 1998).

Columella cells exhibit structural polarity: A basally located nucleus, an apically located peripheral ER membrane system, and starch filled amyloplasts. Due to their density, amyloplasts sediment, according to the normal gravitation on earth, to the bottom of the cell, where they are thought to provide positional information by exerting pressure on the endomembrane system (Sack, 1997). When the direction of gravistimulation changes, amyloplast sedimentation to the new apparent bottom of the cell occurs within 5 min. This has been proposed to be the first event in gravity perception (starch-statolith hypothesis) (reviewed in Kiss, 2000). Supporting evidence for this hypothesis comes from the observation that changes in starch content, due to physiological treatments (Sack, 1991) as well as starch deficient or starchless mutants (Fitzelle and Kiss, 2001; Kiss *et al.*, 1996; MacCleery and Kiss, 1999), result in defects of amyloplast sedimentation and a decreased gravitropic response. Displacement of amyloplasts by high gradient magnetic fields, on the other hand, can cause root curvature (Kuznetsov and Hasenstein, 1997). Interestingly, the velocity of amyloplast sedimentation differs within the cells of the columella tissue with amyloplast sedimentation being faster in cells of the central columella files, as opposed to cells of flanking files. Specific laser ablations and subsequent determination of presentation time (i.e. the minimum time of gravistimulation required for the initiation of bending) revealed that indeed, cells of central columella files, especially from story S2, are more important for gravitropism, than cells of flanking columella files (Blancaflor *et al.*, 1998).

Related to the starch-statolith hypothesis, is the idea that substances or organelles other than amyloplasts may sediment in response to gravity. These might include crystals, such as BaSO₄ found to be involved in gravity perception in rhizoids of the alga *Chara*, or even the

cellular protoplast itself (Staves, 1997). The force of gravity may also be sensed at cellular membranes or by cytoskeletal interactions (Sack, 1997). In addition, it was proposed, that the root cap was not the only site of gravity perception. Rapid changes in proton flux in the upper half of the DEZ were detected after gravistimulation, raising the possibility that there was a second and independent site of gravity perception located in this region (Behrens *et al.*, 1985; Evans and Ishikawa, 1997; Monshausen *et al.*, 1996).

Signal transmission from gravity perceiving cells to the elongation zone

Root bending in response to perception of a gravity stimulus requires signal transmission from the site of gravity perception to the growth response zone. Several factors are proposed to be involved in this process including changes in pH, electric currents, cytosolic free calcium and auxin. These factors can induce the differential elongation of cells in the DEZ either directly or indirectly by activating other signaling mechanisms.

Amongst the earliest events, proposed to be involved in gravity induced signal transduction, are changes in pH, which were observed, both at the site of gravity perception, in root columella cells and the site of root bending, in the DEZ. Alkalinisation of cytosolic pH in columella S2 cells occurs within seconds after gravistimulation of *Arabidopsis* seedlings (Fasano *et al.*, 2001; Scott and Allen, 1999). Measurements of cell wall pH, on the other hand, revealed a decrease of apoplastic pH in the entire columella tissue, as well as in the DEZ along the upper half of the gravistimulated root (Fasano *et al.*, 2001). Moreover, when changes in root cap pH were induced by localized treatments with buffers or microinjection of caged protons, gravitropic root bending was affected (Fasano *et al.*, 2001; Scott and Allen, 1999). The changes in pH could partially also account for alterations in membrane potential and electric currents observed after gravistimulation. Enhanced currents seen on the upper side of the DEZ of gravistimulated maize root tips was previously reported to be carried by protons (Collings *et al.*, 1992). On the other hand, gravity induced transient changes in membrane potential on upper and lower halves of gravistimulated *Lepidium sativum* root cap cells could be the result of changes in H⁺-ATPase mediated proton transport across the plasma membrane (Behrens *et al.*, 1985). The plasma membrane H⁺-ATPase was shown to be primarily responsible for generating the membrane potential in plant cells (Assmann and Haubrick, 1996; Briskin, 1990).

Another second messenger involved in signal transmission during root gravitropism might be calcium. Alterations in cytosolic free calcium concentrations in statocytes, at the site of gravity perception, could so far not be detected (Legue *et al.*, 1997, S. Gilroy, personal communication). However, indirect evidence proposes a role for calcium in gravity induced signal transduction. Columella cells contain high concentrations of the Ca^{2+} binding protein calmodulin and their amyloplasts contain high calcium levels. Inhibitors of Ca^{2+} -ATPases and calmodulin activity, as well as calcium chelators were shown to prevent gravitropic curvature (reviewed in Sinclair and Trewavas, 1997). Furthermore, rapid induction of calcium movement towards the lower half of gravistimulated maize root tips was reported (Bjorkman and Cleland, 1991; Lee and Evans, 1985).

The substance, most extensively discussed to be involved in signal transduction during root gravitropism is the plant hormone auxin. Already before the first isolation of plant hormones, experiments on phototropic curvature of grass coleoptiles led to the assumption, that a chemical substance might promote differential growth during tropic responses (Darwin and Darwin, 1881). Later, modification of early phototropic and gravitropic experiments confirmed the existence and growth promoting nature of the substance, now termed auxin (Went, 1928). Combining ideas from independent observations of N. Cholodny and F. Went, the Cholodny-Went hypothesis was formulated: "Growth curvatures, induced by external factors, are due to an unequal distribution of auxin between the two sides of a curving organ. In the tropisms induced by light and gravity the unequal auxin distribution is brought about by a transverse polarization of the cells, which results in lateral transport of the auxin" (Firn *et al.*, 2000; Went and Thiemann, 1937).

Auxin accumulation on one side of the shoot induces cell elongation. Because roots are more sensitive to auxin than are shoots, concentrations of auxin that promote the growth of shoots inhibit the growth of roots. According to the Cholodny-Went hypothesis, root curvature is therefore thought to be the result of auxin induced inhibition of cell elongation on the lower half of the gravistimulated root. This theory, although around as dogma for almost a century, has been challenged in the light of results inconsistent with the original concept (reviewed in Evans and Ishikawa, 1997; Firn *et al.*, 2000). Mainly it has been claimed, that auxin gradients are not present in many instances of tropic curvature, and that these gradients do not occur with the rapidity required for a regulatory involvement of auxin. Furthermore,

roots treated with high auxin concentrations, that should mask internal gradients of auxin, remained capable of gravitropic curvature (Ishikawa and Evans, 1993).

On the other hand, there is strong evidence, that supports the involvement of auxin gradients in differential cell elongation during root curvature: Redistribution of radio-labeled IAA in root tips of gravistimulated maize roots (Young *et al.*, 1990), and differential expression of auxin responsive promoter fusions to the β -glucuronidase gene, such as *SAUR-GUS*, *AtIAA2-GUS* and *DR5-GUS*, on the lower half of gravistimulated roots provide evidence for an auxin asymmetry during root curvature (Li *et al.*, 1991; Luschnig *et al.*, 1998; Rashotte *et al.*, 2001). Moreover, inhibitors of polar auxin transport also inhibit root gravitropism (Rashotte *et al.*, 2000) and several mutants with either defects in proteins mediating polar auxin transport (*aux1*, *Atpin2*, *Atpin3*) or putative defects in the regulation of polar auxin transport (*rcn1*, *axr1*, *axr3*, *arg1*) also display agravitropic root growth (Friml *et al.*, 2002b and reviewed in Firn *et al.*, 2000; Muday, 2001)).

1.2 Auxin transport in roots

Apart from tropic responses, auxin is thought to regulate many aspects of plant growth and development, including the formation of primary and lateral shoots and roots, and the differentiation of vascular tissue and embryo development (reviewed in Gilroy and Trewavas, 2001). The cellular mechanisms by which a simple molecule like auxin exerts such pleiotropic effects are not known, yet a main aspect in the regulation of these diverse processes seems to be the response of cells and tissues to different auxin concentrations. Concentration gradients are thought to be established in the course of auxin transport, when auxin from shoot and leave apices, the main sites of synthesis, is transported to the base of the root and further down to the root apex (reviewed in Jones, 1998).

Two main pathways of auxin transport within the root are described: A fast and non polar transport, coupled with the transport of assimilates (e.g. sugars) in the phloem and a slower, directional, polar transport pathway in different tissues of the root. While non polar auxin transport includes the transport of physiologically inactive auxin conjugates, polar auxin transport is restricted to the cell to cell transport of free, and therefore active, auxins. The most abundant naturally occurring auxin is indole-3-acetic acid (IAA). Both pathways may be

directly or indirectly linked (Cambridge and Morris, 1996), however, polar auxin transport is thought to be the main developmentally relevant auxin transport (Lomax *et al.*, 1995). Auxin measurements revealed two distinct directions of polar auxin transport in the root (Fig. 2a) (Rashotte *et al.*, 2000): (i) The transport of auxin from the base of the root to the apex of the root in the vascular tissue (acropetal auxin transport) and (ii) the backward transport of auxin from the apex of the root to the base through the outermost epidermal and cortical tissues (basipetal auxin transport).

The cell-to-cell transport of the auxin IAA was postulated to occur through specific carrier proteins or complexes of proteins, that regulate the flux of auxin into and out of the cell. The direction of auxin flow was proposed to be determined by the efflux carrier and its polar localisation at the site of auxin exit (Rubery and Sheldrake, 1974). The chemiosmotic model for polar auxin transport (Fig. 2b) proposes the entry of non-charged, protonated IAA (HIAA) from the acidic apoplast via diffusion or more efficiently via energized uptake by specific influx carriers into the cell (Goldsmith, 1977; Morris *et al.*, 1991). Because of the more basic pH in the cytosol IAA is deprotonated (IAA^-), and, due to its negative charge and thus poor membrane permeability, trapped within the cell. Consequently, IAA^- can only leave the cell through the action of auxin efflux carriers (Raven, 1975; Rubery and Sheldrake, 1974).

Efflux mediated auxin transport can be distinguished from influx mediated auxin transport (i) by the application of inhibitors, that specifically impair either auxin efflux or auxin influx carrier activity, or (ii) in assays, that determine the transport of synthetic auxins, that are only substrates for one type of carrier. Synthetic auxins used for auxin transport measurements are 1-naphthylacetic acid (1-NAA) and 2,4-dichlorophenoxyacetic acid (2,4-D), that are exclusively transported through activity of auxin efflux and auxin influx carriers, respectively ((Delbarre *et al.*, 1996)).

Inhibitors of auxin transport

The most prominent inhibitors of auxin efflux carrier activity are the phytohormones 1-naphthylphtalamic acid (NPA) and 2,3,5-triiodobenzoic acid (TIBA). NPA and TIBA were shown to influence many plant growth and developmental processes that are thought to be controlled by polar auxin transport, including embryo development (Hadfi *et al.*, 1998),

vascular tissue formation (Mattsson *et al.*, 1999), lateral root initiation (Reed *et al.*, 1998) and meristem pattern formation (Sabatini *et al.*, 1999). Both phototropic and gravitropic curvature of organs are nearly completely abolished upon application of these auxin efflux blockers (Li *et al.*, 1991; Rashotte *et al.*, 2001).

The molecular mechanisms by which NPA and TIBA block polar auxin transport are not precisely known. NPA was originally thought to act on a separate, not yet identified, NPA binding protein (NBP). NBP was controversially described as a peripheral (Cox and Muday, 1994) or integral (Bernasconi *et al.*, 1996) membrane protein. New evidence suggests that NPA and TIBA act by blocking actin dependent vesicle cycling between the plasma membrane and an internal membrane compartment (Geldner *et al.*, 2001; Gil *et al.*, 2001). This cycling is also blocked by application of brefeldin A (BFA), an inhibitor of Golgi vesicle secretion (Geldner *et al.*, 2001). BFA is therefore another candidate for inhibition of efflux mediated polar auxin transport (Delbarre *et al.*, 1998; Geldner *et al.*, 2001; Morris and Robinson, 1998).

Recently, a novel class of specific inhibitors of auxin influx carriers was described with the common feature to perturb the accumulation of 2,4-D in cultured tobacco suspension cells (Imhoff *et al.*, 2000). Two of these compounds, 1-naphthoxyacetic acid (1-NOA) and 3-chloro-4-hydroxyphenylacetic acid (CHPAA) were shown to disrupt root gravitropism. In contrast to 1-NOA, CHPAA exhibited in addition to blocking activity at lower concentration (<10 μ M) auxin like activity at higher concentrations (>10 μ M) (Parry *et al.*, 2001).

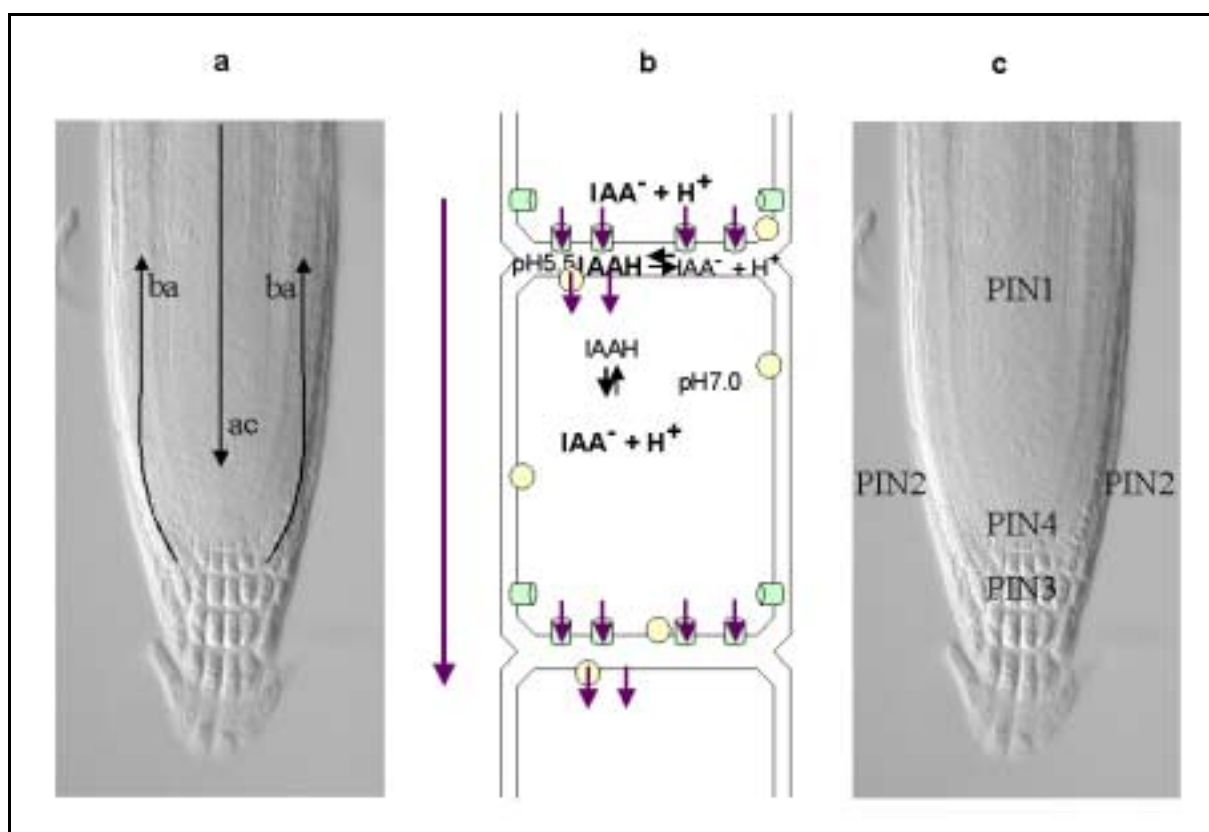


Fig.2: Polar auxin transport in roots and the localization of AtPIN auxin efflux carrier proteins. (a) Arrows indicate direction of acropetal (ac) and basipetal (ba) auxin transport polarities. (b) Chemiosmotic model of polar auxin transport: Protonated IAA (IAAH) enters the cell by diffusion and import via influx carriers (yellow). In the cell IAA is deprotonated (IAA^-) and can only leave the cell via efflux carriers (green). Arrows indicate direction of auxin flow (adapted from Jones, 1998). (c) Approximate localization of AtPIN proteins (PIN1-PIN4) in the Arabidopsis root apex.

Polar auxin transport proteins

Proteins specifically involved in auxin influx or efflux have been identified and mutant plants with defects in genes encoding for these proteins were characterized. The AUX1 protein is thought to mediate auxin influx, while proteins of the AtPIN family are proposed to be involved in auxin efflux. Immunolocalization of the AUX1 and some of the AtPIN proteins revealed their often polar and very specific distribution along the supposed route of acropetal and basipetal auxin transport, in accordance with previous hypotheses (Fig. 2c) (Friml *et al.*, 2002a; Friml *et al.*, 2002b; Gälweiler *et al.*, 1998; Müller *et al.*, 1998; Swarup *et al.*, 2001). Some of the mutants with defects in these genes display agravitropic phenotypes.

The Arabidopsis *AUX1* gene encodes a transmembrane protein that shares homology with transporters of plant amino acid permeases, and appears to play a role in auxin influx (Bennett *et al.*, 1996). A disruption of the *AUX1* gene causes resistance to auxin and ethylene, and

affects root gravitropism in *Arabidopsis* seedlings (Bennett *et al.*, 1996). Agravitropic root growth is compensated by application of the membrane permeable auxin 1-NAA, but not by influx carrier dependent 2,4-D (Marchant *et al.*, 1999). The root growth characteristics of *aux1* can be phenocopied by treating WT seedlings with the auxin influx carrier inhibitors 1-NOA and CHPAA (Parry *et al.*, 2001). Immunolocalization of HA-tagged AUX1 protein in roots of transgenic *Arabidopsis* seedlings revealed a polar localization of the protein at the basal end of protophloem cells, as well as a non polar localization in cells of columella S2, the pLRC and epidermis (Swarup *et al.*, 2001).

Proteins encoded by the *Arabidopsis PIN* gene family consist of 10-12 putative transmembrane segments, and exhibit similarity to bacterial transporters (reviewed in Palme and Galweiler, 1999). Functional assays with AtPIN2, also known as EIR1, AGR1 or WAV6 (Chen *et al.*, 2001; Luschnig *et al.*, 1998; Müller *et al.*, 1998; Utsuno *et al.*, 1998) in yeast suggested auxin carrier activity for the AtPIN2 protein (Chen *et al.*, 1998b; Luschnig *et al.*, 1998). Measurements of auxin transport revealed impaired basipetal auxin transport in roots of the *Atpin2* and stems of the *Atpin1* mutant (Okada *et al.*, 1991; Rashotte *et al.*, 2000). The different phenotypes displayed by the *Atpin1*, *Atpin2*, *Atpin3* and *Atpin4* mutants can be phenocopied by treatment of WT seedlings with inhibitors of auxin efflux (Friml *et al.*, 2002a; Friml *et al.*, 2002b; Fukaki *et al.*, 1998; Gälweiler *et al.*, 1998; Rashotte *et al.*, 2000). In *Arabidopsis* the *PIN* gene family consists of eight members. Six members of this family were cloned and are currently studied in detail. Most striking is the distinct and mostly polar localization pattern of the different AtPIN proteins and their regulated distribution in different organs and various tissues of the *Arabidopsis* plant. While AtPIN1, AtPIN2, AtPIN3 and AtPIN4 are all expressed in roots, only the *Atpin2* mutant displays severe defects in root gravitropism.

The first *AtPIN* gene cloned was *AtPIN1* (Gälweiler *et al.*, 1998). Roots of *Atpin1* mutant plants display normal gravitropic growth. Antibodies, raised against a portion of AtPIN1, revealed the polar localization of the protein at the apical end of phloem cells, basal to the root meristem (J. Friml, personal communication). Other members of the *AtPIN* gene family were isolated in library screens using probes of *AtPIN1* (Friml *et al.*, 2002a; Friml *et al.*, 2002b; Müller *et al.*, 1998). The *Atpin2* mutant, exhibits reduced sensitivity to auxin and ethylene and displays severe defects in root gravitropism (Friml *et al.*, 2002a; Friml *et al.*, 2002b; Müller *et al.*, 1998). Unlike described for *aux1*, application of auxin does not result in

rescue of the *Atpin2* mutant phenotype (A. Müller, personal communication). The AtPIN2 protein was found to be polarly localized at the basal end of LRC (P. Wolff, personal communication), epidermis and cortex cells in Arabidopsis roots (Müller *et al.*, 1998).

In addition to a reduction in phototropic and gravitropic curvature of hypocotyls, the *Atpin3* mutant displays a delay in gravitropic curvature of roots (Friml *et al.*, 2002b, M. Evans, personal communication). In roots, the AtPIN3 protein was shown to be expressed in S1 and S2 cells of the columella tissue. In vertically grown roots, AtPIN3 is non polarly localized in the plasma membrane of S1 and S2 cells, but is polarly relocated to the lateral side of these cells upon gravistimulation (Friml *et al.*, 2002b).

Regulation of AtPIN proteins

The precise mechanisms for the regulation of AtPIN activity are not known and proteins directly interacting with a member of the AtPIN family have not yet been identified. There is, however, evidence for a regulation of AtPIN activity at the level of gene transcription, as well as at the level of post translational protein targeting to the plasma membrane.

Northern blot experiments with an *AtPIN2* specific probe revealed, that application of 1-NAA causes induction of *AtPIN2* gene expression in Arabidopsis roots (A. Müller, personal communication). *In situ* hybridization experiments with an *AtPIN4* specific probe indicated, that in roots of *Atpin1* mutant plants, expression of *AtPIN4* expands to tissues, where WT plants normally do not express *AtPIN4* (J. Friml, personal communication). *AtPIN* gene expression might therefore directly or indirectly be influenced by auxin transport and auxin levels in the plant.

AtPIN activity is also regulated by posttranslational protein trafficking and its (polar) localization in the plasma membrane. In embryos of the *gnom* mutant, vesicle trafficking is disturbed and polarity of AtPIN1 localization is lost (Steinmann *et al.*, 1999). *GNOM* was found to encode a protein, demonstrated to have guanine nucleotide exchange activity for ARF GTPases (Steinmann *et al.*, 1999). These small GTPases are known to play a role in the control of vesicle trafficking between the Golgi apparatus and the plasma membrane and are required for polar localization of auxin efflux carrier proteins (Steinmann *et al.*, 1999). Localization of AtPIN proteins in the plasma membrane was recently found to reflect a

dynamic process of protein cycling between the plasma membrane and an endomembrane compartment (Geldner *et al.*, 2001). BFA treatment abolishes this cycling process and leads to intracellular accumulation of AtPIN proteins, as shown for AtPIN1, AtPIN2 and AtPIN3 (Friml *et al.*, 2002b; Geldner *et al.*, 2001, 2002, P. Wolff, personal communication). Both, directed membrane targeting and cycling of AtPIN proteins are dependent on the actin cytoskeleton (Geldner *et al.*, 2001).

1.3 Aim of the work

The work presented here includes two distantly related projects:

1) The first project deals with the investigation of auxin flows during root gravitropism. Therefore, transgenic Arabidopsis lines carrying the *DR5-GFP* construct as an *in vivo* reporter for cellular auxin levels, were generated. Auxin levels, as represented by *GFP* expression were analyzed in seedling roots before and after change of gravity vector orientation. Genetic and pharmacological analyses were used to identify the role of efflux- and influx mediated polar auxin transport pathways on gravity induced changes in relative auxin levels and the rate of root curvature.

2) The second project deals with the establishment of the split-ubiquitin-system (USPS) for protein interaction as a system to find interaction partners for the AtPIN1 membrane protein. At the beginning of this work, USPS had neither been used for the analysis of protein interaction between membrane proteins of plants nor been employed for screening purposes before. In the first step the potential to monitor the interaction of plant proteins should therefore be analyzed by testing known interaction partners. The next step involved the establishment of the AtPIN1 protein as a bait in this system. The last step required the construction and cloning of a cDNA library from plant tissues in a USPS vector and the screening of this library with the AtPIN1 bait.

2 Materials and methods

2.1 Materials

2.1.1 Plants

<i>Arabidopsis thaliana</i> L.	Cultivar Col0
<i>Arabidopsis thaliana</i> suspension culture	Cultivar Col0
<i>Arabidopsis thaliana</i> L., <i>Atpin2/eir1-1</i>	Cultivar Col0 (Roman <i>et al.</i> , 1995)

2.1.2 Bacteria

<i>E. coli</i> DH10B	F ⁺ mcrAΔ(mrr-hsdRMS-mcrBC)φ80dlacZΔM15lacXΔ74deoRrecA1endA1araD139Δ(ara, leu)7697galUgalKλ ⁻ rpsLnupG
<i>A. tumefaciens</i>	GV3013 C58C1, Rif ^R , Gm ^R (Koncz and Schell, 1986)

2.1.3 Yeasts

JD53	<i>MATα</i> , <i>his3</i> ⁻ Δ200, <i>leu2-3 112</i> , <i>lys2-801</i> , <i>trp1</i> Δ63, <i>ura3-52</i>
------	--

2.1.4 Plasmids

Plasmids used for the generation of constructs described in this thesis are listed below:

<i>pS2-46</i>	contained <i>DR5</i> element (kindly provided by T. Guilfoyle) (Ulmasov <i>et al.</i> , 1997a). amp ^R
<i>pCAT</i>	contained <i>CaMV35S</i> terminator sequence (kindly provided by C. Maas). amp ^R
<i>pGFP-JH</i>	contained <i>GFP5-ER</i> sequence (kindly provided by G. Jach) (Haseloff <i>et al.</i> , 1997). amp ^R
<i>pgj280</i>	contained <i>GFP-LT</i> sequence (kindly provided by G. Jach) (G. Jach, unpublished data). amp ^R
<i>pS001</i>	plant binary vector (kindly provided by B. Reiss) (B. Reiss, unpublished data). amp ^R , sulf ^R
<i>pPINc23</i>	contained <i>AtPIN1</i> cDNA sequence (kindly provided by L. Gälweiler) (Gälweiler <i>et al.</i> , 1998). amp ^R
<i>pC_{ub}-R-URA</i>	contained <i>pMET-C_{ub}-R-URA</i> sequence (kindly provided by N. Johnsson) (Dunnwald <i>et al.</i> , 1999). amp ^R , his
<i>pN_{ub}[*]</i>	contained pCu and N _{ub} , or N _{uba} sequences (N _{ub} [*]) (kindly provided by N. Johnsson) (Dunnwald <i>et al.</i> , 1999). amp ^R , trp
<i>pGAD424</i>	contained the <i>ADH</i> terminator sequence (commercially available). amp ^R
<i>pRS314</i>	yeast ARS/CEN plasmid (Sikorski and Hieter, 1989). amp ^R , trp
<i>pGAP1</i>	contained the <i>GAP1</i> cDNA sequence (kindly provided by A. Molendijk) (A. Molendijk, personal communication). amp ^R
<i>pARAC5[*]</i>	contained the <i>ARAC5-WT</i> , <i>ARAC5-G15V</i> or <i>ARAC5-T20N</i> cDNA sequences (<i>ARAC5[*]</i>) (kindly provided by A. Molendijk) (A. Molendijk, personal communication). amp ^R

<i>pN_{ub}-SSS1</i>	contained the SSS1 sequence (kindly provided by N. Johnsson). amp ^R , trp
<i>pN_{ub}-TPII</i>	contained the TPII sequence (kindly provided by N. Johnsson). amp ^R , trp

2.1.5 Synthetic oligonucleotides

The following synthetic oligonucleotides (primers) were derived from Invitrogen.

Oligonucleotides	Sequence
<i>s2-46up</i>	<i>ggaattcgtcgacggtatcgag</i>
<i>s2-46lo</i>	<i>tgaattgtaattgtaaataag</i>
<i>PIN-U99A</i>	<i>gctctagaattcagatgattacggcgggcggact</i>
<i>PIN-L1948B</i>	<i>taactagtcgacccaccacctagacccaagagaatgtag</i>
<i>PIN-U581C</i>	<i>gctctagaattcatgatctccgagcagtttcca</i>
<i>PIN-L1540D</i>	<i>ggactagtcgacccaatgccgaataaactggag</i>
<i>CUP-U1</i>	<i>tctccccgcgcgagctctggacgateccattaccgacattt</i>
<i>NUIha-L1</i>	<i>ccgccggtcgacggatcccggcgggcgccagcgtaatctggaacatcgatgggtagaatt ccttgtcttgat</i>
<i>ADH1tU1</i>	<i>tccccgggccccgcgccgacagatctatgaatcgtagat</i>
<i>ADH1tL1</i>	<i>tccccgggtacctcgcttatttagaagtgtcaacaac</i>
<i>GAP16U1</i>	<i>gctctagaattcatgatgactaaaggcggaggt</i>
<i>GAP16L1255</i>	<i>taactagtcgacccgctcgctagtcttgagctcaa</i>
<i>ARAC5U199</i>	<i>gcccgggatcctgagtgtcttcgaggtttataaag</i>
<i>ARAC5L766</i>	<i>gcgctcgaggctgactcacaagaacacgcagcgggt</i>
<i>CUP-U595</i>	<i>aattctaccatacgatgttccaga</i>
<i>ADH-L689</i>	<i>gtgaactgcggggtttttcagtat</i>

2.1.6 Antibodies

anti-AtPIN1 rabbit polyclonal antibody (Gälweiler *et al.*, 1998)

goat anti-rabbit IgG horse radish peroxidase conjugated antibody

2.1.7 Enzymes

If not indicated otherwise, enzymes used for experiments in this thesis were obtained from Roche and New England Biolabs.

2.1.8 Chemicals and radiochemicals

If not indicated otherwise, chemicals and radiochemicals used for experiments in this thesis were obtained from Amersham Buchler GmbH & Co KG, J.T. Baker Chemicals, BioRad, Difco Laboratories, Fluka, Merck AG, Serva Feinbiochemica GmbH & Co, Sigma Chemie GmbH.

2.1.9 Other materials

Parafilm M	American National Can.
mRNA Purification Kit	Amersham Pharmacia Biotech
Hybond N	Amersham Pharmacia Biotech
Buchler Flacon tubes	Becton
Reaction tubes	Eppendorf
Petridishes	Greiner GmbH
Pipette tips	Greiner GmbH
Gibco BRL SUPERScript cDNA kit	Invitrogen
Autoradiofilm XOMAT AR	Kodak
Sterile filtration units	Millipore
PicoGreen reagent	Molecular Probes
Qiagen Gel Extraction kit	Qiagen

Plasmid Isolation Midi kit	Qiagen
Plasmid Isolation Maxi kit	Qiagen
RNeasy Maxi kit	Qiagen
Whatman 3MM paper	Whatman

2.1.10 Media for plants

Media were diluted in 1l H₂O.

AM Agar	2.297g MS basal salt medium, 10g sucrose, pH=6, 10 g agar agar.
AM Agarose	2.297g MS basal salt medium, 10g sucrose, pH=6, 8 g agarose.

When required, antibiotics were supplemented to the following final concentration:

Claforan	300 mg/l
Sulfonamide	10 mg/l

2.1.11 Media for bacteria

Media were diluted in 1l H₂O. For solid media 15 g of agar agar was added.

LB medium (Sambrook)	5g yeast extract, 10g trypton, 10g N, pH=7.5.
SOC medium (Sambrook)	5g yeast extract, 20g trypton, 20 mM glucose, 0.5g NaCl, 2.5 mM CaCl, pH=7.5.
YEB medium	10g yeast extract, 10g peptone, 5g NaCl.

When required, antibiotics were supplemented to the following final concentration:

Ampicillin	100 mg/l
Carbenicillin	100 mg/l
Gentamycin	10 mg/l
Rifampicin	100 mg/l

2.1.12 Media for yeasts

Media were diluted in 1 l H₂O. For solid media 20 g of agar agar was added.

YPD medium	10 g yeast extract, 20 g peptone, 20 g glucose.
SD medium	6.7 g nitrogen base without amino acids, pH=5.8, 20 mg L-adenine hemisulfate, 20 mg L-histidine-HCl monohydrate, 100 mg L-leucine, 20 mg L-tryptophane, 20 mg L-uracil, 30 mg L-isoleucine, 150 mg L-valine, 20 mg L-arginine, 30 mg L-lysine, 20 mg L-methionine, 50 mg L-phenylalanine, 20 mg L-threonine, 30 mg L-tyrosine.

The amino acids histidine and tryptophane were omitted from SD media, when selection of yeast cells that had acquired prototrophy for these amino acids (due to transformation events) was required. Furthermore, in the course of USPS growth assays, SD medium lacking uracil (ura⁻ medium) or containing 5'-FOA (1 g/l) (FOA⁺ medium) were prepared. For increased gene expression from the methionine repressible promoter, methionine was omitted from SD media. For increased gene expression from the copper inducible promoter, 100 μM CuSO₄ was added to the medium.

2.1.13 Microscopes

Fluorescence microscope:	Leica MZ12 with mercury HBO 50 W/Ac lamp and FITC filter
Confocal laser scanning microscope:	Leica DMIRBE, TCS4D, with digital imaging processing. A 530+/-15nm band pass filter for FITC specific detection and a 580 nm band pass filter for propidium iodide and autofluorescence detection.

2.1.14 Computer programs

UNIX version 8

DNA star software package

Lasergene

Image Quant 4

Molecular Dynamics

Adobe Photoshop 6.0

Adobe

Diskus

Carl H. Hilgers

Powerpoint 8.0

Microsoft

2.2 Methods

2.2.1 Cloning strategies

Cloning strategies performed in the course of this thesis are described below. Plasmids and primers used for cloning procedures are listed in 2.1.4 and 2.1.5.

Generation of pDR5-GFP

The *DR5* promoter was amplified by PCR from *pS2-46* using the primers *pS2-46up* and *pS2-46lo*. The resulting *DR5* PCR product was cleaved *EcoRI/BamHI* and introduced into *pS001* using these restriction sites. The *CaMV35S* transcriptional terminator was excised *XbaI/HindIII* and introduced downstream of the *DR5* promoter into *pS001* using these restriction sites. The resulting plasmid was termed *pDR5pApS001*.

The *GFP* sequence used for the *pDR5-GFP* construct was generated by excision of an *MscI/SfuI* fragment of *GFP-LT* from *pgj280* and introduction of this fragment into *MscI/SfuI* cleaved *pGFP-JH*. The resulting plasmid was termed *pGFP-LT-ER* and contained the *GFP* sequence *GFP-LT-ER*. *GFP-LT-ER* was excised from *pGFP-LT-ER* by digestion with *BamHI/XbaI* and introduced into *pDR5pApS001* using these restriction sites. The resulting plasmid was termed *pDR5-GFP* (see also 3.1.1, Fig. 3).

Generation of pGAP1-C_{ub}

GAP1 was amplified by PCR from *pGAP1* using the primers *GAP16U1* and *GAP16L1255*. The resulting *GAP1* PCR product was cleaved *EcoRI/SalI* and introduced into *pCub-R-URA*. The resulting plasmid was termed *pGAP1-Cub* see also (see also 3.8.1, Fig.12).

Generation of pN_{ub}m and pN_{uba}m

Sequences for the *pCU* copper inducible promoter and the N_{ub} fragment were jointly amplified by PCR from *pN_{ub}* using the primers *CUP-U1* and *NUIha-L1*. As a result of the design of the *NUIha-L1* primer sequence, the amplified PCR fragment, termed *N_{ub}m*, contained sequences for *pCU*, N_{ub}, the HA epitope and a polylinker downstream of the *HA* sequence. The polylinker contained recognition sites for the restriction endonucleases *AscI*, *SmaI*, *BamHI* and *SalI*. *N_{ub}m* was digested *SacI/SalI* and introduced into *pRS314* using these restriction sites. Furthermore, the *ADH* transcriptional terminator sequence was amplified by PCR from *pGAD424* using the primers *ADH1tU1* and *ADH1tL1*. As a result of the design of the *ADH1tU1* primer sequence, the amplified PCR product, termed *ADHm* contained a polylinker site upstream of the *ADH* terminator sequence. This polylinker site contained recognition sites for the restriction endonucleases *ApaI*, *NotI* and *BglII*. *ADHm* was digested *ApaI/KpnI* and introduced downstream of *N_{ub}m* into *pRS314* using these restriction sites. The resulting plasmid was termed *pN_{ub}m* and differed from the original *pN_{ub}* construct that had frequently been used in USPS, by the addition of a transcriptional terminator sequence, a sequence for the HA epitope and an extensive polylinker site, that later allowed the introduction of many different control genes, as well as the *SalI/NotI* digested cDNA from plant tissues. *pN_{uba}m* was generated by replacement of the N_{ub} fragment in *pN_{ub}m* by *N_{uba}* using the restriction enzymes *SacI/SalI*. *N_{uba}* had been amplified by PCR from *pN_{uba}* using the primers *CUB-U1* and *NUIha-L1*.

Generation of pN_{ub}m-ARAC5, pN_{ub}m-ARAC5-G15V, pN_{ub}m-ARAC5-T20N, and pN_{uba}m-ARAC5-G15V

ARAC5, *ARAC5-G15V* and *ARAC5-T20N* were amplified by PCR from the corresponding *pARAC5** plasmids. PCR fragments of *ARAC5*, *ARAC5-G15V* and *ARAC5-T20N* were digested *BamHI/Sall* and introduced into *pN_{ub}m* using these restriction sites. The resulting plasmids were termed *pN_{ub}m-ARAC5*, *pN_{ub}m-ARAC5-G15V* and *pN_{ub}m-ARAC5-T20N*, respectively (see also 3.8.1, Fig.12). *pN_{uba}-ARAC5-G15V* was generated by excision of *ARAC5-G15V* from *pN_{ub}m-ARAC5-G15V* and introduction into *pN_{uba}m* using the restriction sites *BamHI/Sall*.

Generation of pAtPIN1-C_{ub}, pAtPI-C_{ub} and pAtI-C_{ub}

AtPIN1, *AtPII* and *AtI* were amplified by PCR from *pPINc23* using the primer combinations *PIN-U99A/PIN-L1948B*, *PIN-U99A/PIN-L1540D* and *PIN-U581C/PINL1540D*, respectively. The amplified PCR fragments *AtPIN1*, *AtPII* and *AtI* (see also 3.7.2, Fig.14) were digested *BamHI/Sall* and introduced into *pC_{ub}-R-URA* using these restriction sites. The resulting plasmids were termed *pAtPIN1-C_{ub}*, *pAtPI-C_{ub}* and *pAtI-C_{ub}*.

Generation of pN_{ub}m-SSS1 and pN_{uba}m-SSS1

SSS1 was excised *BamHI/Sall* from *pN_{ub}-SSS1* and introduced into *pN_{ub}m* and *pN_{uba}m* using these restriction sites. The resulting plasmids were termed *pN_{ub}m-SSS1* and *pN_{uba}m-SSS1*.

Generation of pN_{ub}m-TPII and pN_{uba}m-TPII

TPII was excised *BamHI/Sall* from *pN_{ub}-TPII* and introduced into *pN_{ub}m* and *pN_{uba}m* using these restriction sites. The resulting plasmids were termed *pN_{ub}m-TPII* and *pN_{uba}m-TPII*.

2.2.2 Construction and cloning of a cDNA library in *pN_{ub}m*

Isolation of total RNA

Tissues from Arabidopsis suspension culture cells, aerial parts of 4-6 weeks old greenhouse plants and roots of 4-6 weeks old *in vitro* grown plants were homogenized in liquid nitrogen, using mortar and pestle. Total RNA from homogenized tissues was isolated using the Quiagen RNeasy® Maxi Kit. The procedure of total RNA isolation involved the lysis of cells in denaturing guanidine isothiocyanate containing buffer and the application of the cell lysate to RNeasy columns. Total RNA binds to a silica-gel-based membrane in these columns and is finally eluted under low salt conditions. Isolation procedure was performed according to supplier's recommendation. The concentration and purity of the isolated total RNA was determined by measuring the absorbance at 260nm and 280nm in a spectrophotometer. An absorbance of 1 U at 260 nm corresponds to 40 µg/ml RNA when RNA is diluted in water. Pure RNA has an A_{260}/A_{280} ratio of 1.8-2.1. RNA quality was further investigated by application of 3 µg of each RNA sample was mixed with an RNA loading buffer (33% w/v formamide, 8% v/v FA, 0,1% w/v xylene, cyanol, 0,1 % w/v bromphenol blue, 0,1 mg/ml ethidium bromide, running buffer), denatured at 65°C and applied to a denaturing agarose gel (1,2% w/v agarose, 100 mM MOPS, 5 mM NaAc, 1mM EDTA). Electrophoresis was performed at 5 V/cm using 1x FA gel running buffer (100 mM MOPS, 5 mM NaAc, 1 mM EDTA, pH=7, 12,3 M FA, DEPC treated water). RNA ladder (Boehringer) was used to estimate size of RNA fragments. After electrophoresis, RNA was visualized on a transilluminator under UV light (254 nm). Distinct bands representing ribosomal RNA indicated, that the RNA was not degraded. The yield of total RNA obtained from 800 mg fresh weight of each starting material, Arabidopsis suspension culture, aerial parts of Arabidopsis plants and roots of Arabidopsis plants, was 600 µg, 624 µg and 250 µg, respectively. Total RNA of root tissues was repeated three times and a total of 600 µg total RNA from this tissue was obtained.

Isolation of mRNA

For rapid affinity-purification of mRNA from total RNA, prepacked oligo(dT)-cellulose spun columns, from Amersham Pharmacia Biotech, were used. 500µg of total RNA from each

starting material (Arabidopsis suspension culture, aerial parts of Arabidopsis plants and roots of Arabidopsis plants) were united and used for the isolation of mRNA. The technique of mRNA isolation by oligo(dT)-cellulose spun columns is based on binding of poly(a)⁺ RNA (mRNA) to the oligo(dT) matrix under high salt conditions and elution of mRNA from the columns under low salt conditions. The isolated mRNA was glycogen precipitated and resuspended in 15 µl water. All steps in the mRNA isolation procedure were performed according to supplier's recommendations. The concentration and purity of the isolated total RNA was determined by measuring the absorbance at 260nm and 280nm in a spectrophotometer (see also isolation of total RNA). 11 µg of mRNA were isolated from a total of 1500 µg of total RNA.

cDNA synthesis

cDNA synthesis was performed using the GIBCO BRL SUPERSCRIPT™ Plasmid System for cDNA Synthesis. This kit results in the generation of cDNA with cohesive ends for *Sall* ligation at the 5'-end and cohesive ends for *NotI* ligation at the 3'-end, thereby allowing the directional cloning of cDNA fragments. The cDNA synthesis procedure was performed according to supplier's recommendation. The basic principle of the synthesis procedure is outlined below. 6 µg of mRNA were used for cDNA synthesis.

For the synthesis of the 1st cDNA strand, oligo(dT) NotI primer adapters were hybridised to the 3'-poly(a)⁺ tail of the mRNA. These primers provided a substrate for the polymerase activity of the SUPERSCRIPT II reverse transcriptase (RT), the enzyme catalysing 1st strand DNA synthesis from the mRNA template. The amount of SUPERSCRIPT II RT added to the reaction depended on the amount of mRNA material used (200 U/µg of mRNA).

Before the 2nd strand cDNA synthesis, 15 µCi α³²PdCTP were added to the reaction mix to mark the cDNA for subsequent determination of fragment size. The 2nd strand synthesis was catalyzed by *E. coli* DNA polymerase I in combination with *E. coli* RNase H and *E. coli* DNA ligase. Subsequent addition of T4 DNA polymerase resulted in blunt-end cDNA fragments. *Sall* adaptors are ligated to the cDNA by T₄-DNA Ligase. The *Sall* adaptors are short duplex oligomers that are blunt ended at one terminus and contain a 4-base 5'-extension for ligation with *Sall* cohesive ends at the other terminus. Directionality of the cDNA was

achieved by *NotI* digestion of the adaptor ligated cDNA, resulting in cDNA fragments with cohesive ends for *Sall* at the 5'- and cohesive ends for *NotI* at the 3'-end.

The *NotI* digested cDNA was extracted by phenol/chlorophorm and precipitated with 7,5 M NH₄ OAc. To estimate the size range of cDNA fragments, an aliquot of the ³²P-labelled cDNA was applied on an agarose gel. After equilibration of the gel in 7% TCA, the gel was air dried and exposed to a XOMAT KODAK film. The majority of cDNA fragments was found at a size ranging from 0,7-2,2 kb.

Size fractionation of cDNA fragments

Size fractionation of cDNA prior to vector ligation was performed according to the GIBCO SUPERScript protocol. Instead of GIBCO columns, CLONTECH CHROMA SPIN™ columns were used. The CHROMA SPIN™ purification method is based on size-exclusion chromatography. Small molecules are retained in the pores of the column resin and large molecules are allowed to pass through. Different fractions of progressively smaller cDNA fragments were therefore collected upon elution of cDNA from the columns. An aliquot of each fraction was applied to an agarose gel. After equilibration of the gel in 7% TCA, the gel was air dried and exposed to a XOMAT KODAK film. Fractions containing larger cDNA fragments (>500 bp) were selected and fractions containing smaller cDNA fragments (<500 bp) and residual adaptors were discarded.

Quantitation of cDNA concentration by PicoGreen® Reagent

Three cDNA fractions containing cDNA fragments larger than 500 bp were selected by size fractionation. The amount of cDNA present in these fractions was determined using the Molecular Probes PicoGreen dsDNA quantification reagent. PicoGreen becomes highly fluorescent when bound to double stranded DNA and allows the detection of as little as 250 pg/ml of dsDNA. PicoGreen Reagent was therefore added to λ DNA standards at different concentrations (250 pg/ml, 2,5 ng/ml, and 25 ng/ml) and to the aliquots of the cDNA fractions. Fluorescence of standards and cDNA samples was determined in a fluorometer at an excitation of 485 nm and an emission at 525 nm. Known concentrations of DNA standards

and fluorescence emission, allowed the determination of cDNA concentration from known cDNA fluorescence emission. cDNA fractions were therefore found to contain a total of 200 ng cDNA.

Ligation and cloning of the cDNA to the pN_{ubm} vector

After over night digestion of *pN_{ubm}* with *NotI* and *Sall*, vector DNA was precipitated by PEG/NaAc. Test ligations of 50ng *pN_{ubm}* with a 10 ng of a 1,1kb fragment revealed good ligation efficiency of fragment to vector and low background of relegated vector at 50 ng vector/ligation in a 20 µl reaction volume. The proportion of vector to DNA was therefore kept and upscaled for the ligation of cDNA to *pN_{ubm}*. In total 100 ng of cDNA were ligated to 500 ng of *pN_{ubm}*. Ligation was performed at 4° C for 4 days. After ligation, the reaction mix was phenol/chlorophorm extracted and NH₄OAc precipitated. The purified DNA was ligated into freshly prepared DH10B *E. coli* competent cells. Transformed *E. coli* cells were plated on ampicillin containing LB agar plates and incubated at 37°C over night. Colonies were scratched from the plates, inoculated in 5 l of LB medium and immediately used for the isolation of plasmid DNA using the Plasmid Isolation Giga kit from Qiagen.

2.2.3 Methods for the analysis of nucleic acids

Methods for the analysis of nucleic acids, that were exclusively performed in the course of cDNA library construction and cloning are described in 2.2.2. All other methods for the analysis of nucleic acids are depicted below.

Small scale plasmid isolation from E. coli

Small scale plasmid isolation from *E.coli* was performed by alkaline lysis according to Sambrook and Fritsch, 1998.

Large scale plasmid isolation from E. coli

The Plasmid Isolation Midi kit for midi preparations from Qiagen was generally used for the isolation of plasmid DNA in the range of 50-100 µg of DNA/preparation. For the isolation of plasmid DNA from *E. coli* cells transformed with the cDNA library, the Plasmid Isolation Giga kit for giga preparations from Qiagen was used. This kit allows the isolation from large bacterial culture volumes and results in yields of plasmid DNA in the range of 5-10 g. Isolation procedure was performed according to manufacturer's protocol. The amount of plasmid DNA obtained from the isolation procedure was evaluated by determination of light absorbance at 260nm in a spectrophotometer.

PCR amplification

A PCR reaction mix of 100 µl contained DNA template (100 ng), 0.8 µl 25 mM dNTPs, 5 µl of each primer of a primer pair ([primer]=10 pmol/µl), 10 µl of 10x buffer (provided by manufacturer) and 1µl Taq polymerase. The PCR reaction was performed by incubation of the PCR reaction mix at three temperatures corresponding to the denaturing, annealing and extension steps in each cycle of amplification. In a typical reaction the DNA was denatured at 95°C, the primers annealed at 40-60°, and the extension was processed at 72°C. 30-40 amplification cycles were used.

DNA cleavage by digestion with restriction endonucleases

For the digestion of DNA with restriction endonucleases, buffers supplied by manufacturers were used. Cleavage of DNA was performed at recommended optimal temperatures, usually at 37°C. 5-10 U of enzyme were used. Digestion of plasmid DNA was performed for 1-3 hrs, while digestion of PCR fragments was performed o/n. Enzyme reactions were stopped by heat inactivation of restriction enzymes upon transfer of the restriction mix to 65° for 20 min.

DNA dephosphorylation

In order to prevent religation of cleaved vector DNA, 5'-phosphate groups at cleaved ends of plasmid DNA were enzymatically removed. Dephosphorylation was performed by addition of 1-2 U of alkaline phosphatase to the restriction digest mix for 20 min. Phosphatase activity was inhibited by heat inactivation upon transfer of the reaction mix to 65°C for 20 min.

Purification of PCR products

After PCR reactions or after enzymatic cleavage of PCR fragments, PCR products were purified using a PEG/NaAc precipitation procedure. Equal amounts of DNA solution and PEG/NaAc solution (26% vol/vol PEG 6000, 6,5 mM MgCl₂, 0,6 M NaAc, pH=6,7) were mixed and incubated at R.T. for 10-15 min. DNA was precipitated by centrifugation for 5 min, twice washed with absolute ethanol and left to air dry for 10-15 min. DNA was resuspended in desired volume of water.

Purification of plasmids

After enzymatic digestion of plasmid DNA, cleaved plasmids were purified from enzymes and small DNA fragments by PEG/NaAc extraction (according to the protocol for purification of PCR products) or by isolation from agarose gels. For the latter procedure, the Quiagen gel extraction kit was used. Procedure was performed according to supplier's recommendations.

Purification of DNA by phenol/chloroform extraction

Equal volumes of DNA and phenol/chloroform/isoamyl alcohol (25:24:1) were mixed, vortexed and centrifuged. The upper, aqueous phase was carefully removed and transferred to a fresh reaction tube. This extraction procedure was repeated with chloroform/isoamyl alcohol (24:1). DNA in the aqueous phase was precipitated by addition of 10% v/v 7,5 M NH₄OAc and 2.5% v/v absolute ethanol at -20° C. After precipitation, salt from the DNA pellet was removed by a washing step in 70% ethanol.

DNA ligation

To ligate DNA fragments with linearized vectors, 1-2 U of T4 DNA-Ligase were used. Typically the amount of fragment mixed with plasmid in the ligation mix was at a ratio of 3:1. For ligation of fragments into binary vectors and for ligation of cDNA to the *pN_{ubm}* vector, the ratio of fragment to plasmid was changed to 10:1 and 1:5, respectively. Ligation was performed in a small volume (5-20 μ l), typically at 16°C o/n. Ligation of cleaved PCR fragments was performed at 4°C for 2-3 days. This procedure resulted in higher ligation efficiency and was applied also for the ligation of cDNA fragments to the *pN_{ubm}* vector.

Separation of DNA fragments by agarose gel electrophoresis

DNA fragments were mixed with DNA loading buffer (8% w/v sucrose, 1 mM EDTA, 0,02% w/v SDS, 0,005% w/v bromphenol blue, 0,05 % w/v xylene cyanol) and analyzed by agarose gel electrophoresis. The agarose concentration depended on the size of fragments to be resolved ((Sambrook and Fritsch, 1998)). Electrophoresis was performed at 5 V/cm using TBE buffer (90 mM Tris/Cl (pH=8,3), 90 mM boric acid, 2,5 mM EDTA, 100 μ g/l EtBr). 1kb ladder DNA size marker was used to estimate the size of DNA fragments. After electrophoresis, DNA was visualized on a transilluminator under UV light (254 nm).

2.2.4 Methods for the analysis of proteins

Protein extraction from yeast cells

Yeast cells were grown to $OD_{600nm}=1,5$ at 30°C and harvested by centrifugation for 10 min at RT. After decanting the supernatant, the pellet was resuspended in 300 μ l lysis buffer (50mM Hepes pH 7,5; 150 mM NaCl; 5 mM EDTA; 1% Triton X-100; 1:40 2M NEM). The lysate was transferred to a reaction tube containing 200 μ l of glass beads and 2,5 μ M PMSF. To break the cells the suspension was repeatedly vortexed and cooled. After centrifugation, 50 μ l of the supernatant were transferred to a reaction tube containing 100 μ l 2x SDS loading buffer (10% glycerol; 3% SDS; 3% β -mercaptoehtanol; 0,3% bromophenol blue; 1 mM PMSF). 5 μ l of the supernatant were used for determination of protein concentration. After determination

of protein concentration, the protein extracts were either directly loaded on a polyacrylamide gel, or stored at -20°C . Before gel loading, membrane proteins were denatured at 45°C for 30 min and soluble proteins were denatured at 95°C for 10min.

Determination of protein concentration

200 μl of 5x Bradford solution (BioRad) were mixed with the protein sample to a final volume of 1 ml. After 5 min incubation at R.T., the absorption of the color complex was measured at 595 nm in a spectrophotometer. The protein concentration was estimated with the help of a standard curve made with BSA (Bradford, 1976).

Separation of proteins in SDS polyacrylamide gels

The electrophoresis of protein extracts was performed in a 10% polyacrylamide running gel (4 ml rotiphorese 30 containing 30% acrylamide and 0,8% bisacrylamide, 3ml 1,5 M Tris/Cl, pH=8,8, 120 μl 10% SDS; 600 μl glycerol, 40 μl APS). The separation gel mix was prepared, degassed and the polymerisation started by the addition of 80 μl TEMED. The stacking gel (1,25 ml rotiphorese 30 containing 30% acrylamide and 0,8% bisacrylamide, 2,5 ml 0,5 M Tris/Cl, pH=6,8; 100 μl SDS, 40 μl APS, 20 μl TEMED, 6,15 ml H_2O) was prepared similarly and loaded on top of the separation gel. Before loading, samples were mixed with loading buffer and denatured. Electrophoresis was performed at a steady current of 10 mA while the samples were in the stacking gel and at 20 mA once the samples reached the running gel.

Western blot

After SDS polyacrylamide electrophoresis, proteins were transferred to a polyvinylidene difluoride membrane (PVDF membrane) (Millipore). The PVDF membrane and gel were wetted in methanol, washed with water and twice equilibrated in transfer buffer (24.24 g Tris/Cl, 12.36 g boric acid) for 15 min. The gel was placed adjacent to the PVDF membrane and pressed between sheets of 3MM paper and pads on the transfer cassette in the following

order starting from the side of the cathode: pad, 3MM paper, gel, membrane, 3MM paper, pad. The assembled transfer cassette was placed vertically into the electrophoresis tank and filled with transfer buffer. Electrophoresis was performed at 20 V o/n (with agitation).

Ponceau staining

After completion of the transfer, the PVDF membrane was washed in water and stained for 10 min in Ponceau staining solution (0.2% v/v Ponceau, 3% v/v Trichloroacetic acid). The stain was removed with several washes in water with a few drops of NaOH.

Immunostaining of Western blots

The membrane with the transferred proteins was incubated in TN buffer (10 mM Tris/Cl, pH=7.5, 150 mM NaCl) with blocking buffer (TN buffer; 3,5% milk powder) for 30 min. The binding of the anti-AtPIN1 antibody was done at a dilution of 1:10,000 in blocking buffer for 90 to 120 min at R.T. Unbound antibodies were removed by washing with TN buffer with 0.05% NP40, 5x for 5min. After addition of the secondary antibody (anti-rabbit antibody coupled to alkaline phosphatase, raised in goat) at a dilution of 1:15,000 in blocking buffer, the membrane was incubated for 60-90 min at R.T. Subsequently, the membrane was washed 5 x with TN buffer containing 0.05% NP40 and once with TN buffer (without detergent). The membrane was then incubated in chemi-luminescent solution (50 µl NBT, 37.5 µl BCIP in 10 ml of TN buffer) and exposed to X-ray film XOMAT AR 5.

2.2.5 Methods for the cultivation and transformation of bacteria

Preparation of electrocompetent E. coli cells

A single colony of *E. coli* DH10B cells was inoculated into 50 ml of LB medium and incubated o/n at 37°C with continuous shaking. 10 ml of the o/n culture were diluted in 500 ml of fresh LB medium, and incubated at 18°C to OD₆₀₀=0.4. Cells were harvested by centrifugation for 15min, at 4°C and resuspended in 500 ml ice-cold water. This washing step

was repeated twice with 250 and 50 ml of ice-cold water, respectively. The supernatant was discarded and cells were gently resuspended in 800 μ l 7% DMSO. The samples were aliquoted in 60 μ l portions, snap frozen in liquid nitrogen and stored at -70°C .

Electroporation of E. coli cells

DNA was added to an aliquot of thawed electrocompetent cells and transferred to an electroporation cuvette. The electroporator was set to 25 μ F, 2,5 kV and 200 Ω . A single electroporation pulse was given and 0.8 ml of SOC medium immediately added. After incubation at 37°C for 1 h, cells were plated on selective LB medium and incubated o/n at 37°C . Transformed colonies were isolated.

Preparation of electrocompetent A. tumefaciens

A single colony of *A. tumefaciens* was inoculated into 16 ml of YEB medium and grown o/n at 28°C . The o/n culture was used to inoculate 400 ml of YEB medium and grown to $A_{600\text{nm}}=0.5$. Cells were harvested by centrifugation and successively resuspended in 200 ml, 100 ml and 10 ml of ice-cold 1 mM Hepes (pH=7.5). Finally cells were resuspended in 800 μ l of 1 mM Hepes (pH=7.5) and 10% v/v glycerol, aliquoted and either directly used for transformation or frozen at -70°C .

Electroporation of A. tumefaciens cells

An aliquot of frozen electrocompetent *A. tumefaciens* was thawed on ice and mixed with 1 μ l of ligation mix. The electroporator was set to 25 μ F, 2,5 kV and 200 Ω . A single electroporation pulse was given and 0.8 ml of YEB medium immediately added. After incubation at 28°C for 2 hrs, cells are plated on selective YEB medium and incubated for 2 d at 28°C . Transformed colonies were isolated.

2.2.6 Methods for the cultivation and transformation of yeasts

Yeast transformation and co-transformation

A single yeast colony was resuspended in YPDA liquid medium and incubated o/n at 30°C. 30 ml of o/n culture were then inoculated in 300 ml YPDA liquid medium and incubated for about 3 hrs at 30°C until an $OD_{600nm}=0.7$ was reached. Yeast cells were harvested by centrifugation. The pellet was washed in 150 ml of sterile water and immediately centrifuged at RT. The resulting pellet was resuspended in 2 ml of LiAc buffer (100 mM LiAc, pH=7.5) and aliquoted (100 μ l/aliquot). For the transformation of yeast cells, 10 μ l of sheared and denatured salmon sperm DNA (2mg/ml) and plasmid DNA (0.5 μ g/transformation) were added to an aliquot of competent yeast cells. For a yeast transformation, only one type of plasmid DNA was added/aliquot, while for a yeast co-transformation two types of plasmid DNA (e.g. bait and prey vector) were added/aliquot. After addition of 600 μ l transformation buffer (100 mM LiAc, pH=7.5, 40% v/v PEG 3350, 1 mM EDTA, pH=8, 10 mM Tris/Cl, pH=8) the suspension was incubated at RT for 20-60 min. 70 μ l DMSO were added and the suspension was heat shocked for 10 min at 42°C. After centrifugation, the cells were resuspended in 100 μ l of TE buffer (1 mM EDTA, 10 mM Tris/Cl, pH=8). The transformed yeast cells were plated on selective SD plates and incubated at 30°C for 2 d.

Analysis of yeast growth phenotypes

Single colonies from yeast strains carrying different plasmids or plasmid combinations were picked and incubated in selective liquid SD medium for 2 d. Yeast cells within the liquid medium were then counted using a counting chamber and diluted to 10^5 , 10^4 , 10^3 and 10^2 cells/3.8 μ l of liquid medium. 3.8 μ l of each dilution were dropped onto selective SD plates supplemented with FOA (FOA⁺) or lacking uracil (ura⁻) and incubated at 30°C for 2 d.

2.2.7 Methods for the cultivation and transformation of plants

Transformation of Arabidopsis WT and eir1-1 plants

Agrobacterium clones carrying pDR5-GFP were grown in 2 ml of YEB medium with gentamycin (10 mg/l), kanamycin (100 mg/l) and rifampicin (100 mg/l) o/n at 28°C. *A. tumefaciens* cultures were 20x diluted and further cultivated for 12-14 hrs. Before transformation Silwet L-77 (500 µl/l) and 5% sucrose were added to the *A. tumefaciens* culture. Arabidopsis WT and *eir1-1* plants were grown under greenhouse conditions at a density of 8 plants/pot (9 cm diameter). The first emerged floral bolts were cut off to encourage growth of multiple secondary bolts. Transformation was performed 5-10 days after clipping. The plants were dipped for 30 s into *A. tumefaciens* culture and covered with a plastic dome for 24 hrs to maintain high humidity.

In vitro selection of transformed Arabidopsis WT and eir1-1 plants

Seeds of transformed Arabidopsis and *eir1-1* plants were surface sterilized by addition of 5% w/v calcium hypochloride and 0.1 % v/v Triton X-100. After washing the seeds 3x in sterile water, seeds were dried under the flow hood for 2 d. Seeds were plated on AM agar plates containing 10 mg/l sulfonamide for selection of transgenic plants and 300 mg/l Claforan to prevent growth of residual *Agrobacteria*, that might not have been killed in the sterilization procedure. After vernalization of seeds for 3 d at 4°C in the dark, plates were transferred to climate chambers and kept at a 16 hrs day and 8 hrs night rhythm. Transgenic T1 plants were selected and transferred to the greenhouse.

Preparation of seedlings for microscopy

Sterile seeds were sown on AM agar medium. After vernalisation in the dark for 3 days at 4°C, plates were transferred to climate chambers where seeds were germinated and grown at a 16 hrs day and 8 hrs night rhythm. 12 hrs before microscopic analyses or gravistimulation, seedlings were transferred to microscope slides covered with a thin layer (1 mm) of AM medium containing 0.8 % agarose, and supplemented with auxins and auxin transport

inhibitors, respectively. Seedlings on microscope slides were gravistimulated by rotating the stage to 135 °. For better resolution of cellular borders, seedlings were stained with 10 µM propidium iodide prior to analysis by CLS microscopy.

Measurement of root curvature

Kinetic measurements of root gravitropic curvature were performed in the group of M. Evans (Ohio/USA) by using automated root image analysis software (Mullen *et al.*, 1998).

Evaluation of IAA content in root tips of Arabidopsis WT and eir1-1 seedlings

Measurements of IAA content in root tips of Arabidopsis WT and *eir1-1* seedlings were performed in the group of G. Sandberg (Umea/Sweden). Free IAA was measured in the first 1 mm of root tips of Arabidopsis WT and *eir 1-1* seedlings by gas chromatography and mass spectrometry (Friml *et al.*, 2002a).

3 Results

In order to understand the role of polar auxin transport during root gravitropism auxin changes at cellular resolution in living tissues were visualized. The synthetic auxin responsive promoter *DR5* was therefore linked to *GFP* in a transcriptional fusion construct. Transgenic *Arabidopsis* plants harboring *pDR5-GFP* were generated and used for studies on gravitropic root growth. After a short description of the *pDR5-GFP* construct and the characterization of transgenic *Arabidopsis* lines expressing *DR5-GFP*, the distribution of GFP fluorescence in root tips of *Arabidopsis* before and after gravistimulation is reported. Subsequently, the effect of pharmacological treatments with auxins and inhibitors of polar auxin transport on changes in the pattern of *DR5-GFP* expression and the rate of root curvature is described. The use of the split-ubiquitin-system for the search for interaction partners of the AtPIN1 protein is reported in 3.8.

3.1 Generation of transgenic DR5-GFP Arabidopsis plants

3.1.1 The *pDR5-GFP* construct

For the generation of the *pDR5-GFP* transcriptional fusion construct, an ER-targeted GFP variant was constructed and cloned in combination with the *DR5* auxin responsive promoter into the plant binary vector pS001 (see also Materials and Methods).

To obtain a suitable GFP reporter, in a first cloning step, a 450 bp DNA sequence of the ER targeted GFP variant, *mGFP5-ER* (Haseloff *et al.*, 1997), was excised *MscI/SfuI* and replaced by a 450 bp *MscI/SfuI* flanked DNA sequence from another GFP variant, *GFP-LT* (Materials and Methods) (Jach *et al.*, unpublished results). The DNA sequence of the newly generated GFP variant, *GFP-LT-ER*, was a combination of DNA sequences coding for chromophore and folding mutations characteristic for GFP-LT and sequences coding for ER target- (basic chitinase ER target signal) and ER retention signals (KDEL ER retention signal), characteristic for *mGFP5-ER*. In a second cloning step, the synthetic *DR5* auxin responsive promoter (Ulmasov *et al.*, 1997), consisting of the *DR5* auxin response element and a *CaMV35S* minimal promoter, together with a *TMV* leader sequence were amplified by

PCR and introduced into the plant binary vector *pS001* (Reiss *et al.*, unpublished data). The *CaMV35SpA* transcription terminating sequence was further added resulting in *pDR5pApS001*. For the final construction of the *pDR5-GFP* transcriptional fusion, *GFP-LT-ER* was introduced between the *DR5* auxin responsive promoter and the *CaMV35S* terminator of *pDR5pApS001* (Fig. 3). *GUS* was inserted into *pDR5pApS001* as a control (data not shown).

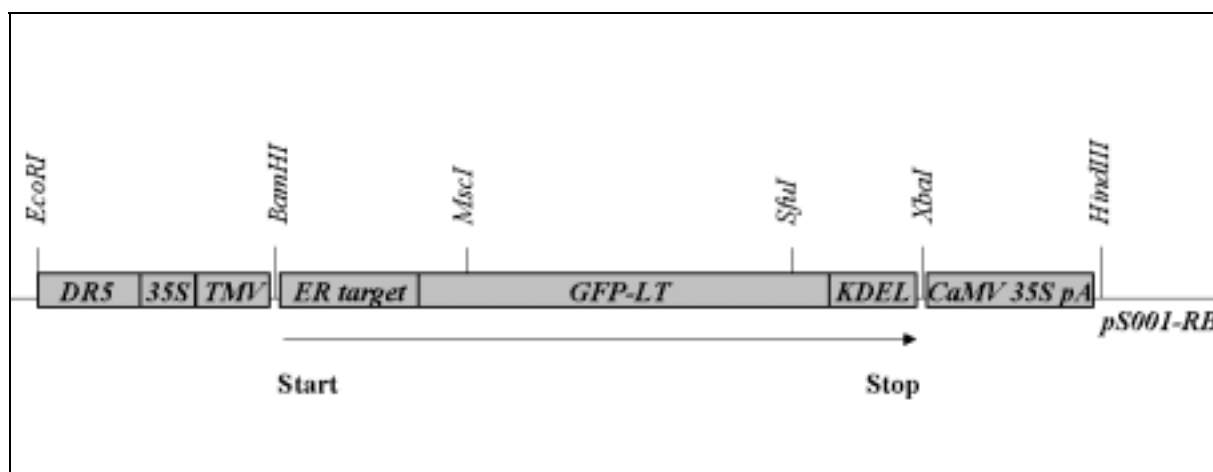


Fig. 3: Schematic diagram of *pDR5-GFP*. *DR5*: *DR5* auxin response element, *35S*: *CaMV35S* minimal promoter, *TMV*: *TMV* leader sequence, *ER target*: coding sequence of ER basic chitinase target signal, *GFP-LT*: coding sequence of GFP, *KDEL*: coding sequence of KDEL ER-retention signal, *CaMV35SpA*: *CaMV35S* transcriptional terminator. Start and Stop mark beginning and end of GFP reporter sequence, respectively. Arrow indicates direction of gene transcription. Restriction sites relevant for the construction of *pDR5pApS001* are indicated.

3.1.2 Analysis of Arabidopsis *DR5-GFP* plants

Selection of transgenic Arabidopsis DR5-GFP plants

Arabidopsis plants were transformed with the *pDR5-GFP* construct (T0 plants) and first transgenic offspring, termed T1 was selected (see Materials and Methods). Subsequently, the T2 progeny of eight independent T1 lines, *DR5-GFP* 1-8, was analyzed for single or multiple loci T-DNA insertions by segregation analysis (Tab. 1). According to Mendelian rules a ratio of three antibiotic resistant to one antibiotic sensitive seedlings is characteristic for a single locus insertion. Homozygous plants for all *DR5-GFP* T-DNA single locus insertion lines were selected by segregation analysis in the T3 generation.

Independent T2 lines	Ratio sulf ^R /sulf ^S	Lines with a single locus insertion
DR5-GFP 1	23/1	-
DR5-GFP 2	3/1	+
DR5-GFP 3	3/1	+
DR5-GFP 4	21/1	-
DR5-GFP 5	3/1	+
DR5-GFP 6	5/1	+
DR5-GFP 7	4/1	+
DR5-GFP 8	3/1	+

Tab. 1: Selection of transgenic *Arabidopsis* lines that contain a single locus insertion for the *pDR5-GFP* T-DNA. DR5-GFP 1-8: T2 generation of 8 DR5-GFP lines derived from independent transformation events in T0. Ratio sulf^R/sulf^S: 150 seeds of each DR5-GFP line were germinated on medium supplemented with the antibiotic sulfonamide. Single locus insert lines (+) vs. multiple locus insert lines (-) were selected by an approximate 3:1 segregation for sulfonamide resistant (sulf^R) vs. sulfonamide sensitive (sulf^S) seedlings. Slight deviations from a strict 3:1 segregation are the result of limited sample size.

DR5-GFP expression in transgenic *Arabidopsis* plants

To determine the sites of *DR5-GFP* expression (in the absence of exogenous auxin) one-week-old seedlings and three to four weeks old plants were analyzed by fluorescence microscopy. In seedlings strong GFP signals were found in the root tip (Fig. 4h, see also 3.2), at the site of adventitious root initiation (data not shown), and at the margins of cotyledons (Fig. 4e). In addition to GFP expression in root tips of main and adventitious roots, as well as cotyledon margins, adult plants exhibited localized strong fluorescence in tips of lateral roots (data not shown), tips of primary and cauline leaves (Fig. 4d), dormant lateral buds (Fig. 4c), the seed funiculus (Fig. 4a) and guard cells of the upper leaf side (Fig. 4b). Weaker GFP signals were often found in the vasculature of roots and hypocotyls (Fig. 4 f,g). No qualitative difference in *GFP* expression pattern of lines DR5-GFP 1 to 8 was observed, although DR5-GFP lines 1, 4, 5, 6, and 7 exhibited stronger GFP fluorescence than lines 2, 3, and 8. The stronger *GFP* expressing lines DR5-GFP 5, 6 and 7 were used for further experiments. GFP signals were comparable to staining patterns obtained with DR5-GUS control plants (data not shown).

Induction of DR5-GFP expression by exogenous auxin application

The *DR5* auxin response element is known to respond to active auxins at concentrations between 10^{-8} and 10^{-5} M (Ulmasov *et al.*, 1997). To test the auxin sensitivity of the *DR5-GFP* reporter, one week old seedlings were incubated with 10^{-8} , 10^{-7} , 10^{-6} , 10^{-5} and 10^{-4} M IAA for twelve hours and analyzed by fluorescence microscopy. GFP induction in all organs of the seedling was already evident in treatments with 10^{-7} M IAA but fluorescence intensity seemed to increase with auxin concentrations up to 10^{-5} M. No apparent difference in GFP intensity of seedlings treated with 10^{-5} and 10^{-4} M IAA was observed. Auxin induction of DR5-GFP seedlings is depicted in Fig. 4 e-l.

As a derivative of an early auxin response element, activation of *DR5* occurs within 5 minutes after auxin application (Ulmasov *et al.*, 1997b). GFP fluorescence, however, is only visible once enough GFP molecules have accumulated. The lag time between *GFP* gene expression and detectable fluorescence depends on many factors, such as promoter strength (and in this case also local auxin concentration for induction of *DR5*), rate of GFP folding, fluorescence intensity of a given GFP variant, and accumulation of sufficient GFP molecules to reach a detectable threshold. To determine the lag time of *DR5-GFP*, one week old DR5-GFP seedlings were treated with 5 μ M IAA by incubation in liquid medium. *DR5-GFP* expression was then analyzed in time intervals of 30 min using fluorescence microscopy. GFP induction was first detected in roots and started one hour after auxin treatment. Induction in all organs of the seedling was complete after 1.5-2.5 hours (data not shown). In comparison to DR5-GFP, DR5-GUS control plants revealed similar sensitivity to exogenous auxin applications with complete staining of the seedlings upon induction with 10^{-7} M IAA and a slightly shorter lag time of 1-1.5 hours (data not shown).

Evaluation of GFP stability in DR5-GFP seedlings

GFP is known to be a very stable reporter protein and, once produced, was shown to be fluorescent for many days (Deichsel *et al.*, 1999). In order to analyze GFP stability in DR5-GFP seedlings, *DR5-GFP* expression was induced by exogenous auxin application and GFP fluorescence was analyzed after auxin depletion. One week old DR5-GFP seedlings were therefore incubated in liquid medium containing 5 μ M IAA. After 2.5 hours some seedlings

were removed from the medium and analyzed by fluorescence microscopy. Auxin induced *DR5-GFP* expression was complete in the entire seedling. Remaining seedlings were transferred to auxin free medium and incubated for two, four, eight and twelve hours before microscopy. During the first eight hours seedlings were transferred to fresh auxin free medium every one hour. However, even after twelve hours of washing, the tissues of the seedlings that had been induced by exogenous auxin were still fluorescent (data not shown).

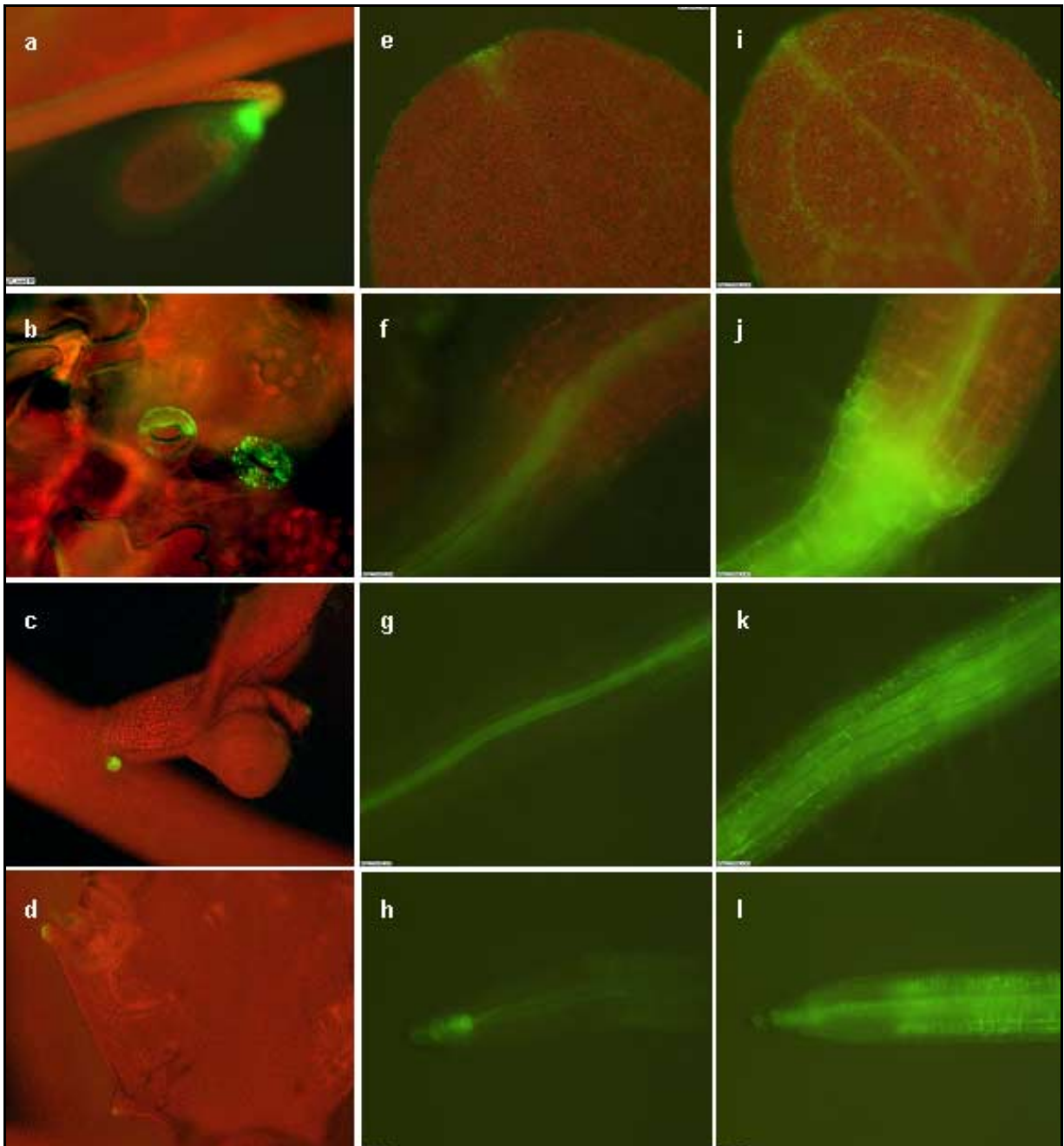


Fig.4: GFP fluorescence pattern of transgenic *DR5-GFP* plants. Fluorescence microscopy images of GFP signals in 4-6 weeks old *Arabidopsis* plants (a-d) and in 1 week old seedlings before (e-h), and after application of 1 μ M IAA (i-l). GFP signals found in the seed funiculus, in guard cell of the upper leaf side, in lateral buds and in tips of cauline leaves are depicted in a, b, c and d, respectively. Apical parts of roots, basal parts of roots, hypocotyls and cotyledons of *DR5-GFP* seedlings are depicted before (e, f, g, and h, respectively) and after application of auxin (i, j, k, and l).

3.2 *DR5-GFP* expression during root gravitropism

In order to analyze the effect of gravity on GFP signal distribution in the Arabidopsis root tip *DR5-GFP* seedlings were grown for five days on vertically oriented AM agar plates. Seedlings were then transferred to microscope slides that were covered with a thin layer of AM agarose and again placed vertical with roots aligned along the gravity vector for twelve hours. For gravistimulation microscope slides were rotated 135° from the vertical. Seedlings remained on agarose covered microscope slides during microscopy. *DR5-GFP* expression pattern in the root tip of live seedlings was analyzed using confocal laser scanning (CLS) microscopy.

DR5-GFP expression in the Arabidopsis root tip of vertically grown roots

The Arabidopsis root has a radial organization with concentric cell layers of epidermis, cortex and endodermis encircling the vascular system of the stele (from outside to inside). A longitudinal section of the root apex (schematically depicted in Fig. 5a) revealed the tissues of the root meristem, that contain epidermis, cortex, endodermis and columella initials and display stem cell activity. All initials encircle a group of four non-dividing central cells, termed the quiescent center (QC). Epidermis and columella initials give rise to the root cap. The root cap consists of three horizontal stories (S1, S2, S3) and four vertical files of columella cells surrounded by the cells of the distal and proximal lateral root cap (dLRC, pLRC) (according to Blancaflor *et al.*, 1998).

In order to facilitate the determination of cell identity in the root apex, cell walls were stained with propidium iodide (see Materials and Methods) before CLS microscopy. In vertically grown roots of six-day-old *DR5-GFP* seedlings, GFP fluorescence appeared very localized in QC, columella initial and mature columella cells S1, S2 and S3 (Fig. 5b).

DR5-GFP expression in the Arabidopsis root tip of gravistimulated roots

Upon 135° gravistimulation first changes in GFP signal distribution were visible after one and a half hours. Adjacent to columella S2, fluorescent signals started to appear asymmetrically in cells of the dLRC, on the lower half of the gravistimulated root (Fig. 5c). Slightly later also dLRC cells adjacent to columella S1 and S3 became fluorescent. Three hours after gravistimulation the entire LRC was asymmetrically stained on the lower half of the root (Fig. 5d). No GFP signals were found in the elongation zone (data not shown). Longer gravistimulation (for up to twelve hours) as well as a continuous gravity stimulus obtained by rotating the plate further (for up to 24 hours) resulted in an increase of GFP signal intensity in the LRC of the lower half of the root. However, extension of fluorescence pattern to other tissues (e.g. to epidermal cells) was not observed (data not shown). To exclude the possibility that after gravistimulation cells in the elongation zone were not anymore sensitive to auxin induction of the *DR5* element, roots were gravistimulated for five hours and subsequently treated with 5 µM IAA for another 2 hours. Microscopic analysis revealed that *DR5-GFP* expression was induced in the elongation zone at the site of root bending (data not shown).

Previous experiments showed that there was a lag time of at least one and a half hours between *DR5-GFP* expression and visible GFP fluorescence. Gravistimulation experiments for periods shorter than one and a half hours were therefore performed such, that the plates were rotated to 135° for five, 15 and 30 min, respectively, and subsequently back-rotated to the vertical for three hours to allow GFP accumulation. It was found that a stimulus of 15 min was enough to induce *DR5-GFP* expression in dLRC cells adjacent to columella S2 and S3 (data not shown). Therefore, auxin accumulation (as represented by the *DR5-GFP* reporter) in the dLRC and pLRC cells on the lower half of the gravistimulated root was induced shortly after gravistimulation.

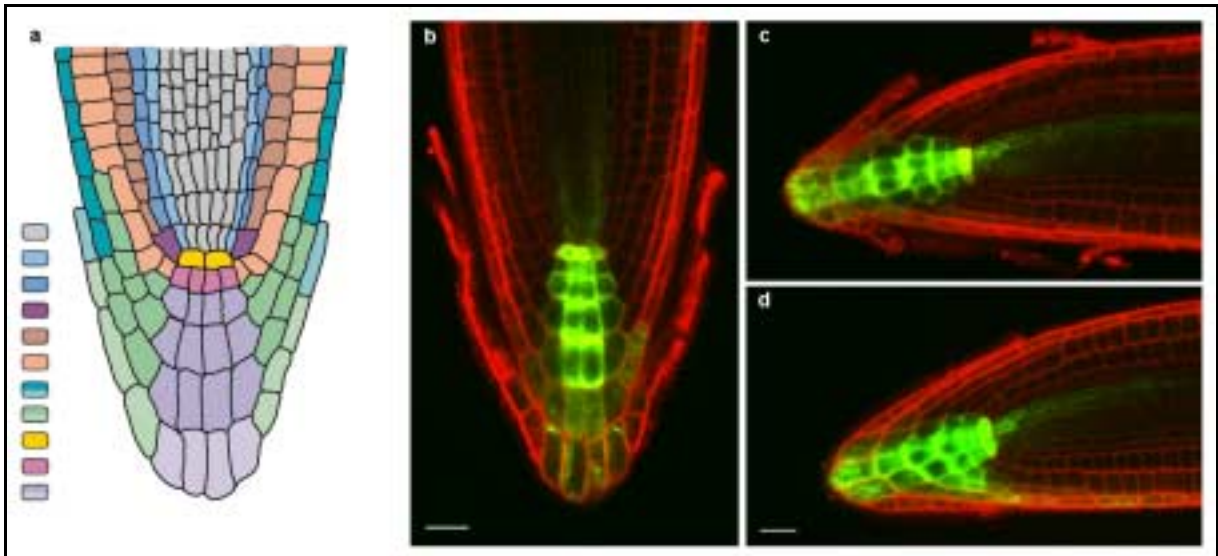


Fig. 5: Changes in gravity vector orientation induce asymmetric DR5-GFP expression in LRC cells. a) Schematic representation of the Arabidopsis root apex. The colour code labels different tissues (top to bottom: stele, pericycle, endodermis, cortex/endodermis initial, cortex, epidermis, proximal LRC, distal LRC, QC, columella initial, columella). b) CLS microscopy images of GFP signals in quiescent center, columella initials and columella of vertically grown roots. c) After 1.5 hrs of gravistimulation GFP signals expand from columella S2 to lower half of LRC resulting in complete staining of LRC after 3 hrs (d). Scale bars represent 20 μm.

3.3 The effect of exogenous auxin application on *DR5-GFP* expression during root gravitropism

To investigate the effect of gravity induced changes of polar auxin transport on the distribution of exogenously applied auxins, *DR5-GFP* seedlings were treated with IAA, 1-NAA and 2,4-D. These auxins are known for their different cell-to-cell transport characteristics, with IAA being a substrate for both efflux and influx carriers, while 1-NAA and 2,4-D are substrates exclusively for efflux- and influx carriers, respectively (see 1.2). Analogous to experiments described in 3.2, five day old seedlings were grown on vertically oriented AM agar plates and subsequently transferred to agarose covered microscope slides. For auxin treatments described below, the agar covering the microscope slides was supplemented with IAA, 1-NAA, and 2,4-D, respectively. Microscope slides were kept in vertical position for twelve hours and either used for the analyses of vertically grown seedlings or gravistimulated by rotation to 135° for five or 24 hours. *DR5-GFP* expression in root tips was analyzed by CLS microscopy.

3.3.1 Effect of IAA

In the presence of 1 μ M IAA, GFP fluorescence was observed in QC, columella initials and columella cells with additional strong signals in the entire lateral root cap and epidermis of vertically grown roots (Fig. 6a). After gravistimulation for five hours a slight asymmetry in signal distribution was observed. GFP signal intensity in the dLRC, adjacent to columella S2 and S3 increased on the lower half of the gravistimulated root, while intensity decreased on the upper half (Fig. 6b). After longer gravistimulation for 24 hours this effect was more pronounced, but no asymmetry in signals of the pLRC was observed (Fig. 6c).

3.3.2 Effect of 1-NAA

Vertically grown roots treated with 1 μ M 1-NAA were fluorescent in QC, columella initial and mature columella cells. Similar to IAA treated roots, LRC and epidermis were stained, although fluorescence intensity in epidermis as well as pLRC cells was less bright for 1-NAA compared to IAA treatments (Fig. 7d). Identical GFP fluorescence pattern in vertical roots were obtained when roots were treated with a combination of 1 μ M IAA and 10 μ M 1-NOA, an inhibitor of influx carrier mediated polar auxin transport (data not shown). After gravistimulation for 5 hours, asymmetry in signal distribution was observed with signal decay in dLRC on the upper and signal increase in dLRC on the lower half of the root (Fig. 6e). After 24 hours of gravistimulation asymmetric signal distribution was clearly evident with fluorescence distribution almost entirely confined to dLRC, pLRC, and epidermis on the lower half of the root (Fig. 6f). Interestingly, under these conditions GFP fluorescence was also observed on the lower half of the root in epidermal cells of the elongation zone at the site of root bending (Fig. 7).

3.3.3 Effect of 2,4-D

Roots kept on 1 μ M 2,4-D displayed GFP fluorescence in virtually all tissues of the root tip (Fig. 6g). Identical GFP fluorescence pattern in vertical grown roots were obtained when roots were treated with a combination of 1 μ M IAA and 10 μ M NPA, an inhibitor of efflux carrier mediated polar auxin transport (data not shown). Gravistimulation for five and 24 hours did

not result in change of staining pattern. Signal intensity remained equally strong on both halves of the gravistimulated root tip (Fig. 6 h, i).

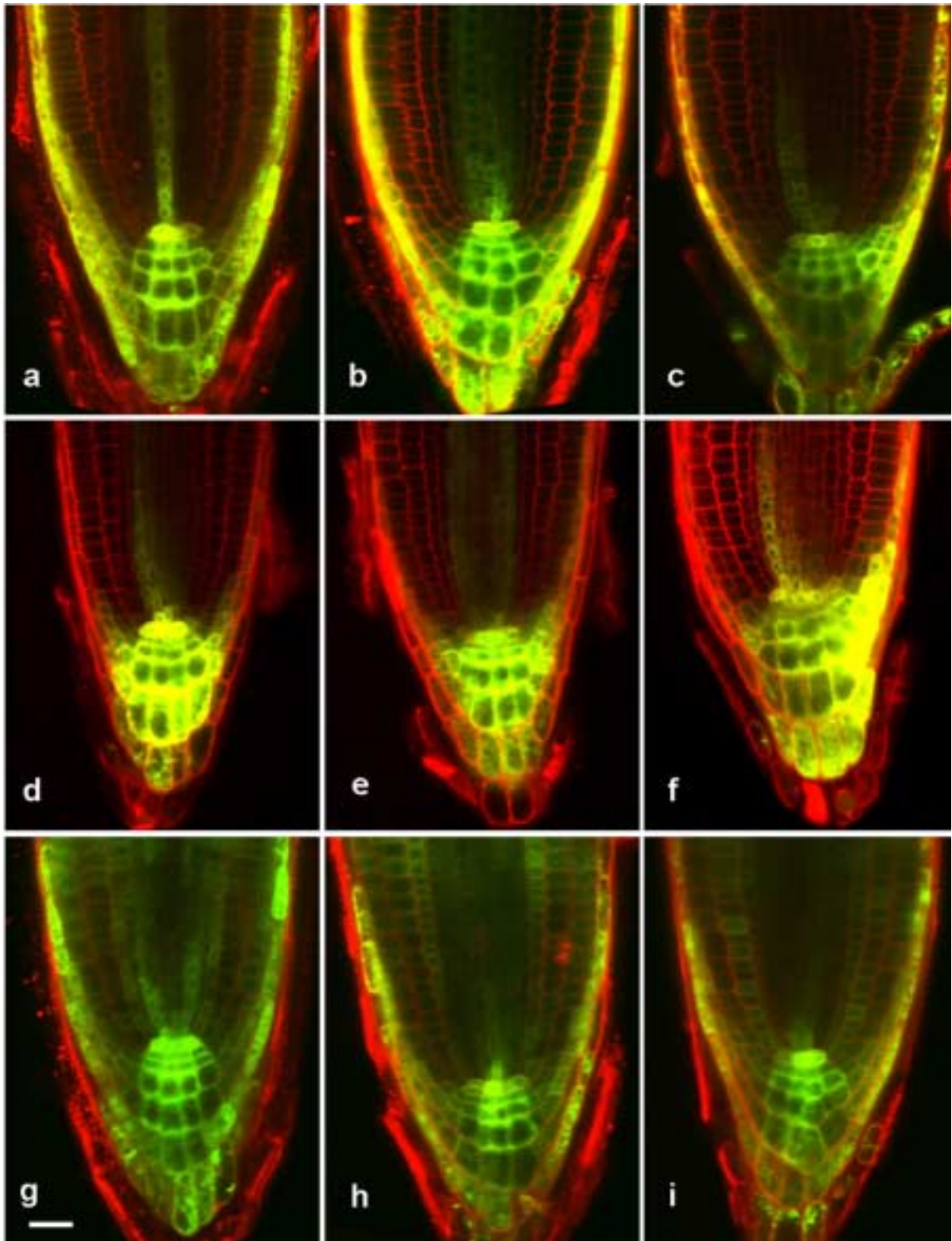


Fig. 6: Asymmetric GFP signals are observed in gravistimulated roots even under continuous auxin supply. CLS microscopy images of GFP signals in roots grown on 1 μ M IAA, 1 μ M 1-NAA, and 1 μ M 2,4-D before (a, d, g), and after 5 hrs (b, e, h), and 24 hrs (c, f, i) of gravistimulation, respectively. Images are aligned with root tips to the vertical for better comparison; note that lower half of gravistimulated roots is at the right hand side (b, c, e, f, h, i). Scale bar represents 20 μ m.

Application of IAA, 1-NAA and 2,4-D caused clear differences in accumulation and redistribution of auxin (as represented by *DR5-GFP* expression) before and after gravistimulation, respectively. Under continuous auxin supply only roots grown on IAA and 1-NAA, both substrates for the auxin efflux carrier, were capable of establishing auxin asymmetry in response to gravity.

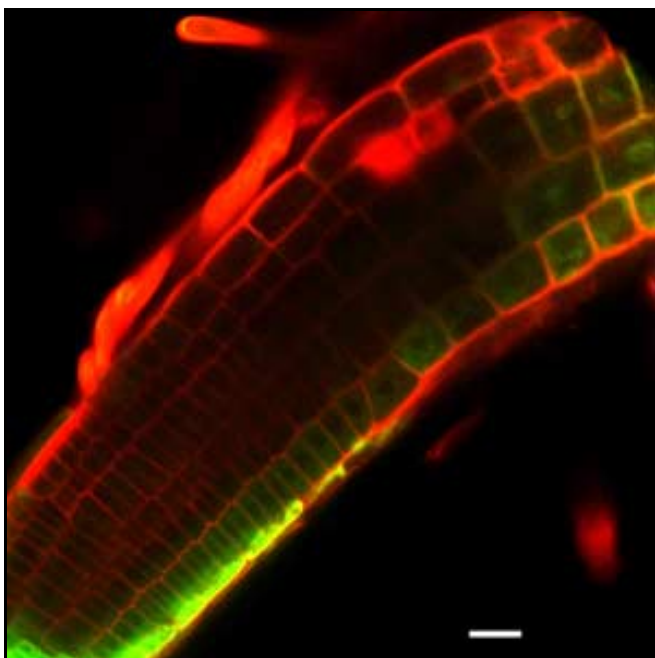


Fig. 7: Asymmetric GFP signal distribution is observed in epidermal cells of gravistimulated roots grown on 1-NAA. CLSM microscopy image of GFP signal in roots treated with 1 μ M 1-NAA and gravistimulated for 24 hrs. Scale bar represents 20 μ m.

3.4 The effect of exogenous auxin application on gravity induced root curvature

To correlate gravity induced changes in GFP signal distribution of auxin treated roots with root bending, kinetic measurements of root curvature were performed (see 2.2.7). Similar to experiments described in 3.3, roots were transferred to medium containing 1 μ M of IAA, 1-NAA or 2,4-D twelve hours before gravistimulation. When roots were gravistimulated, initiation of root bending in the elongation zone was followed and the angle of root curvature was determined at different timepoints (Fig. 8). The strongest downward curvature was observed in roots treated with 1-NAA. After 20 hrs of gravistimulation in the presence of 1-NAA roots still bent to about 56 % compared to untreated control roots. Gravitropic curvature of IAA treated roots was close to zero despite a slight but significant downward curvature. Roots grown on 2,4-D showed no or even tenuous negative gravitropic curvature.

Taken together results described in 3.3 and 3.4, the strongest root curvature and the most prominent difference in gravity induced auxin distribution on the upper and the lower half of the root (as represented by *DR5-GFP* expression) was observed for roots grown in the presence of 1-NAA. Roots grown in the presence of IAA displayed an asymmetry in auxin distribution in dLRC cells of gravistimulated roots, but not in pLRC cells and showed a strong reduction in gravitropic curvature. 2,4-D treated roots did not reveal a difference between auxin distribution on lower and upper half of gravistimulated roots and also did not exhibit a curvature response. The extent of auxin asymmetry in the root tip therefore correlated with the degree of root curvature.

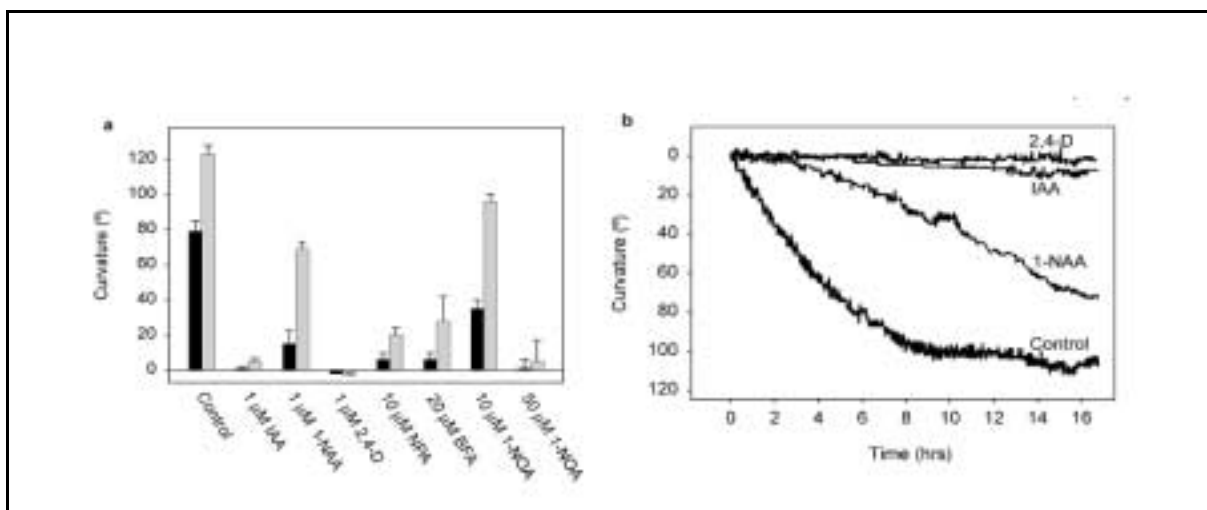


Fig. 8: Disruption of root gravitropism by application of auxin and auxin transport inhibitors correlates with altered *DR5-GFP* expression patterns. a) Total curvature 5 hrs and 20 hrs (black and grey bars, respectively) after stimulation at 135 °. Values represent means \pm SE, $n = 7-10$ for all treatments. b) Example kinetics of curvature in the apical 300 μm of roots treated as indicated.

3.5 The effect of auxin transport inhibitors on *DR5-GFP* expression during root gravitropism

To further assess the contribution of auxin efflux and influx carriers to auxin flux during gravitropic root growth, seedlings were treated with inhibitors of polar auxin transport that specifically block auxin transport via efflux and influx carriers. Seedlings were treated as described in 3.3. Agarose covering microscope slides was supplemented with NPA, TIBA, and BFA, inhibitors of auxin efflux and 1-NOA, an inhibitor of auxin influx. *DR5-GFP* expression in root tips was analysed by CLS microscopy.

3.5.1 Effect of NPA and TIBA

Treatment with 10 μ M NPA resulted in altered *GFP* expression pattern in the root apex of vertically grown roots (Fig. 9a). *GFP* fluorescence appeared in QC, columella initials and columella S1 cells, but extended from these cells into initials of epidermis, endodermis and vasculature. Staining in columella cells S2 and S3 was less intense in the outermost vertical files. Compared to control roots, that were not grown on auxin transport inhibitors, NPA treatment resulted in an enlarged and slightly upward shifted area of *GFP* signal distribution. A similar pattern was observed when roots were treated with 10 μ M of the auxin transport inhibitor TIBA (data not shown). Gravistimulation for either 5 (data not shown) or 24 hours resulted in staining patterns identical to those observed in vertically grown, NPA treated roots. (Fig 9b). Thus, no asymmetric signal distribution occurred.

3.5.2 Effect of BFA

DR5-GFP expression pattern of roots grown vertically on 20 μ M BFA was similar to untreated control roots (Fig. 9c). Only a small portion (2-5%) of roots displayed additional *GFP* signals in initials of epidermis, endodermis and vascular cells, an effect similar, but less pronounced, to that observed for NPA treatments (data not shown). After gravistimulation for 5 (data not shown) or 24 hours there was no change in *GFP* signal distribution and no signal asymmetry was detected (Fig. 9d).

3.5.3 Effect of 1-NOA

In the presence of 20 and 50 μ M 1-NOA *DR5-GFP* expression pattern in vertically grown roots was nearly identical to that observed in root tips of vertically grown control roots with *GFP* signals in QC, columella initials and mature columella cells (Fig. 9e, g). However, fluorescence intensity was slightly stronger in QC cells, compared to a more evenly distributed fluorescence intensity in root tips of seedlings that were not treated with 1-NOA. Gravistimulation for 5 hours resulted in asymmetric signal distribution in the LRC on the lower half of the gravistimulated root (data not shown). Fluorescence intensity was weaker than in controls. After 24 hours of gravistimulation signal asymmetry was more pronounced

and bright fluorescence was observed in cells of the dLRC, adjacent to columella S2 and S3 (Fig. 9f, 9h). There was no significant difference in signal pattern for the different concentrations of 1-NOA. Interestingly, unlike in 24 hours stimulated control roots, the strong asymmetrically distributed staining pattern was restricted to the dLRC and did not extend to the pLRC.

Thus, the auxin efflux carrier blockers NPA, TIBA and BFA completely inhibited asymmetric auxin accumulation (as reflected by *DR5-GFP* expression) on the lower half of the gravistimulated root. In the presence of the auxin influx carrier blocker 1-NOA, on the other hand, auxin was asymmetrically distributed to the dLRC but not to the pLRC.

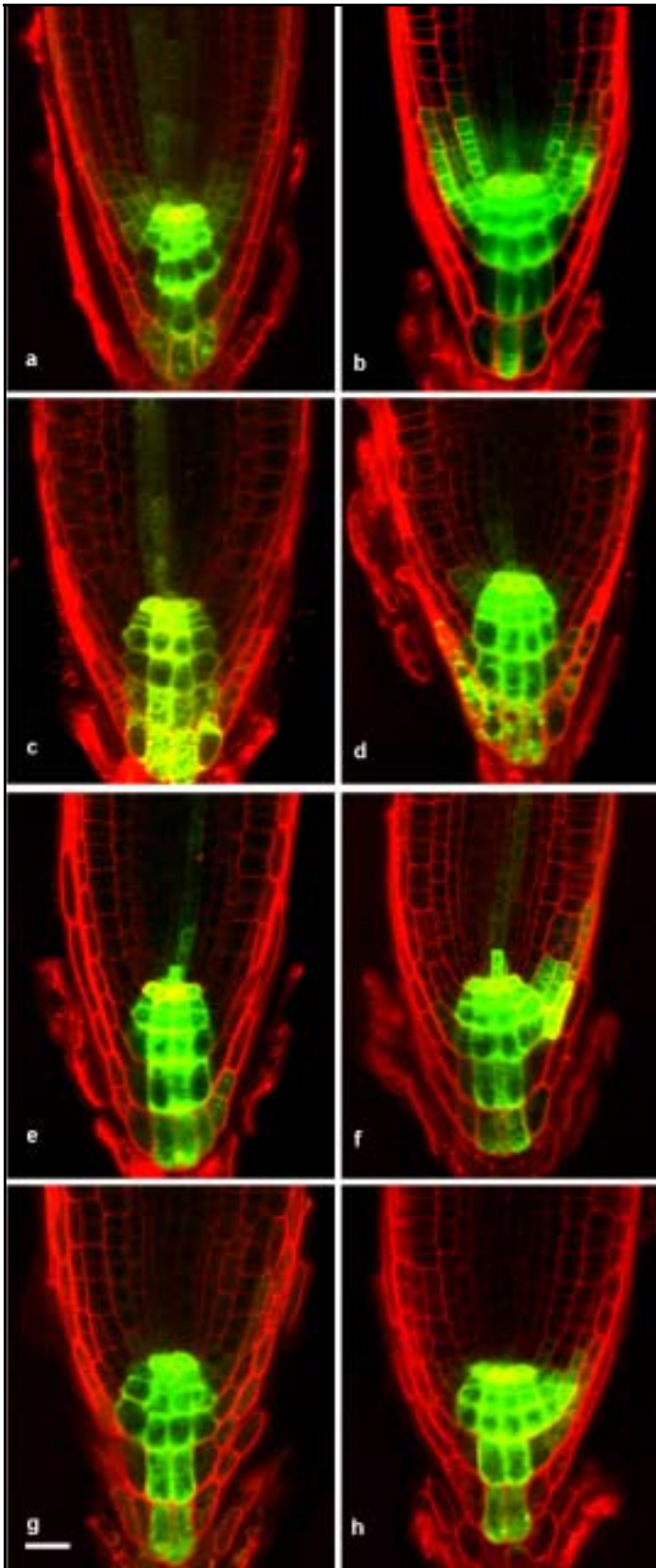


Fig. 9: Auxin transport inhibitors influence *DR5-GFP* expression. CLS microscopy images of GFP signal in roots grown on 10 μ M NPA, 20 μ M BFA, 10 μ M and 50 μ M 1-NOA before (a, c, e, g), and after 24 hrs (b, d, f, h) of gravistimulation. Images are aligned with root tips to the vertical for better comparison; note that lower half of gravistimulated roots is at the right hand side (b, d, f, h). Scale bar represents 20 μ m.

3.6 The effect of auxin transport inhibitors on gravity induced root curvature

Analogous to auxin treated roots in 3.4, the angle of root curvature was also determined for roots treated with inhibitors of polar auxin transport. Seedlings were transferred to medium containing either 10 μ M NPA, 20 μ M BFA or 10 and 50 μ M 1-NOA. The angles of curvature after 5 and 20 hrs of gravistimulation are depicted in Fig 8a. Treatments with NPA and BFA resulted in comparable and strong reduction of root bending with angles of curvature of only 17-25% compared to untreated controls. Treatments with 10 μ M 1-NOA also resulted in a reduction of root bending, however less pronounced. In the presence of 50 μ M 1-NOA gravitropic root bending was almost completely abolished.

Taken together results reported in 3.5 and 3.6, inhibitors of auxin efflux carrier activity therefore resulted in inhibition of asymmetric auxin accumulation (as reflected by *DR5-GFP* expression) in LRC cells on the lower half of gravistimulated roots, as well as in a strong reduction of root bending. The auxin influx carrier inhibitor 1-NOA, on the other hand, led to inhibition of asymmetric auxin accumulation in the pLRC, but not the dLRC. Interestingly higher concentrations of 1-NOA nearly eliminated root bending, while asymmetric auxin distribution to the dLRC on the lower half of the root still occurred.

3.7 *DR5-GFP* expression in the root tip of the *eir1-1* mutant

It was shown that inhibition of auxin efflux prevents asymmetric GFP signal distribution in the LRC after gravistimulation. Another approach for the investigation of gravity induced regulation of polar auxin transport, was the analysis of *DR5-GFP* expression in mutants with defects in polar auxin transport. Therefore the mutant *eir1-1* was transformed with the *pDR5-GFP* construct. *eir1-1*, allelic to *Atpin2*, *agr1* and *wav6* (see also 1.2.), displays a strong agravitropic phenotype and is a null mutant for the putative auxin efflux carrier AtPIN2. AtPIN2 was shown to be localized in pLRC, cortex and epidermis, predominantly at the basal side of the cell.

T1 *eir1-1* plants, transgenic for the *DR5-GFP* T-DNA were selected and T2 progeny seedlings were used for further analyses. One-week-old seedlings were transferred to agarose covered microscope slides and vertically aligned along the gravity vector. 12 hrs later

(agravitropic root growth was clearly visible) *GFP* expression was analyzed using CLS microscopy. Fluorescence pattern in the root tip was found to be enlarged with strong GFP signals not only in QC, columella initials and columella cells, but also in the dLRC (Fig. 10b). A slight asymmetry of the GFP signal on one half of the root was observed but, due to agravitropic root growth, could not be correlated with the direction of the gravity vector. In addition, free IAA levels were measured in the first mm of *eir1-1* mutant root tips by mass spectrometry. When these were compared to wild type, mutant root tips contained a 2.5 times higher level of auxin (Fig. 10b) correlating with enhanced *DR5-GFP* expression in the mutant root cap.

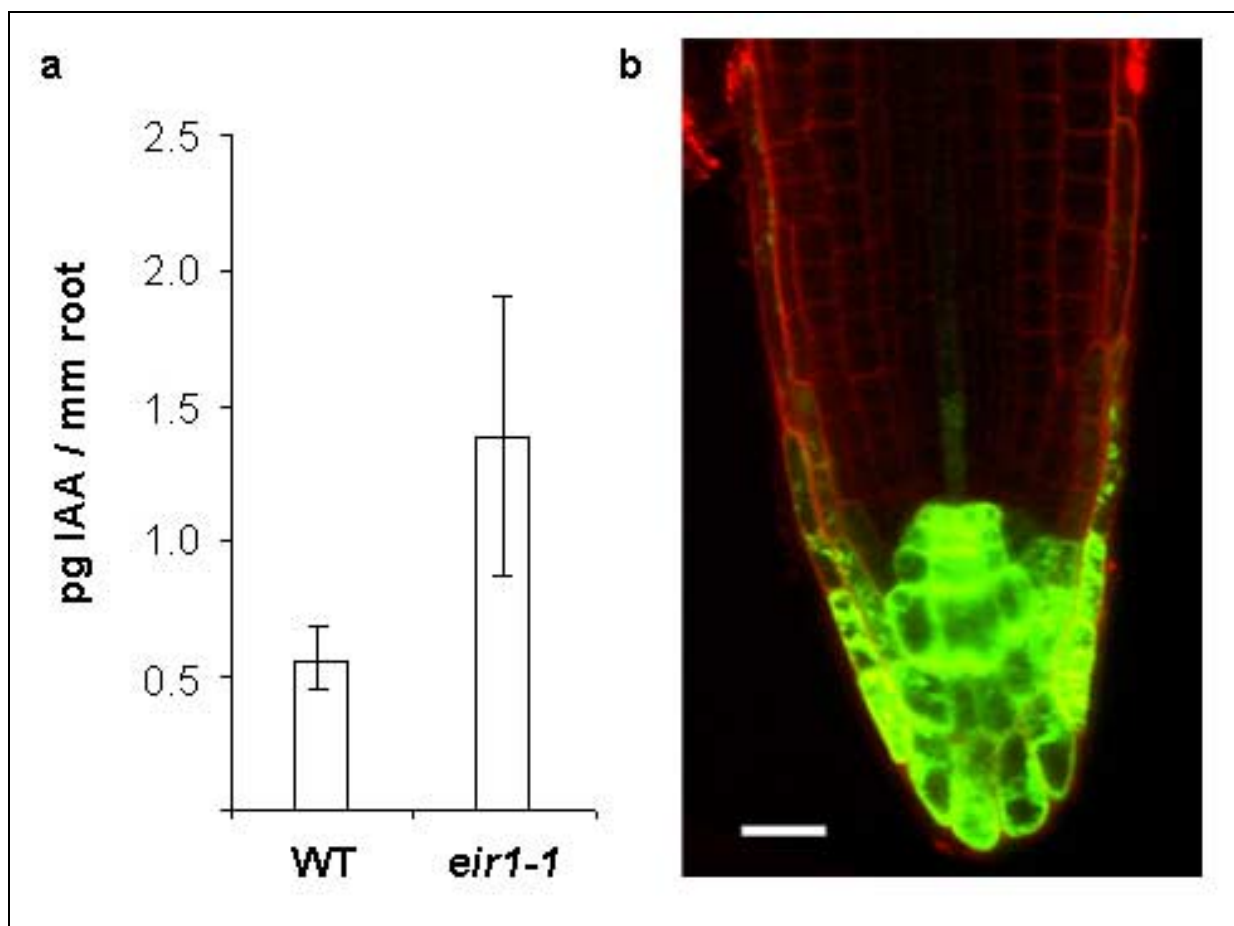


Figure 10: *Eir1-1* mutants have substantially elevated auxin levels in the root tip. a) Levels of free IAA of young seedlings determined by mass spectrometry. For each line data were sampled from 10 measurements in two different experiments and are represented as means and SD. b) Auxin biosensor signal reveals increased auxin levels in LRC of *eir1-1* mutant root tip. Scale bar represents 20 μm.

3.8 Identification of AtPIN1 interaction partners with the split-ubiquitin-system

With the aim to screen for proteins, that interact with AtPIN1, a plant cDNA library was constructed and introduced into a yeast expression vector. For detection of proteins interacting with AtPIN1, the split ubiquitin system, also called USPS (ubiquitin/split/protein/sensor), was used (Johnsson and Varshavsky, 1994a; Johnsson and Varshavsky, 1994b).

The USPS is based on the ability of N-terminal and C-terminal halves of ubiquitin (N_{ub} and C_{ub}), to assemble into a functional ubiquitin moiety. Proteins of interest are tested for interaction, by linking one protein to the N_{ub} - and the other protein to the C_{ub} fragment. If the proteins interact or come into close proximity to each other, N_{ub} and C_{ub} fragments reconstitute a functional ubiquitin protein. Reassembly of the ubiquitin halves is detected through the action of ubiquitin specific proteases (UBPs), that cleave off a reporter, that has been attached to the C-terminus of the C_{ub} fragment (Fig. 11). UBPs are present in the cytosol and the nucleus of all eukaryotic cells and recognize only the reconstituted ubiquitin, but not its separate halves.

Similar to the yeast two hybrid technique, the USPS employs live yeast cells for the analysis of protein interaction. In contrast to the yeast two hybrid system, USPS allows the detection of protein interaction in various cellular compartments, provided that N_{ub} and C_{ub} are attached to parts of the protein which localize to the cyto- or nucleoplasm, where UBPs are present. Thus interaction of proteins at the plasma membrane, at the translocation pore of the ER, as well as in the cyto- and nucleoplasm of the cell have been reported (Dünnwald *et al.*, 1999; Johnsson and Varshavsky, 1994a; Stagljar *et al.*, 1998; Wittke *et al.*, 1999; Wittke Wittke *et al.*, 2000).

In order to get familiar with the USPS, the interactions of plant proteins, that had been proven to interact in the yeast two hybrid system and in a co-immuno-precipitation assay, were demonstrated with the USPS. Subsequently, the *AtPIN1* gene was introduced into a USPS C_{ub} bait vector and used to establish the ideal conditions for the screening procedure. Finally, a cDNA library from plant tissues was generated and introduced into a USPS N_{ub} prey vector. In a test trial, this library was screened for putative interaction partners of AtPIN1.

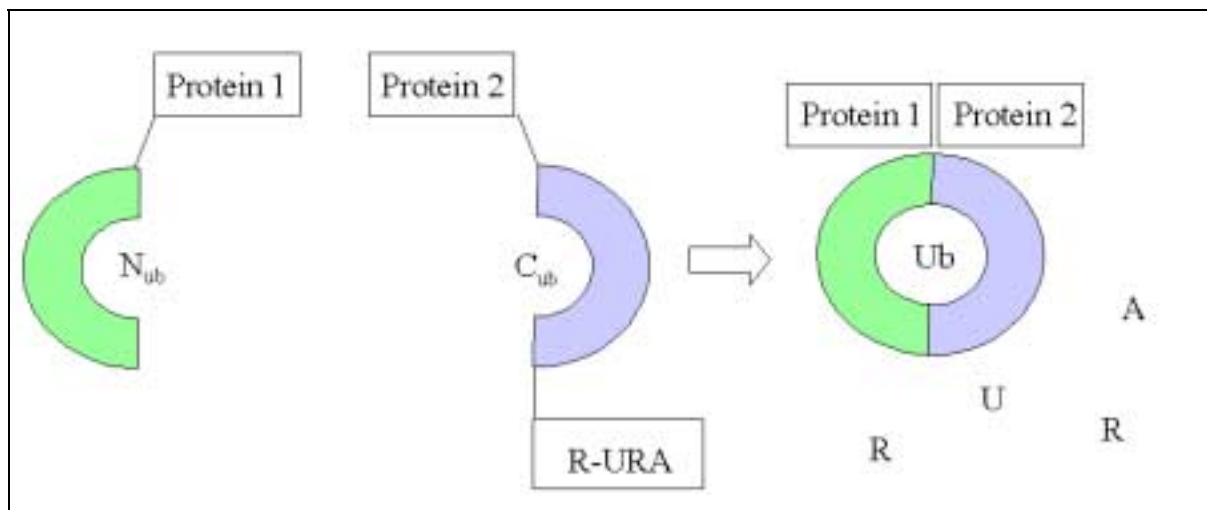


Figure 11: Schematic diagram for the basic mechanism of the split-ubiquitin-system. When protein 1 fused to the N_{ub} fragment interacts with protein 2 fused to the C_{ub} fragment and the R-URA reporter enzyme, a functional ubiquitin (Ub) protein forms. Reconstitution of Ub is detected by cleavage and degradation of the R-URA enzyme.

3.8.1 The use of USPS to detect the interaction of plant proteins

The Arabidopsis proteins ARAC5, a small Rho GTPase, and RhoGAP1 (GAP1), a corresponding GTPase activating protein, were used to demonstrate the possibility of detecting protein interactions using the USPS technique. ARAC5, like most other Rho GTPases, is anchored to the plasma membrane by its C-terminal isoprenyl moiety (reviewed in Valster *et al.*, 2000.). In its active form, ARAC5 is bound to GTP, while in its inactive form it is bound to GDP. The single amino acid exchanges G15V and T20N in the ARAC5 protein sequence are predicted to result in a constitutively active (ARAC5-G15V) and a constitutively inactive form (ARAC5-T20N) of ARAC5, respectively (Zerial and Huber, 1995). GAP1 is a cytosolic protein and binds specifically to the GTP-bound form of ARAC5 (reviewed in Valster *et al.*, 2000).

Using a co-immuno-precipitation assay, GST-GAP1 was shown to interact with recombinant GFP-ARAC5-G15V but not with GFP-ARAC5-WT as present in transgenic plant extracts. It is likely that GFP-ARAC5 WT in these experiments was largely in the GDP-bound form due to intrinsic hydrolysis occurring during the extraction and precipitation procedure, indicating that GAP1 does not bind the GDP bound form of ARAC5 (A. Molendijk, personal communication). In the yeast two hybrid system various GAP1 isoforms have been shown to interact with constitutively active ARAC GTPases (Borg *et al.*, 1999; Wu

et al., 2000). GAP1 specifically co-immuno-precipitates with constitutively active, but not with constitutively inactive ARAC GTPases as expressed in bacteria, confirming a specific interaction between GTP-bound ARAC and GAP1 (Wu *et al.*, 2000). Interestingly, yeast two hybrid screens also revealed an interaction between RLK kinases, interactors that normally only bind the active form of ARAC5, and ARAC5 WT, indicating that internal GDP/GTP exchange factors of yeast cells can activate WT ARAC5 (A. Molendijk, personal communication). For the investigation of ARAC5 and GAP1 interaction in the USPS, a fusion of GAP1 to the C_{ub} fragment and a reporter enzyme was used as a bait, while the fusion of the N_{ub} fragment to the ARAC5 protein was used as a prey.

The USPS GAP1 bait vector

The USPS bait construct (*pC_{ub}*) was based on the *pRS313* ARS/CEN plasmid (see also 2.2.1). It contained a yeast promoter, repressible by methionine (*pMET*), the DNA sequence of the C_{ub} fragment and the DNA sequence of the reporter protein (*R-URA*). The *GAP1* cDNA was introduced between *pMET* and C_{ub}, maintaining the DNA reading frame of C_{ub}-*R-URA*. The resulting plasmid was termed *pGAP1-C_{ub}* (Fig. 12a).

The USPS ARAC5 prey vector

In order to obtain a USPS prey construct, that would be suitable for the introduction of a cDNA library and the subsequent library screening, the original USPS prey construct was modified (see also 2.2.1). The modified USPS prey construct (*pN_{ub}m*) contained a yeast promoter, inducible by Cu²⁺ (*pCU*) and the DNA sequence of the N_{ub} fragment, as well as the DNA sequence of the HA-epitope, an extensive multiple cloning site, and the yeast *ADH* transcriptional terminator (*ADHpA*). *pN_{ub}m* was based on the ARS/CEN plasmid *pRS314* (see also 2.2.1). The cDNAs of *ARAC5*, *ARAC5-G15V* and *ARAC5-T20N* were introduced between the HA-epitope sequence and the *ADHpA* following the N_{ub}-HA reading frame. The resulting plasmids were termed *pN_{ub}m-ARAC5*, *pN_{ub}m-ARAC5-G15V*, and *pN_{ub}m-ARAC5-T20N* (Fig. 12b).

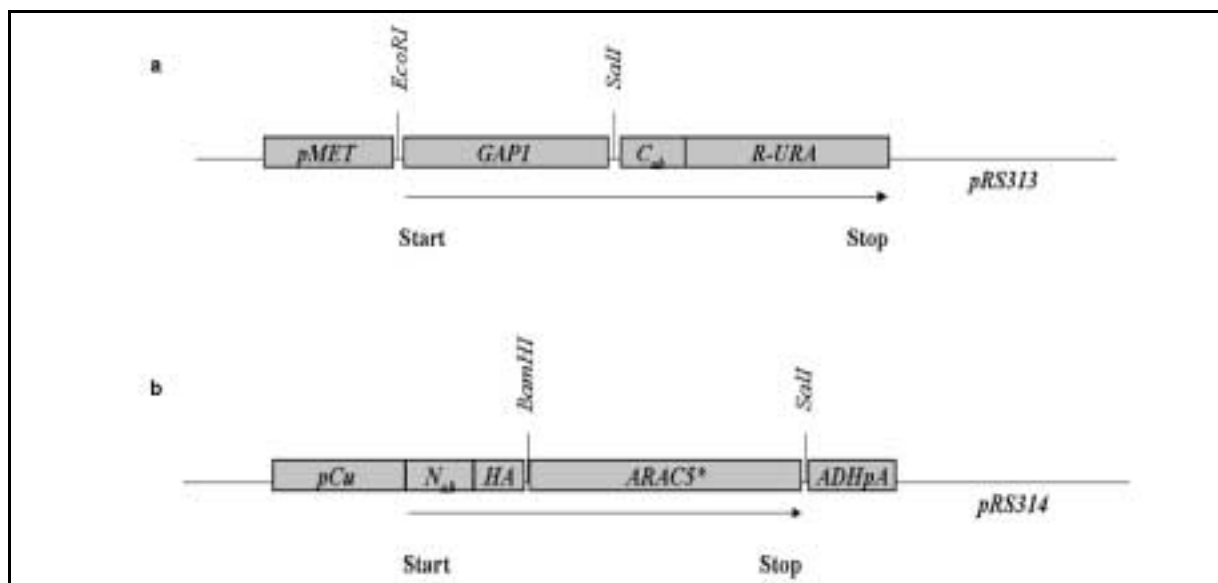


Fig. 12: Schematic diagram of *pGAPI-C_{ub}* and *pN_{ub}m-ARAC5.** a) *pGAPI-C_{ub}* contains a methionine repressible promoter (*pMET*), the *GAPI* cDNA sequence and the sequences coding for the *C_{ub}* fragment and the R-URA reporter enzyme. b) *pN_{ub}m-ARAC5** contains a Cu^{2+} inducible promoter (*pCu*), sequences coding for the *N_{ub}* fragment (*N_{ub}*) and an HA epitop (*HA*), cDNA sequences of *ARAC5* or mutants of *ARAC5* (summarized by *ARAC5**) and an ADH transcriptional terminator (*ADHpA*). Start and Stop mark beginning and end of sequence coding for the translational fusion protein, respectively. Arrows indicate direction of gene transcription. Restriction sites relevant for the construction *pGAPI-C_{ub}* and *pN_{ub}m-ARAC5** are indicated.

Test for interaction of GAPI-C_{ub} and N_{ub}-ARAC5

Yeast cells were cotransformed with the *pGAPI-C_{ub}* construct and with *pN_{ub}m*, *pN_{ub}m-ARAC5*, *pN_{ub}m-ARAC5-G15V* or *pN_{ub}m-ARAC5-T20N*, respectively. Cleavage of the R-URA reporter served as a read out in the USPS interaction assay.

The R-URA reporter is a slightly modified derivative of the enzyme orithidine-5'-phosphate-decarboxylase, involved in the synthesis of the amino acid uracil. In contrast to the naturally occurring uracil synthesising enzyme (URA), R-URA contains an additional arginine residue (R) at its N-terminus. When linked to the *C_{ub}* fragment, R-URA is active and allows the growth of yeasts on medium lacking uracil (ura^-). Cleavage of R-URA due to protein interaction, however, results in rapid degradation of the enzyme, caused by the arginine residue at the now free N-terminus (N-end rule, reviewed in Varshavsky, 1997). Consequently, the ability of yeasts to grow on ura^- medium is lost. The interaction dependent growth phenotype of yeasts is mirror imaged, when ura^- medium is replaced by medium containing the prototoxin 5-FOA (FOA^+). R-URA degrades 5-FOA to 5-fluorouracil, which is toxic for the cell. The rapid degradation of R-URA due to protein interaction, on the other

hand, allows the cells to grow on 5-FOA (FOA^R) (Johnsson and Varshavsky, 1994b). Protein interaction therefore results in the ability of yeasts to grow on FOA⁺ and the inability of yeasts to grow on ura⁻ medium.

Double transformants of yeasts expressing the GAP1-C_{ub}-R-URA fusion and different N_{ub}-ARAC5 fusions, were applied in droplets of three dilutions (10⁵, 10⁴, and 10³ cells/droplet) to ura⁻ and FOA⁺ plates. After incubation at 30°C for two days, the growth phenotypes of the yeast double transformants were determined (growth assays) (Fig. 13). Yeast cells harbouring the GAP1-C_{ub} fusion protein in combination with the empty vector revealed the typical growth pattern for lack of protein interaction in the USPS system: Growth of yeasts on ura⁻ medium and no growth on FOA⁺ medium. A similar growth pattern was obtained for cells expressing the GAP1-C_{ub} fusion protein together with the N_{ub}-ARAC5-T20N fusion protein. Interaction of GAP1 with ARAC5-G15V and to a lesser extent also with WT ARAC5, on the other hand, was reflected by growth of yeasts on FOA⁺ and no growth on ura⁻ plates. The USPS system therefore revealed the interaction between GAP1 and ARAC5-G15V, but not between GAP1 and ARAC5-T20N, confirming results obtained in previous studies with other methods.

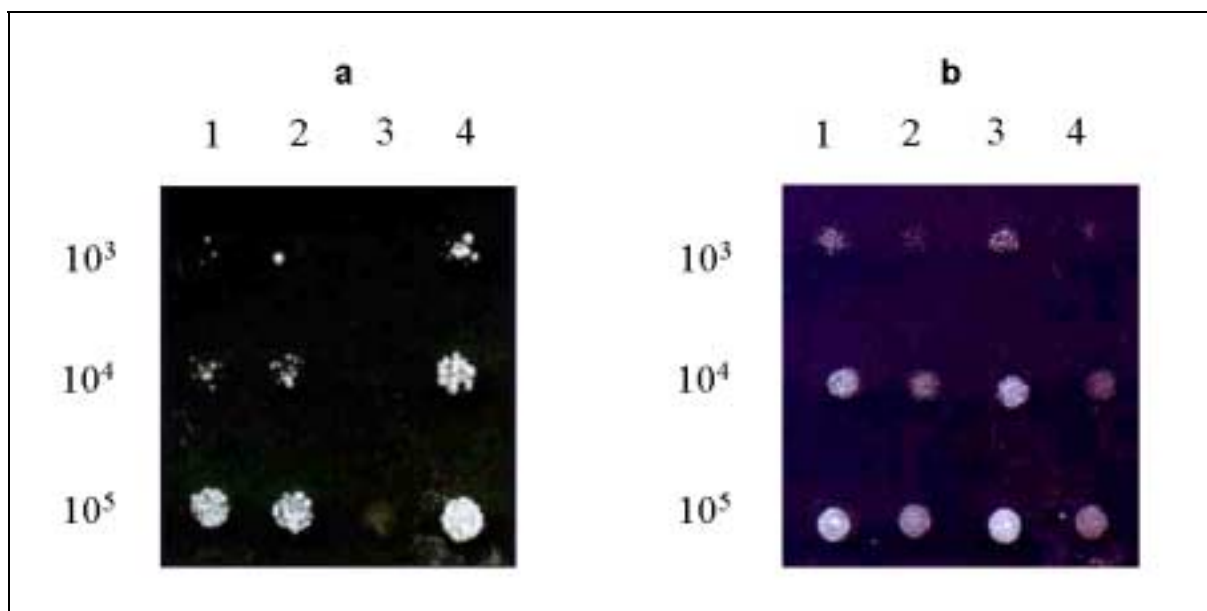


Fig. 13: Growth assays on ura⁻ (a) and FOA⁺ (b) revealed interaction between GAP1 and ARAC5 and GAP1 and ARAC5-G15V. Yeast cells co-expressing the GAP1-C_{ub} fusion protein together with ARAC5 WT (1), ARAC5-T20N (2), ARAC5-G15V (3) as fusions to N_{ub}, and N_{ub} expressed from the empty *pN_{ub}m* vector (4) were applied in three different dilutions (10⁵, 10⁴, and 10³ cells/droplet) on selective media.

3.8.2 The establishment of AtPIN1-C_{ub} as a bait in USPS

The AtPIN1 protein contains a hydrophilic loop in the middle, flanked by five to six transmembrane segments at the N- and C- terminus (Gälweiler *et al.*, 1998). A possible model for the topology of AtPIN1 is depicted in Fig 14. The orientation of the AtPIN1 protein in the membrane and the spatial orientation of the transmembrane domains, however, are not yet known.

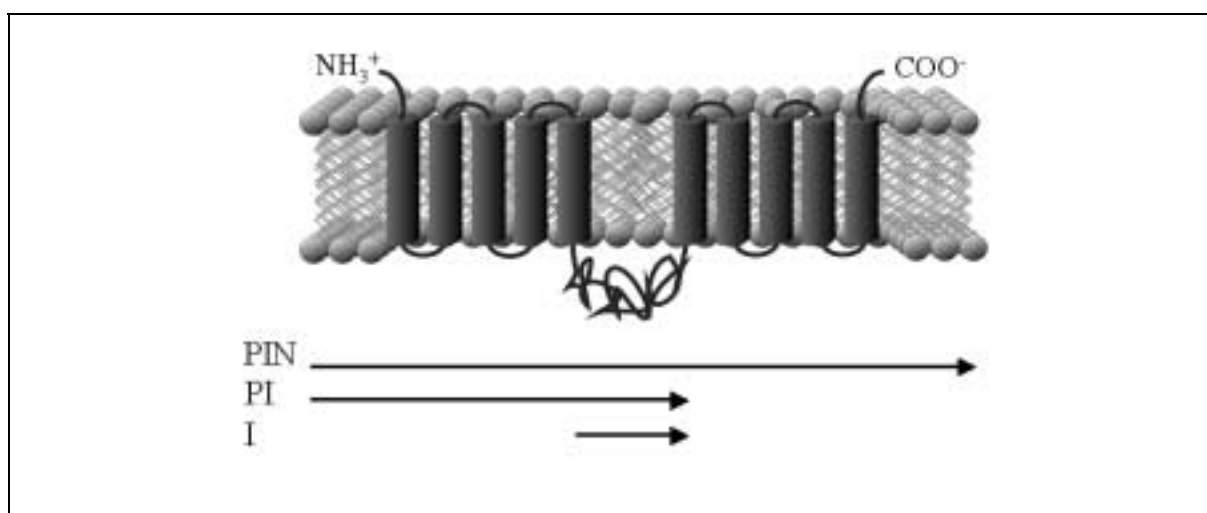


Fig. 14: Putative topology of the AtPIN1 protein. 5 transmembrane segments at N-terminus (NH₃⁺) and C-terminus (COO⁻) of the AtPIN1 are predicted to flank a hydrophilic loop. Arrows termed PIN, PI and I indicate parts of the AtPIN1 protein that are expressed in fusions to C_{ub} from the constructs *pAtPIN1-C_{ub}*, *pAtPII-C_{ub}* and *pAtII-C_{ub}*, respectively.

The USPS AtPIN1 bait vector

The cDNA of AtPIN1 was inserted into the *pC_{ub}* bait vector and the resulting plasmid was termed *pAtPIN1-C_{ub}* (see also 2.2.1). In addition, two different truncated sequences of the AtPIN1 cDNA were cloned into the bait vector: (i) The DNA sequence encoding the N-terminal transmembrane domains and the hydrophilic loop of AtPIN1, resulting in the plasmid *pAtPII-C_{ub}* and (ii) the DNA sequence encoding the hydrophilic loop of AtPIN1, resulting in the plasmid *pAtII-C_{ub}* (Fig. 14) (see also 2.2.1).

Yeast cells were co-transformed with the bait plasmids *pAtPIN1-C_{ub}*, *pAtPII-C_{ub}*, and *pAtII-C_{ub}* in combination with the empty prey vector *pN_{ub}m*. Expression of the protein-C_{ub} fusions was analysed in a Westernblot with protein extracts from yeast cells (Fig. 15). For

detection of the fusion proteins the anti-AtPIN1 antibody, which recognizes the hydrophilic loop of AtPIN1, was used (Gälweiler *et al.*, 1998). AtPIN1-C_{ub}, AtPI1-C_{ub} and AtI1-C_{ub} fusion proteins were detected at the estimated size of 115 kDa, 100 kDa and 82 kDa, respectively.

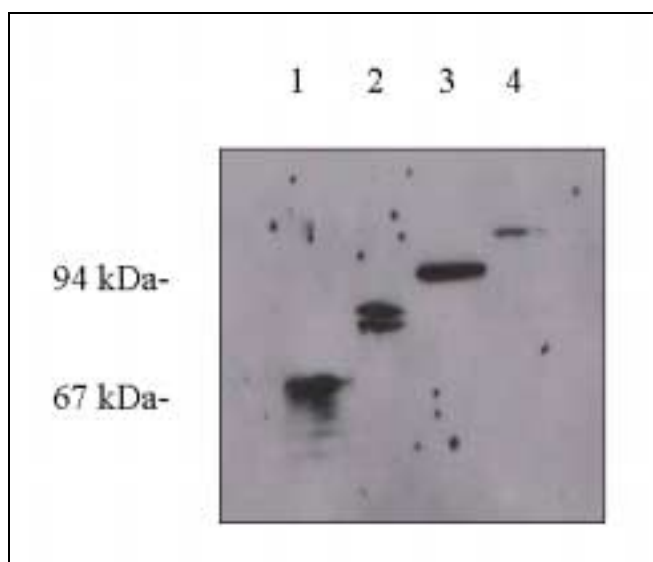


Fig. 15: AtPIN1 and truncated versions of AtPIN1 are expressed as fusions to C_{ub}. Western blot of yeast protein extracts: Expression of AtPIN1 (4), AtPI (3) and AtI (2) as translational fusion proteins with C_{ub}-R-URA, 1) AtPIN1 control protein.

Establishment of optimal screening conditions for the AtPIN1-C_{ub} bait

Screening a cDNA library with the AtPIN1 bait was planned to be performed on FOA⁺ plates. Interaction of a protein derived from a cDNA clone and AtPIN1 would be detected by the ability of yeasts to grow on FOA⁺ (due to R-URA reporter cleavage). The amount of R-URA reporter expressed from the translational fusion of a bait construct, such as *pAtPIN1-Cub* is crucial for the detection of protein interaction during the screening process. Prior to the screening procedure, yeast cells harbouring the bait construct therefore have to be tested for the relative amount of R-URA in the cell: (i) Enough R-URA enzyme has to be produced in order to repress growth of yeasts on FOA, a prerequisite for subsequent screening for FOA^R yeasts. (ii) Too much R-URA enzyme, on the other hand, might mask putative interaction between proteins, i.e. if a substantially greater amount of bait compared to prey is present, there will always be a portion of R-URA enzyme that is not cleaved and therefore degrades FOA to the toxic 5-fluorouracil. Regulation of promoter strength in the *pC_{ub}* construct allows the optimal adjustments of the bait expression level.

The promoter of the pC_{ub} construct is most active without addition of methionine to the yeast growth medium and is repressed by the addition of methionine in a concentration dependent manner. Yeast cells harbouring the $pAtPIN1-C_{ub}$, $pAtPII-C_{ub}$, and $pAtII-C_{ub}$ constructs were therefore streaked on FOA plates without or with methionine (10, 15, 70 μ M) and incubated at 30° C for 2 days. Growth assays revealed, that while plates containing methionine still allowed the growth of yeast cells (data not shown), plates without methionine led to complete repression of yeast growth (Fig. 16). As expected, control streaks on ura^- plates without or with methionine (10, 15, 70 μ M) displayed opposite growth phenotypes, with growth of yeasts only in the absence of methionine (Fig. 16). $pAtPIN1-C_{ub}$, $pAtPII-C_{ub}$, and $pAtII-C_{ub}$ constructs therefore required full promoter strength in order to prevent yeast growth on FOA⁺ and downregulation of *R-URA* expression was not necessary. In the following experiments only $pAtPIN1-C_{ub}$, carrying the entire AtPIN1 cDNA was used as a bait. $pAtPII-C_{ub}$ and $pAtII-C_{ub}$ were used as control plasmids, since a putative interaction partner was isolated using the hydrophilic loop of AtPIN1 in a bait construct of the yeast two hybrid system (L. Gälweiler, personal communication).

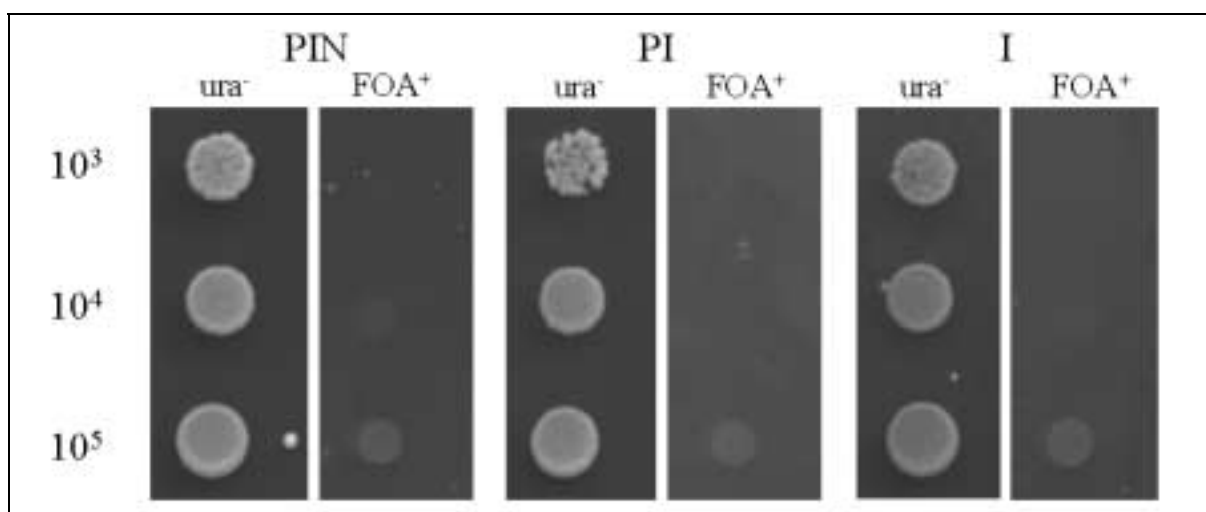


Fig. 16: Growth phenotypes of yeasts carrying $pAtPIN1-C_{ub}$, $pAtPII-C_{ub}$, and $pAtII-C_{ub}$ constructs reflect expression of R-URA reporter. Growth assays on ura^- and FOA⁺ medium without addition of methionine reveal growth phenotypes of $pAtPIN1-C_{ub}$ (PIN), $pAtPII-C_{ub}$ (PI), and $pAtII-C_{ub}$ (I). Yeast cells were applied in three different dilutions (10⁵, 10⁴, and 10³ cells/droplet).

To further test the AtPIN1- C_{ub} bait in the USPS, the interaction of yeast proteins with AtPIN1, as well as the interaction of ARAC5 with AtPIN1 was tested. The *S. cerevisiae* genes *TPH1* and *SSS1* were cloned into the pN_{ubm} vector and the resulting plasmids were termed $pN_{ubm-TPH1}$ and $pN_{ubm-SSS1}$. *TPH1* encodes the cytosolic enzyme triosephosphate-isomerase and *SSS1* encodes a protein that is part of a protein complex that forms an aqueous channel

through which polypeptides are translocated across the ER membrane (Dünnwald *et al.*, 1999). In addition, the N_{ub} fragment in the constructs $pN_{ubm-TPII}$, $pN_{ubm-SSS1}$ and $pN_{ubm-ARAC5}$ was replaced by a mutated N_{uba} fragment, resulting in plasmids termed $pN_{ubam-TPII}$, $pN_{ubam-SSS1}$ and $pN_{ubam-ARAC5}$. Instead of an isoleucine at position 13 of the N_{ub} fragment, N_{uba} contains an alanine, which leads to reduction of N_{uba} affinity to the C_{ub} fragment. N_{uba} and C_{ub} only associate, when the proteins linked to these fragments form a stable protein complex. Unlike WT N_{ub} , N_{uba} therefore does not allow the detection of transient interaction of proteins (Johnsson and Varshawsky, 1994a).

Yeast cells were co-transformed with the prey constructs $pN_{ubm-TPII}$, $pN_{ubm-SSS1}$, $pN_{ubm-ARAC5}$, $pN_{ubam-TPII}$, $pN_{ubam-SSS1}$ and $pN_{ubam-ARAC5}$ in combination with the bait construct $pAtPIN1-C_{ub}$. Yeast cells transformed with bait and prey constructs were applied in droplets of three dilutions (10^5 , 10^4 , and 10^3 cells/droplet) to FOA⁺ plates. After incubation at 30°C for two days, the growth phenotypes of the different yeast double transformants were determined (Fig. 17a). Resistance to FOA revealed the interaction of AtPIN1 with SSS1, when SSS1 was expressed as a fusion to the WT N_{ub} fragment. This is not surprising, since membrane targeting of AtPIN1 requires the transition of the protein through the ER translocation pore. The Nub-SSS1 fusion protein was demonstrated to form a functional complex at the ER translocation pore in yeast cells and interaction with SSS1 was previously observed for other membrane proteins (M. Dünnwald and N. Johnsson, personal communication). Interaction of AtPIN1 with SSS1 as detected in the USPS could therefore be the reflection of close proximity of the proteins during the translocation process. This interpretation is supported by the fact, that interaction between AtPIN1 and SSS1 is lost, when SSS1 is linked to the N_{uba} fragment, which does not allow detection of transient interactions. A control assay revealed the interaction of GAP1- C_{ub} and the N_{uba} -ARAC5-G15V fusion, demonstrating the functionality of N_{uba} (data not shown). No interaction was detected between AtPIN1 and ARAC5 or TPI1.

Gene expression from the prey constructs can be up-regulated by addition of Cu²⁺ to the medium. Such an up-regulation would be favourable for strongly expressed baits or very low level expressed preys. Both cases would mask protein interaction due to a surplus of bait and therefore uncleaved R-URA reporter molecules. Apart from the regulation of bait expression, also regulation of prey expression was investigated. Growth assays on Cu²⁺ containing medium were performed for yeast double transformants containing the AtPIN1 bait and the

ARAC5, TPI1 and SSS1 prey constructs as fusions to either N_{ub} or N_{uba} (17b). Growth of yeasts revealed interaction between AtPIN1 and SSS1, when SSS1 was linked to N_{ub} . In addition, slight interaction was observed for AtPIN1 and TPI1, when TPI1 was linked to N_{ub} . No interaction was observed for ARAC5 and all N_{uba} linked prey proteins. Slight interaction between AtPIN1 and TPI1 under Cu^{2+} induction might indicate an unspecific association of C_{ub} and N_{ub} fragments due to high levels of TPI1 prey in the cell. Indeed, high levels of TPI1 protein were detected in protein extracts of Cu^{2+} treated yeast cells (data not shown).

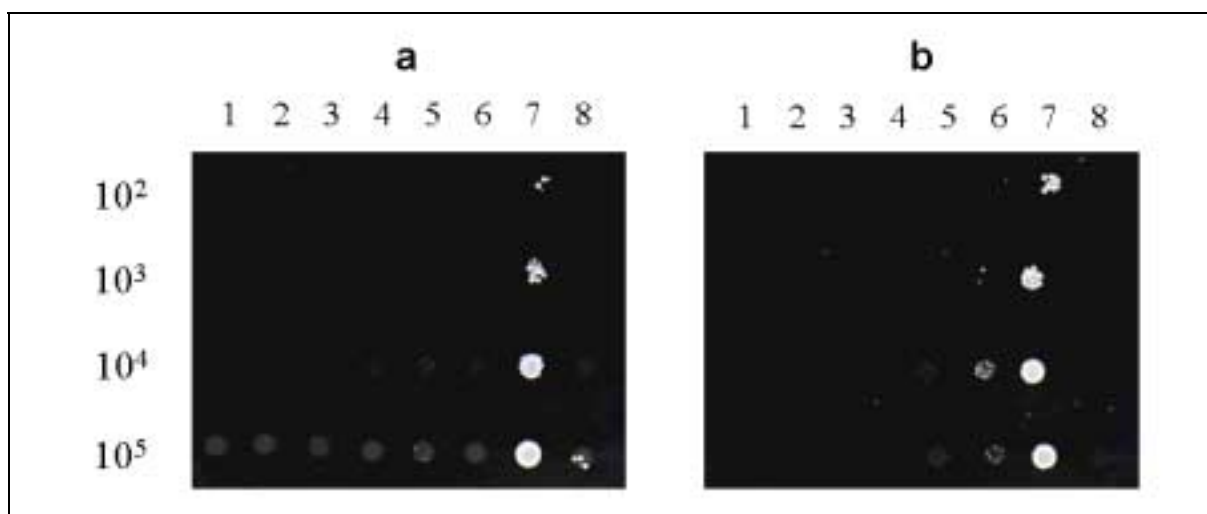


Fig. 17: AtPIN1 interacts with SSS1 on medium without copper and with SSS1 and TIM1 on medium with copper. Growth assays on FOA^+ medium without (a) and with addition of copper (b). Yeast cells were co-transformed with AtPIN1- C_{ub} and with N_{ubm} (8), N_{ubm} -SSS1 (7), N_{ubm} -TIM1 (6), N_{ubm} -ARAC5 (5), N_{uba} m (4), N_{uba} m-SSS1 (3), N_{uba} m-TIM1 (2), and N_{uba} m-ARAC5 (1). Yeast cells were applied in three different dilutions (10^5 , 10^4 , and 10^3 cells/droplet).

These analyses showed that i) AtPIN1 could be used as a bait in USPS if the bait promoter was fully active, i.e. on medium without methionine. ii) FOA^R upon interaction of AtPIN1 and SSS1 linked to N_{ub} indicated, that transient interaction or close proximity of AtPIN1 to another protein could be detected by USPS. iii) Because of the low expression level of the AtPIN1 bait upregulation of prey genes was not required. Therefore we set out for a USPS library screen without addition of methionine and Cu^{2+} .

3.8.3 The construction and cloning of a plant cDNA library for USPS

The construction of the cDNA library involved the isolation of total RNA and subsequently messenger RNA (mRNA) from plant tissues, the reverse transcription of the mRNA into copy DNA (cDNA) and the ligation of the cDNA into the *pN_{ub}m* vector (for details see Materials and Methods). Total RNA was separately isolated from the following *Arabidopsis thaliana* tissues and organs: Suspension culture cells, aerial parts of 4-6 weeks old greenhouse plants and roots of 4 weeks old *in vitro* cultured plants. Equal amounts (in grams) of total RNA from each source were mixed and used for the isolation of mRNA. The mRNA was transcribed into cDNA using the GIBCO BRL SUPERSCRIPT™ Plasmid System. This system results in cDNA with a *NotI* restriction site at the 3' end and cohesive ends for *SallI* at the 5' end. After digestion with *NotI* and separation of the cDNA from linker fragments (size fractionation), the cDNA was ligated to *pN_{ub}m*.

The ligated cDNA library was cloned in *E. coli* cells and positive transformants were selected. Transformation of *E. coli* with the cDNA library yielded 3×10^6 independent clones with a background of 0.39% religated empty vector. In order to preserve the primary transformations, bacterial colonies were aliquoted with 40,000-80,000 clones/aliquot. Each aliquot was separately used for the generation of glycerol stocks and the isolation of plasmid DNA. The size of the cloned cDNA fragments ranged between 0.5-1.2 kb. Sequence analyses of 30 clones from the library revealed no redundancy. One third of the cDNA sequences were in frame fusions with *N_{ub}-HA* (data not shown).

3.8.4 A small scale screen for interaction partners of AtPIN1

Since it was not clear, how many putative positive interaction partners would be obtained from the screening procedure of the cDNA library with the AtPIN1 bait, a test trial for the screening procedure was performed. Yeast cells containing the *pAtPIN1-Cub* bait construct were transformed with 50,000 independent clones of the *pN_{ub}m* cDNA library. Transformed yeast cells were plated on FOA⁺ plates and incubated at 30°C for 3-5 days. Out of 5000 transformed yeast colonies (as evaluated from the transformation efficiency) 10 colonies displayed FOA^R. All of the 10 colonies exhibited growth on FOA⁺ and no growth on ura⁻ plates (data not shown). cDNA inserts of these clones were amplified by PCR and sequences

of the PCR products were analysed. All of the genes were full length with additional sequences at the 5' untranslated region. The size of the PCR products ranged from 300-1000 bp. Start codons were in frame with *Nub-HA* (data not shown). Blast searches in the *Arabidopsis thaliana* data base revealed, that 7 out of 10 clones were identical to a gene that encodes a glycine rich protein of Arabidopsis (384 bp coding region) and 3 out of 10 clones were identical to a gene that encodes an Arabidopsis protein of unknown function (669 bp coding region). The small scale screening procedure therefore led to the isolation of two putative interaction partners of AtPIN1.

4 Discussion

Roots respond to gravity by directional growth toward the center of the earth. Changes in orientation of the gravity vector induce root curvature, eventually resulting in realignment of the root tip to along the new gravity vector. Root curvature is the result of a series of events, including gravity perception, signal formation in gravity perceptive cells and transmission of the signal to the growth response zone where root bending occurs. Auxin has been proposed to control differential cell elongation during root curvature by inhibiting cell elongation at the site of accumulation (Cholodny-Went hypothesis).

Despite correlative evidence for an asymmetric auxin distribution following gravistimulation, little is known about the cell to cell movement of auxin in this process. Recently gravity induced relocation of the AtPIN3 auxin efflux carrier component in columella cells of the Arabidopsis root tip provided new evidence for an important role of lateral polar auxin transport (Friml *et al.*, 2002b). Furthermore, results from different types of experiments suggested that also basipetal auxin transport was essential for a gravitropic response (Rashotte *et al.*, 2000; Young *et al.*, 1990; Young *et al.*, 1996). What are the contributions of these distinct polar auxin transport mechanisms in the establishment of an auxin asymmetry? Is one single transport mechanism required before the other can occur, e.g. does basipetal auxin transport depend on lateral auxin transport? Or do they act independently of each other, by allowing simultaneous lateral auxin transport processes along different regions of the gravistimulated root and in addition basipetal auxin transport to the basis of the root? What are the contributions of efflux and influx carriers to gravity induced auxin redistribution, considering that mutations in genes for either of them caused defects in gravitropic root growth? To start to address these questions and analyze gravity induced auxin flux on a cellular level, we generated a *DR5-GFP* fusion construct and employed it as an auxin biosensor in live cells of Arabidopsis roots.

4.1 *DR5-GFP* as an auxin biosensor

Choosing a GFP variant for the DR5-GFP construct

GFP emits green fluorescence upon excitation with blue or UV light. It is widely used for its unique properties of being an easily detectable *in vivo* reporter protein that does not require exogenous substrates or cofactors. GFP fluorescence can be detected at cellular and even subcellular levels within the tissue. Despite these advantages over other reporter proteins, GFP fluorescence detection depends on the accumulation of a certain number of GFP molecules within the cell. As a result the GFP reporter is generally less sensitive than enzymatic reporters (such as GUS or luciferase) that are capable of amplifying a signal by enzymatic activity of just a few reporter molecules. It is therefore important to choose a GFP variant that best meets all requirements for the given task.

Since the first cloning of *GFP* cDNA from the jellyfish *Aequorea victoria* (Prasher *et al.*, 1992), many modifications have been made to the original DNA sequence. One of the most important was the change of codon usage in a region that was shown to be incorrectly spliced in plants (Haseloff *et al.*, 1997). On the basis of this modified GFP (mGFP), other mutations were introduced and fall within two categories: i) Mutations within the chromophore region S65-Y66-G67, resulting in altered spectral properties and ii) mutations outside the chromophore region, leading to faster protein folding and better protein solubility. Both types of mutations contribute to higher sensitivity of the GFP reporter with respect to mGFP.

For the *DR5-GFP* transcriptional fusion construct, we chose to target GFP to the ER. *DR5-GUS* expression indicated that high expression levels of *DR5-GFP* could be expected in very localized regions, such as the Arabidopsis root tip (Rashotte *et al.*, 2001; Sabatini *et al.*, 1999). It was reported that compartmentalization of GFP counteracts mildly toxic effects that were observed upon high levels of *GFP* expression (Haseloff and Amos, 1995). In addition, restriction of GFP to a defined subcellular compartment could lead more quickly to the accumulation of a detectable amount of GFP molecules, thereby increasing the sensitivity of the *DR5-GFP* reporter. Extensive studies on expression levels and fluorescence intensities of many GFP variants in different subcellular compartments (such as cytoplasm, vacuole, ER, plasma membrane, mitochondria) revealed, that for ER and plasma membrane targeting best results were obtained with GFP-LT (G. Jach, personal communication). On the amino acid-

but not the nucleotide level GFP-LT is identical to EGFP, commercially available from CLONTECH (G. Jach, personal communication). It differs from mGFP in two amino acid exchanges: i) S65T in the chromophore region, conferring better excitation with blue than UV light and ii) F64L outside the chromophore region, improving GFP folding. It is worth noting, that GFP variants containing the S65C chromophore mutation, that results in comparable spectral properties, are not suitable when targeted to ER and plasma membrane. The oxidative state of cysteine most probably leads to loss of fluorescence in these compartments (G. Jach, personal communication).

A common feature of all *GFP* variants is the fact, that chromophore and folding mutations lie, flanked by the restriction sites *MscI* and *SfuI*, within a 450 bp region of the 720 bp complete *GFP* sequence. GFPs with different properties, even GFPs with altered emission spectra such as YFP, CFP or BFP, can therefore be exchanged for each other by simple replacement of the inner *MscI/SfuI* DNA sequence. Using this strategy, a new and strongly fluorescent ER targeted GFP was generated by replacement of the *MscI/SfuI* flanked DNA sequence of mGFP5-ER (Haseloff *et al.*, 1997) by the characteristic *MscI/SfuI* DNA sequence of GFP-LT. The *GFP-LT-ER* DNA sequence was then employed for the construction of the *pDR5-GFP* auxin inducible reporter construct and the subsequent generation of transgenic DR5-GFP Arabidopsis lines.

Relating DR5-GFP expression to endogenous auxin levels of the plant

DR5-GUS fusions were shown to be auxin inducible in transient expression studies with carrot protoplasts (Ulmasov *et al.*, 1997a) as well as in stably transformed tobacco and Arabidopsis plants (Friml *et al.*, 2002a; Mattsson *et al.*, 1999; Sabatini *et al.*, 1999; Ulmasov *et al.*, 1997a). *DR5-GUS* was induced in a concentration dependent manner by only active auxins and 'auxin maxima' as depicted by the *DR5-GUS* element were shown to correlate with direct auxin measurements in Arabidopsis roots (Sabatini *et al.*, 1999).

The results that were obtained with the *DR5-GFP* reporter were comparable to what was previously reported for *GUS*. Similar to *DR5-GUS*, *DR5-GFP* was shown to be induced by exogenously applied IAA in a concentration dependent manner in all tissues of the Arabidopsis seedling. Similar concentrations of exogenously applied IAA were required for

both *DR5-GFP* and *DR5-GUS* expression, indicating that the GFP reporter in this fusion was not less sensitive than GUS. A strong GFP signal was also found in the root tip of Arabidopsis seedlings. In addition, localized GFP signals were detected at the site of lateral and adventitious root initiation, dormant lateral buds and tips of leaves, correlating with sites of elevated auxin levels in these tissues, as previously postulated from bioassays and auxin measurements (Davies, 1995).

However, the reflection of endogenous auxin concentrations is an indirect one and even though *DR5* seemed to be inducible in all tissues of the Arabidopsis seedling, it cannot be excluded that signalling pathways required for *DR5-GFP* expression may change under certain physiological conditions. Also, *DR5-GFP* expression labelled sites of the plant where the concentration of endogenous auxin passed the threshold that is required for detectable induction of the *DR5* promoter. Above this threshold, however, even gradients of relative auxin levels were to a certain extent reflected by different intensities of GFP fluorescence. Another factor that has to be considered, is the nature of the GFP reporter: (i) the time needed for chromophore formation as well as (ii) the time required for GFP degradation. Therefore, changes in auxin distribution could only be detected with a certain delay and detection was most probably restricted to changes that resulted in elevated auxin levels at sites, where previous auxin concentrations were too low to lead to GFP fluorescence. Observation of signal decay faster than the average time of GFP stability, on the other hand, had to be attributed to increased proteolysis in these cells.

Nevertheless, the *DR5-GFP* biosensor is an excellent tool for studying the involvement of auxin during gravitropic root growth. Low basal activity, no tissue preference for inducibility, and detection in live cells on a single cell level offer possibilities in the analysis of auxin changes, that other methods cannot fulfill. Thus, bioassays and auxin measurements by mass spectrometry detect auxin changes in tissues or even organs, but not on a cellular level. Also promoter-*GUS* fusions require tissue disruptive histochemical analyses with the additional disadvantage that signals can often not be related to single cells due to dye diffusion. Furthermore only the GFP reporter allows optical sectioning of plant organs by CLS microscopy to identify staining patterns in tissues underneath the surface layers. An advantage that became obvious in the analysis of auxin treated root tips: Only optical sectioning revealed that IAA, 1-NAA and 2,4-D resulted in different *DR5* induction patterns. An effect, that had never been observed before. Therefore, keeping in mind the limitations of the *DR5-GFP*

reporter, changes in fluorescence patterns will be treated as indirect evidence for changes in auxin accumulation in the following discussion of experimental results.

4.2 Gravity induced asymmetric auxin accumulation in the LRC

Root tips of vertically grown DR5-GFP roots displayed strong fluorescent signals in the cells of the QC, columella initials and mature columella. An auxin 'maximum' in this region was previously reported for *DR5-GUS* and was found to correlate with direct auxin measurements (Sabatini *et al.*, 1999; Swarup *et al.*, 2001). Elevated auxin levels in these cells could be due to an AUX1 mediated import of auxin from the root vasculature into protophloem cells of the proximal root meristem (Swarup *et al.*, 2001). Alternatively, an auxin 'maximum' in the root tip could be the result of an independent site for auxin biosynthesis in the root meristem (K. Ljung, personal communication). Subsequent auxin flux into QC and columella cells of the root tip could then be mediated by the AtPIN4 efflux carrier protein, that was shown to be expressed in the distal root meristem (Friml *et al.*, 2002a).

Changes in GFP signal distribution were observed, when roots were gravistimulated by rotating the plates 135° from the vertical. Apart from GFP fluorescence in QC, columella initial and mature columella cells, signals started to appear in dLRC cells adjacent to columella S2 and S3 on the lower half of the gravistimulated root. As gravistimulation persisted, the entire LRC displayed GFP fluorescence on its lower half. This chronological appearance of GFP signals in the cells of the LRC gave the impression of an auxin 'movement', implicating auxin transport from columella cells to cells of the dLRC and further on to cells of the pLRC. Interestingly, the AtPIN3 auxin efflux carrier protein was shown to be located in columella S2 in an apolar fashion, but was demonstrated to relocate laterally upon gravistimulation (Friml *et al.*, 2002b). Gravity induced lateral auxin transport from columella S2 to the cells of the dLRC via AtPIN3 is therefore likely.

Further basipetal auxin transport from dLRC to pLRC could be mediated by auxin influx and efflux carrier proteins, AUX1 and AtPIN2, respectively. Both proteins were shown to be expressed in cells of the pLRC, with AtPIN2 being polarly localized at the basal end of LRC cells (Müller *et al.*, 1998, P. Wolff personal communication). Longer gravistimulation (for up to 24 hrs) led to an increase in fluorescence intensity in the LRC, but additional signals in

epidermis or other tissues of the distal and central elongation zone (DEZ, CEZ), where AUX1 and AtPIN2 are also expressed, were not observed. This was in contrast to earlier results obtained with radiolabelled IAA (IAA*) and promoter-*GUS* fusions, such as *SAUR-GUS* and *AtIAA-GUS*, where gravity induced asymmetric auxin distribution on the lower half of the root was detected, but IAA* or GUS staining patterns extended to the elongation zone at the site of root bending (Li *et al.*, 1991; Luschnig *et al.*, 1998; Rashotte *et al.*, 2001; Young *et al.*, 1990). Similar experiments with the *DR5-GUS* reporter, however, revealed GUS staining patterns exclusively in the LRC and not in the epidermis of the elongation zone (Rashotte *et al.*, 2001, P. Wolff personal communication), identical to what was observed for *DR5-GFP*. Therefore either (i) there was no transport of auxin to the elongation zone and retardation of cell elongation at the site of root bending was due to other (auxin induced) signals, such as e.g. calcium, or (ii) auxin transport to the elongation zone occurred, but auxin levels in this region were below *DR5-GFP* (and *DR5-GUS*) detection. The latter explanation seems to be more likely, because in the presence of exogenous 1-NAA application, gravity induced asymmetric GFP staining of epidermal cells was actually observed in the root elongation zone.

In order to demonstrate auxin as a signal linking gravity perception and curvature response earlier time periods in the range of 5 min, the time when amyloplasts sediment (MacCleery and Kiss, 1999), and approximately 20 min, the average latent period of manually rotated *Arabidopsis* roots before gravitropic curvature is first detectable (Mullen *et al.*, 2000), were investigated. The GFP reporter, however, was shown to exhibit a lag time of at least one and a half hours between *GFP* gene expression and detection of GFP fluorescence. Roots were therefore exposed to short-term gravistimulation and subsequently rotated back to the vertical for 3 hrs. This allowed detection of asymmetric signal distribution after 15 min of stimulation (data not shown).

When root bending was complete (after around 24 hours), asymmetric GFP fluorescence in the LRC on one half of the root faded within a few hours. This suggests increased protein degradation in the ER of these cells, since GFP has been reported to be stable for several days (Deichsel *et al.*, 1999) In addition, signal decrease indicates decay of auxin levels after establishment of the new position in the gravitational field. Interestingly, when root bending seemed to be complete, in some cases, staining of the LRC on the other side, opposite to the previously applied gravity stimulus was observed (data not shown). In these cases CLS

microscopy revealed, that root tips seemed to have oriented away from the new gravity vector in a way, that suggested a kind of ‘surplus bending’ of the root. This was in accordance with previous reports, in which roots were described to undergo root bending by first curving to an angle that was larger than the original angle used for gravistimulation and consequently had to ‘correct’ this angle, by an additional slight backward bending (Ishikawa and Evans, 1993). GFP signals appearing on the LRC side opposite to the direction of the previously applied gravity vector, could be a reflection of auxin induced backward bending before final growth along the new gravity vector.

4.3 The role of polar auxin transport in gravity induced asymmetric auxin accumulation

Two lines of evidence previously showed the importance of polar auxin transport during root gravitropism: (i) the analysis of the agravitropic *Atpin2/eir1-1* and *aux1* mutant phenotypes, as well as (ii) the observation, that inhibitors of polar auxin transport resulted in abolishment of gravitropic root growth (see also 1.2). Investigation of *DR5-GFP* expression pattern in the *Atpin2/eir1-1* mutant background as well as auxin efflux and influx blocker treatments demonstrated impaired auxin flux and allowed the identification of the cells to which auxin transport was hindered. Further analysis of *DR5-GFP* expression in roots treated with auxin and data of root curvature kinetics, revealed the different contributions of efflux and influx mediated auxin transport during root gravitropism.

The importance of auxin efflux

Treatments with NPA and TIBA resulted in altered ‘auxin maxima’ in vertically grown roots. GFP distribution shifted towards the base of the root, with a signal decrease in cells of the columella S2 and S3 and additional appearance of signals in endodermis, cortex and vascular initials. A similar pattern was observed with *DR5-GUS* upon NPA treatment (Sabatini *et al.*, 1999), as well as in the background of the *Atpin4* mutant (Friml *et al.*, 2002a). BFA, an inhibitor of vesicle trafficking, that was shown to prevent polar localization of auxin efflux carrier protein AtPIN1 and other membrane proteins (Geldner *et al.*, 2001), had a similar, however less pronounced, effect on fluorescence pattern in vertically grown roots. This shift

in GFP distribution could be due to an inhibition of AtPIN4 dependent auxin flux from the proximal to the distal root meristem, leading to auxin depletion in the distal most root apex. When roots grown on NPA, TIBA and BFA were gravistimulated, no shift in fluorescence pattern was observed, even after 20 hrs of gravistimulation, and root curvature was strongly reduced. As expected, these substances effected auxin efflux in all parts of the root and inhibited the transport of auxin into the distal root meristem, as well as the transport of auxin from columella cells to the cells of the dLRC.

A different fluorescence pattern was found in the background of the *Atpin2/eir1-1* mutant. AtPIN2 was shown to be localized on the basal side of the plasma membrane in cells of the pLRC, as well as in epidermis and cortex cells of the root elongation zone (Refs, see also 1.2). Loss of AtPIN2 activity led to defects in basipetal auxin transport and agravitropic root growth (Chen *et al.*, 1998a; Luschnig *et al.*, 1998; Müller *et al.*, 1998; Rashotte *et al.*, 2000; Utsuno *et al.*, 1998). Indeed, GFP distribution in the root apex of these mutants, was found not only in QC, columella initials and mature columella cells, but also in the cells of the dLRC on both sides of the root axis, indicating impaired auxin transport from dLRC to pLRC cells. Accumulation of auxin in dLRC of the entire root cylinder indicates that there is a constant and even lateral flow of auxin from columella cells to the dLRC, which in the case of *pin2/eir1-1* mutants cannot be compensated by efficient basipetal transport from this region. Elevated levels of free IAA in root tips of *Atpin2/eir1-1* seedlings compared to WT plants correlated with the enlarged *DR5-GFP* expression pattern.

Further evidence for the efflux mediated auxin transport in response to gravity came from experiments with auxin treated, gravistimulated roots. 1-NAA, 2,4-D and IAA, substrates for either efflux or influx carriers or both, were exogenously applied to roots and GFP fluorescence pattern was investigated before and after gravistimulation. Signal distribution for these auxins in vertically grown roots was different, with 2,4-D causing GFP expression in virtually all tissues of the root tip, and IAA and 1-NAA leading to selective staining of dLRC and pLRC, as well as the epidermis cell layer. These variations in staining pattern were due to different transport characteristics of these auxins and not to different sensitivity of the DR5 element, as could be shown by combined treatments of auxins and auxin transport inhibitors. Gravistimulation under continuous supply of auxin revealed, that fluorescence patterns in 2,4-D treated roots remained identical to 2,4-D treated vertical controls, while GFP distribution in 1-NAA treatments and to a lesser extent in IAA treatments, shifted to the lower half on the

gravistimulated roots. Root curvature experiments demonstrated that the extent of auxin asymmetry in these experiments correlated with the degree of root bending: (i) Roots grown on 1-NAA displayed asymmetric auxin distribution in the entire LRC and elongation zone and exhibited strong gravitropic bending, while (ii) roots grown on 2,4-D displayed no and (iii) roots kept on IAA only reduced auxin asymmetry and root bending. Hence, gravity induced auxin transport to the lower half of the root was not confined to endogenous auxin, but also occurred for exogenously applied auxins, provided the auxin was a substrate for the efflux carrier. Furthermore these results suggest, that root curvature does not depend on absolute auxin levels at one half of the root, but rather on the proportion of auxin levels on the upper to that on the lower half of the root.

The importance of auxin influx

Not only mutants with defects in auxin efflux carrier activity, but also a mutant with defect in auxin influx carrier activity (*aux1*) exhibits agravitropic phenotypes (Bennett *et al.*, 1996). The effect of 1-NOA, an inhibitor of auxin influx, on *DR5-GFP* expression and root gravitropism was tested. In vertically grown roots treated with 1-NOA, *GFP* expression pattern was nearly identical to that of untreated controls, except for an increase in fluorescence intensity of signals in the QC and columella initials. Increased auxin levels in cells of the QC and columella initials, could be due to impaired auxin influx from these cells into cells of columella S1, where AUX1 was shown to be located (Swarup *et al.*, 2001).

Upon gravistimulation, root curvature at the application of 50 μ M 1-NOA was almost completely abolished. Under this and also lower concentrations of 1-NOA, strong asymmetric signal distribution in the cells of the dLRC was detected after 24 hrs. Cells of the pLRC were not stained at all. Fainter signals in dLRC compared to untreated controls 5 hrs after gravistimulation were observed and might be due to decreased auxin levels in columella cells, as a consequence of reduced acropetal AUX1 mediated auxin transport (data not shown). High concentration of auxin in the dLRC 24 hrs after gravistimulation indicates, that influx carrier activity is not needed for a lateral auxin transport from columella cells to the dLRC. Further, basipetal auxin transport from the dLRC to the pLRC, however, does require auxin influx carrier activity, correlating with AUX1 localization in pLRC cells (Swarup *et al.*, 2001).

Results obtained with the *DR5-GFP* auxin biosensor showed that, as proposed by the Cholodny-Went hypothesis, gravity induced root curvature does indeed go along with an auxin accumulation on the lower half of the gravistimulated root. Gravity induced auxin flow on the lower half of the root occurs in the root tip and involves efflux mediated lateral auxin transport in cells of the root columella and efflux as well as influx dependent basipetal auxin transport in LRC and epidermis cells. The transport of auxin from columella to dLRC cells might be mediated by relocation of AtPIN3 auxin efflux carrier protein in columella cells and loss of AtPIN3 activity was shown to result in a delay of graviresponse (Friml *et al.*, 2002b, M. Evans, personal communication). Other members of the AtPIN protein family, recently shown to be located in the root tip (I. Paponov, personal communication), may additionally be involved in the fine tuning of this process.

Basipetal auxin transport from dLRC to pLRC is dependent on activity of the AtPIN2 auxin efflux carrier protein and supported by activity of auxin influx carrier, possibly AUX1. Localisation of AtPIN2 and AUX1 proteins in the pLRC suggests, that the accumulation of auxin in the dLRC of the *Atpin2/eir1-1* mutant and in 1-NOA treated roots was the result of block of auxin transport in these cells. Moreover localisation of AtPIN2 and AUX1 in epidermis cells of the elongation zone indicates, that auxin flow from the pLRC to the site of root bending is also mediated by these proteins. *DR5-GFP* expression revealed auxin flux to the elongation zone only at elevated auxin levels, in the presence of 1-NAA.

Analysis of the *Atpin2/eir1-1* mutant as well as root curvature measurements of 1-NOA treated roots together with other data recent data (Rashotte *et al.*, 2000) revealed, that functional basipetal auxin transport is required for root gravitropism. But in addition, these results demonstrate that basipetal auxin transport is dependent on lateral auxin redistribution in the root tip, as could be seen from (i) the flux of auxin to the dLRC and subsequently to the pLRC of gravistimulated roots, (ii) the inhibition of this flux in the presence of NPA application and (iii) the accumulation of auxin in the dLRC upon inhibition of basipetal auxin transport.

4.4 A preliminary model for Arabidopsis root gravitropism and its regulation

According to the current view on gravity induced root curvature, physically distinct regions within the Arabidopsis root participate in sensing of and responding to a gravity stimulus. Thus, columella cells at the root apex were shown to be primarily involved in gravity perception, while cells in the root elongation zone were found to perform the bending response. The work presented here, provides strong evidence, that gravity induced flows of auxin from columella cells to the elongation zone serve as the messenger that connects the sites of gravity perception and growth response. So how can this information be combined with existing data on the regulation of gravity perception and induction of root curvature?

Gravity induced flow of auxin along the lower half of the root was shown to commence in dLRC cells and proceed through the entire LRC to the elongation zone. Auxin signals in dLRC cells were first observed in cells adjacent to columella S2, indicating that export of auxin following gravistimulation initiated from S2 cells. The importance of root columella cells for gravity perception and early signal formation was demonstrated before, when laser ablation of columella cells was shown to inhibit root curvature (Blancaflor *et al.*, 1998). Ablation of defined groups of cells revealed that among other stories, removal of columella S2 resulted in strongest reduction of root curvature. Moreover, the auxin efflux carrier protein AtPIN3 is located in cells of columella S2 and was demonstrated to relocate laterally upon gravistimulation. This lateral relocation corresponds with the observed flow of auxin to the dLRC and the fact, that this flow is efflux carrier dependent

But how is the regulation of subcellular localization of AtPIN3 connected with the positional information provided by amyloplast sedimentation? It has been proposed that sedimentation of statoliths is either directly sensed by membrane structures within the cell, or indirectly via interaction with the cytoskeleton (reviewed in Chen *et al.*, 1999). Recently it was discussed that statolith sedimentation locally disrupts the actin cytoskeleton, which leads to changes in tensions that act on receptors in different plasma membrane regions (Yoder *et al.*, 2001). A receptor protein perceiving the gravity stimulus has not been identified. However, stretch sensitive receptors, such as stretch activated ion channels or receptors triggering the activation of the H⁺-ATPase could be imagined to be involved in this process. In fact, an increase of apoplastic- and a decrease of cytoplasmic pH in columella cells was reported to occur two minutes after gravistimulation (Fasano *et al.*, 2001; Scott and Allen,

1999). Such changes in pH could directly or indirectly effect AtPIN3 activity. The mechanisms for a pH mediated regulation are not known but might involve pH dependent control of endo- and exocytosis, as has been reported to occur in animal cells (Cosson *et al.*, 1989; Gluck *et al.*, 1982). Membrane localization of AtPIN3 and other AtPIN proteins was shown to be controlled by highly dynamic vesicle trafficking, involving endo- and exocytosis processes (Geldner *et al.*, 2001) This is particularly interesting in the context of gravity induced change of AtPIN3 relocation and implies that dynamic cycling allows a tight control of direction and velocity of AtPIN3 protein targeting and consequently the direction of auxin flow.

Once auxin flow from columella cells to dLRC cells was induced, auxin was transported from dLRC to proximal LRC cells and further to the elongation zone. This basipetal transport of auxin required auxin influx as well as auxin efflux carrier activity, possibly mediated by AUX1 and AtPIN2, respectively. Basipetal auxin transport was demonstrated to be essential for root gravitropism (Rashotte *et al.*, 2000) and was shown to be influenced by reversible protein phosphorylation events (Rashotte *et al.*, 2001). Thus, mutants with defects in RCN1, a regulatory subunit of the protein phosphatase 2A (PP2A), displayed agravitropic root growth and an increased rate of basipetal auxin transport (Deruere *et al.*, 1999; Rashotte *et al.*, 2001). *DR5-GUS* expression in *rcn1* mutants revealed, that unlike WT plants, *rcn1* mutants do not exhibit asymmetric auxin distribution along the lower half of gravistimulated roots. Increased basipetal auxin transport was proposed to be responsible for this effect, by preventing asymmetric auxin accumulation due to immediate removal of auxin from this region. Data presented in this thesis allow to raise an alternative explanation for this observation: Impaired lateral auxin transport possibly by inhibition of AtPIN3 activity/relocation might in fact (additionally) be responsible for loss of asymmetric auxin accumulation in gravistimulated *rcn1* roots. Other evidence for the regulation of polar auxin transport by protein phosphorylation and dephosphorylation events has come from the analysis of plants overexpressing the serine threonine protein kinase PID. *35S-PID* plants exhibit severe defects in the root meristem. and roots of hemizygous *35S-PID* seedlings display agravitropic phenotypes (Christensen *et al.*, 2000). Moreover, the broad spectrum kinase inhibitor staurosporine was shown to inhibit auxin efflux (Delbarre *et al.*, 1998).

Evidence for another possible regulatory mechanism acting on AtPIN proteins, came from the analysis of agravitropic *axr1* mutants. The AXR1 protein is related to the N-terminal half

of the ubiquitin activating enzyme E1 and is thought to be involved in the auxin induced degradation of repressors of the auxin response. The analyses of WT and *axr1* plants carrying a translational fusion of the entire AtPIN2 genomic coding region fused to the amino terminus of the β -glucuronidase reporter gene revealed auxin dependent changes in expression pattern. While in WT seedlings, the construct was unstable in response to changes in auxin homeostasis (Sieberer *et al.*, 2000), the construct became stabilized in the *axr1* background. Proteolytic degradation of AtPIN2 via activation of AXR1 could therefore be essential for the establishment of an auxin gradient in response to the gravitropic stimulus.

Finally, the question remains, as to how asymmetric auxin distribution mediates differential growth in the elongation zone. In roots, increased auxin levels are known to decrease cell elongation (Ishikawa and Evans, 1993). Auxin accumulation in DEZ and CEZ along the lower half of the root might therefore inhibit root growth in this region. Measurements on root curvature, however, revealed, that in addition to inhibition of cell elongation in DEZ and CEZ on the lower half of the root, initiation of cell elongation in DEZ on the upper half of the root occurs during root curvature (Mullen *et al.*, 1998). The initiation of cell elongation in this region could possibly be the result of gravity induced decreased auxin levels on the upper flank of the root. Lower auxin concentrations promote cell elongation in roots, by acting on gene expression and inducing ionic and metabolic changes that stimulate growth and loosen the cell wall (reviewed in Cosgrove, 1997). Decrease of fluorescence activity on the upper half of gravistimulated roots in the presence of 1-NAA indicated a gravity induced decrease of relative auxin levels on the upper half of the root. Alternatively other signaling mechanisms might be involved in the induction of cell elongation in this region. Thus, calcium oscillations were observed in the elongation zone during gravitropic root growth and application of calcium in the DEZ was shown to promote root curvature (Bjorkman and Cleland, 1991; Ishikawa and Evans, 1992; Lee and Evans, 1985). Evidence suggests, that calcium and auxin signaling processes must be tightly linked, since root gravitropism is inactivated upon the application of calcium chelators, as well as upon inhibition of polar auxin transport (Bjorkman and Cleland, 1991; Rashotte *et al.*, 2000). Similarly gravity induced changes in electric currents along the site of root elongation, that were proposed to be the reflection of proton movements (Behrens *et al.*, 1985), might either activate auxin gradients or in turn be activated by auxin gradients.

4.5 The split-ubiquitin-system as a method to find interaction partners of AtPIN1

An important aspect of differential regulation of polar auxin transport lies in the understanding of AtPIN protein regulation. The identification of proteins that interact with AtPIN proteins is therefore of specific interest. Candidates for AtPIN protein interaction may include (plasma membrane) proteins that participate in the formation of an efflux carrier complex, proteins that link AtPIN1 to the cytoskeleton and regulate AtPIN protein cycling and (polar) localization, and regulatory proteins, that are part of the cellular signaling network. Interactions may be stable and result in the formation of multi-protein complexes, or transient, as could be expected for an interaction with regulatory proteins.

The split-ubiquitin-system (USPS) was used as a technique for searching interaction partners of AtPIN1. Unlike the yeast two hybrid system, that has been successfully used for the isolation of binding partners, screening with the USPS is not limited to the analysis of soluble proteins or soluble domains of membrane proteins. This is of particular interest in the case of AtPIN proteins, since N- and C- terminal membrane spanning domains, but not the hydrophilic loop, are highly conserved among members of the AtPIN family (Friml *et al.*, 2002a; Friml *et al.*, 2002b; Gälweiler *et al.*, 1998; Müller *et al.*, 1998). A common mechanism for AtPIN regulation might therefore act on these domains.

In a three step approach the screening of a cDNA library with the AtPIN1 bait was prepared: (i) The interaction of two plant proteins, the membrane associated small GTPase ARAC5 and the cytosolic GTPase activating protein GAP1 was demonstrated with the USPS technique. (ii) The *AtPIN1* gene was cloned into a USPS bait vector and AtPIN1 protein expression and possible unspecific interaction with ARAC5 and yeast control proteins was tested. (iii) A cDNA library was constructed, introduced into a USPS prey vector and an aliquot of this library was screened for interaction partners of AtPIN1.

As a reporter for detection of protein interaction, the R-URA enzyme was used. R-URA was attached to the C-terminus of the bait-C_{ub} construct. Protein interaction, as demonstrated between GAP1 and ARAC5, led to cleavage and degradation of the R-URA enzyme and resulted in the ability of yeasts to grow on FOA⁺. The growth phenotype on FOA⁺ was opposite to that what we obtained on ura⁻ medium, thereby allowing the investigation of R-URA enzyme activity by two physiologically distinct mechanisms. When bait constructs, such as GAP1-Cub and AtPIN1-Cub were co-expressed with the WT Nub fragment (from the

empty *pN_{ubm}* vector) in yeast cells, no protein interaction was detected. This was in contrast to results obtained with the transcriptional activator PLV, another reporter used in USPS, that detected the association of C_{ub} with WT N_{ub} fragments independent of protein-protein contacts (Stagljar *et al.*, 1998, N. Johnsson, personal communication). Detection of protein interaction by R-URA therefore was more stringent than detection by PLV and allowed the use of WT N_{ub} fragment for the screening procedure.

Besides the detection of stable protein interactions, the WT N_{ub} fragment was reported to detect transient (short lived) protein interactions and close spatial proximity of proteins (Johnsson and Varshavsky, 1994a). The N_{uba} fragment, mutated for decreased affinity to C_{ub}, on the other hand, exclusively reveals the stable interaction between proteins (Johnsson and Varshavsky, 1994a). This was also observed when AtPIN1 interaction with other proteins, such as ARAC5 and the yeast proteins SSS1 and TPI1 was tested. When fused to the N_{uba} fragment, none of the proteins revealed interaction with AtPIN1. When linked to the WT N_{ub} fragment, on the other hand, interaction between AtPIN1 and SSS1, a protein of the ER translocation pore in yeasts, was observed.

The interaction between AtPIN1 and SSS1 possibly revealed the spatial proximity of the proteins during AtPIN1 translocation across the ER membrane. In plant cells, AtPIN1 is targeted via the ER to the plasma membrane and the transport of AtPIN1 to the ER would also be expected in yeast. If and how many AtPIN1 proteins then actually reach the plasma membrane of yeast cells is not known. Attempts to analyze AtPIN1 localization in yeasts included the expression of an *AtPIN1-GFP* fusion in the *pC_{ub}* construct (data not shown). GFP fluorescence, however, could not be detected, which might have been the result of low expression level of *AtPIN1-GFP*. Immunolocalization experiments of yeasts with the anti-AtPIN1 antibody may help to identify the site of AtPIN1 localization in yeast.

For screening of AtPIN1 interaction partners, a cDNA library from tissues of Arabidopsis whole plants and suspension culture cells, where *AtPIN1* was known to be expressed (Friml *et al.*, 2002a; Gälweiler *et al.*, 1998, L. Gälweiler, personal communication), was generated. The cDNA library was cloned into the *pN_{ubm}* vector as a fusion to DNA sequences encoding for the N_{ub} fragment and an HA-epitope. The HA epitope was introduced into the prey vector in order to facilitate subsequent biochemical analyses of protein interaction between AtPIN1 and putative candidates that would be identified in the screening procedure.

Prior to the screening of the cDNA library with the AtPIN1 bait, gene expression from bait and prey promoters was regulated. This is essential, since the USPS readout depends on the proportion of cleaved and uncleaved reporter enzyme in the cell. The ideal case would be, if there was no cleaved R-URA reporter in the absence of protein interaction and no uncleaved reporter in the presence of protein interaction. Since reporter cleavage depends on the interaction of bait and prey proteins, the amount of bait and prey in the cell influences the proportion of cleaved and uncleaved reporter enzyme: (i) An excess of bait molecules compared to prey molecules results in uncleaved R-URA reporter, despite protein interaction and prevents detection of protein interaction. (ii) An excess of prey molecules compared to bait molecules, on the other hand, is generally less disturbing, but may lead to detection of unspecific protein interaction (i.e. detection of close proximity due to saturation of the cell with N_{ub} molecules). It is therefore important to adjust the amount of bait and thus R-URA reporter in the cell: (i) Enough R-URA molecules have to be produced in order to confer sensitivity of yeast cells to FOA in the absence of protein interaction. (ii) The amount of R-URA enzyme, however, should not be too high in order to allow detection of protein interaction. Since the promoter of the bait constructs is repressible by methionine, yeast cells harboring AtPIN1 and GAP1 baits were grown on medium containing different concentrations of methionine. The highest possible concentration of methionine (i.e. the strongest repression of the bait promoter) that still allowed the growth of yeasts on ura⁻ medium, but that prevented growth of yeasts on FOA⁺ medium, was selected for use during the interaction/screening growth assay. In the case of AtPIN1, protein expression was low and required full promoter strength (i.e. growth in the absence of methionine). In the case of GAP1, protein expression was slightly higher, than in the case of AtPIN1 and required addition of 25 μ M methionine to the medium (data not shown). Concerning expression of the prey constructs, up-regulation of prey gene expression by addition of Cu²⁺ is only necessary, if the expression of bait genes is very high. This was not the case for AtPIN1 and GAP1 and growth assays with these baits were therefore performed on medium without addition of Cu²⁺.

In order to get an idea for the amount of putative interaction partners obtained in the screening of a cDNA library with the AtPIN1 bait, a test trial for the screening procedure was performed. The test trial involved the transformation of yeast cells, that contained the AtPIN1 bait, with an aliquot of the cDNA library in the prey construct. Selection of 5,000 transformed yeasts on FOA⁺ led to the isolation of two different putative interaction partners of AtPIN1. This was more than ten times more than what was reported for a USPS screen for interaction

partners of yeast transcription factors using a genomic library of yeasts (Laser *et al.*, 2000). Screening a larger amount of transformed yeast cells, e.g. 50,000-100,000 as was reported for other screens (Laser *et al.*, 2000) with AtPIN1 would therefore approximately yield 20-40 different FOA^R clones. Taking further into consideration that an upscale of the yeast screen would involve the use of the entire plant cDNA library, the isolation of more than 40 different clones can be expected.

Blast search of the Arabidopsis data base revealed that from the two different clones isolated in the pre-screening procedure, one contained a gene, encoding an Arabidopsis protein of unknown function and the other contained a gene, encoding an Arabidopsis protein of the family of glycine rich proteins. This gene was represented seven times among the FOA^R clones.

The existence of glycine rich proteins (GRPs) has been reported for a number of species from bacteria, animals and plants (reviewed in Sachetto-Martins *et al.*, 2000). The common feature among all different GRPs is the presence of glycine repeat domains which organize into loops and may constitute the basis for protein-protein interactions or for subcellular compartment association. The function of GRPs is not yet known, but their diversity in structure, gene expression pattern and subcellular protein localization indicates that GRPs represent a diverse and not necessarily related set of proteins (reviewed in Sachetto-Martins *et al.*, 2000). Among the multiple functions in which GRPs of plants were proposed to be involved, the following are particularly interesting in the light of a putative interaction with AtPIN1: (i) Some GRPs were found to be cell wall attached, where they are proposed to act as ligand attachment regions. Interaction of AtGRP-3 with a cell wall associated kinase was recently demonstrated (Park *et al.*, 2001). (ii) Other reports suggest a role of GRPs as linkers between the cell wall and the intercellular compartment by mediating membrane-cytoskeleton or membrane-cell wall interconnection (Marty *et al.*, 1996; Sachetto-Martins *et al.*, 2000). These GRPs were also suggested to be involved in vesicle trafficking and internal cellular transport due to their amino acid similarity to animal vesicle associated membrane proteins (Archer *et al.*, 1990; Marty *et al.*, 1996). However, a role for GRP-AtPIN1 interaction during these processes is speculative.

4.6 Perspectives

The work presented in this thesis, describes the use of the *DR5-GFP* auxin response reporter for the *in vivo* detection of relative auxin levels during gravitropic root growth of Arabidopsis roots. The gravity induced cell-to-cell flow of auxin along the lower half of the root was reported. Pharmacological and genetic analyses allowed the correlation of auxin flow with root curvature, as well as the identification of influx- and efflux carrier dependent auxin transport pathways. To analyze the contribution of different AtPIN proteins to gravity induced auxin transport, the expression pattern of *DR5-GFP* in the *Atpin2/eir1-1* mutant was investigated. Analogous to this experiment, investigation of *DR5-GFP* expression during root gravitropism of *Atpin3* and *Atpin4* mutants will be of interest. AtPIN3 and AtPIN4 proteins are expressed in the Arabidopsis root tip, and the *Atpin3* mutant was shown to exhibit a delayed graviresponse. Crosses of *DR5-GFP* plants with *Atpin3* and *Atpin4* mutant plants have already been performed in the course of this thesis.

Furthermore, *DR5-GFP* plants and crosses of *DR5-GFP* plants with *Atpin* mutants represent a useful tool for pharmacological studies on the regulation of polar auxin transport. In this context, the relation between calcium and auxin flows during root gravitropism will be investigated by application of calcium chelators and release of caged calcium and the subsequent analysis of *DR5-GFP* expression. Similarly, the influence of phosphorylation and dephosphorylation events on polar auxin transport during root gravitropism will be analyzed by testing the effect of different phosphatase and kinase inhibitors on the cell-to-cell auxin flow in roots. Furthermore, treatment of *DR5-GFP* plants with drugs that interfere with AtPIN protein localization, such as inhibitors of vesicle trafficking and actin destabilizing agents, promises to shed light on the involvement of protein dynamics and mobility on auxin transport. Parallel immuno-localization experiments of AtPIN proteins would allow a correlation between changes in protein localization and alterations in auxin distribution. The utilization of *DR5-GFP* plants is manifold and not restricted to the analysis of relative auxin levels in roots. *In vivo* analyses of auxin changes during gravi- and phototropic curvature of hypocotyls, as well as the analyses of relative auxin levels in various organs of mutant plants with defects in auxin sensitivity or polar auxin transport, are already in progress.

A different approach for the investigation of AtPIN regulation involves the isolation of interaction partners of AtPIN proteins. In this report the screening of a plant cDNA library for

interaction partners of AtPIN1 using the split-ubiquitin-technique for detection of protein interaction was described. In a first approach, an aliquot of the cDNA library was screened with the AtPIN1 bait, and led to the isolation of two different putative interaction partners, a protein of unknown function and a glycine rich protein. The specificity of the interaction of AtPIN1 with both proteins in the USPS has further to be confirmed by testing (i) a possible interaction of the putative interactors with other bait proteins, (ii) the interaction of AtPIN1 with the putative interacting proteins, when these proteins are fused to the N_{uba} instead of the N_{ub} fragment, and (iii) the interaction of AtPIN1 with the putative interacting proteins, when N_{ub} and C_{ub} fragments of the fusion proteins are exchanged. If these additional tests validate a true interaction in USPS, other methods for the verification of this interaction, such as a co-immunoprecipitation assays, have to be employed. Finally, a screening for interaction partners of AtPIN1 and possibly also other AtPIN proteins with the entire cDNA library should result in the isolation of further putative interacting candidates.

5 Bibliography

- Archer, B.T., 3rd, Ozcelik, T., Jahn, R., Francke, U. and Sudhof, T.C. (1990) Structures and chromosomal localizations of two human genes encoding synaptobrevins 1 and 2. *J. Biol. Chem.*, **265**, 17267-17273.
- Assmann, S. and Haubrick, L. (1996) Transport proteins of the plant plasma membrane. *Curr. Opin. Cell Biol.*, **8**.
- Barlow, P. and Rathfelder, E. (1985) Distribution and redistribution of extension growth along vertical and horizontal gravireacting maize roots. *Planta*, **165**, 134-141.
- Behrens, H.M., Gradmann, D. and Sievers, A. (1985) Membrane potential responses following gravistimulation in roots of *Lepidium sativum*. *Planta*, **163**, 463-472.
- Bennett, M.J., Marchant, A., Green, H.G., May, S.T., Ward, S.P., Millner, P.A., Walker, A.R., Schulz, B. and Feldmann, K.A. (1996) Arabidopsis AUX1 gene: a permease-like regulator of root gravitropism. *Science*, **273**, 948-950.
- Bernasconi, P., Patel Bhavesh, C., Reagan Jeff, D. and Subramanian Mani, V. (1996) The N-1-naphthylphthalamic acid-binding protein is an integral membrane protein. *Plant Physiol.*, **111**, 427-432.
- Bjorkman, T. and Cleland, R.E. (1991) The role of extracellular free-calcium gradients in gravitropic signalling in maize roots. *Planta*, **185**, 379-384.
- Blancaflor, E.B., Fasano, J.M. and Gilroy, S. (1998) Mapping the functional roles of cap cells in the response of *Arabidopsis* primary roots to gravity. *Plant Physiol.*, **116**, 213-222.
- Borg, S., Podenphant, L., Jensen, T. and Poulsen, C. (1999) Plant cell growth and differentiation may involve Gap regulation of Rac activity. *FEBS Lett.*, **453**, 341-345.
- Bradford, M. (1976) A rapid and sensitive method for the quantification of microgram quantities of protein utilizing the principle of protein-dye-binding. *Anal. Biochem.*, **72**, 248-254.
- Briskin, D. (1990) Ca²⁺-translocating ATPase of the plasma membrane. *Plant Physiol.*, **94**, 397-400.
- Buer, C.S., Masle, J. and Wasteneys, G.O. (2000) Growth conditions modulate root-wave phenotypes in *Arabidopsis*. *Plant & Cell Physiol.*, **41**, 1164-1170.

- Cambridge, A. and Morris, D. (1996) Transfer of exogenous auxin from the phloem to the polar auxin transport pathway in pea. *Planta*, **199**, 583-588.
- Chen, J.G., Ullah, H., Young, J.C., Sussman, M.R. and Jones, A.M. (2001) ABP1 is required for organized cell elongation and division in Arabidopsis embryogenesis. *Genes. Dev.*, **15**, 902-911.
- Chen, R., Hilson, P., Sedbrook, J., Rosen, E., Caspar, T. and Masson Patrick, H. (1998a) The Arabidopsis thaliana AGRAVITROPIC 1 gene encodes a component of the polar-auxin-transport efflux carrier. *Proc. Natl. Acad. Sci. USA*, **95**, 15112-15117.
- Chen, R., Hilson, P., Sedbrook, J., Rosen, E., Caspar, T. and Masson, P.H. (1998b) The arabidopsis thaliana AGRAVITROPIC 1 gene encodes a component of the polar-auxin-transport efflux carrier. *Proc. Natl. Acad. Sci. USA*, **95**, 15112-15117.
- Chen, R., Rosen, E. and Masson, P. (1999) Gravitropism in higher plants. *Plant Physiol.*, **120**, 343-350.
- Christensen, S.K., Dagenais, N., Chory, J. and Weigel, D. (2000) Regulation of auxin response by the protein kinase PINOID. *Cell*, **100**, 469-478.
- Collings, D., White, R. and Overall, R.L. (1992) Ionic current changes associated with the gravity-induced bending response in roots of *Zea mays* L. *Plant Physiol.*, **100**, 1417-1426.
- Cosgrove, D. (1997) Cellular mechanisms underlying growth asymmetry during stem gravitropism. *Planta*, **203**, 130-135.
- Cosson, P., de Curtis, I., Pouyssegur, J., Griffiths, G. and Davoust, J. (1989) Low cytoplasmic pH inhibits endocytosis and transport from the trans-Golgi network to the cell surface. *J. Cell Biol.*, **108**, 377-387.
- Cox, D.N. and Muday, G.K. (1994) NPA binding activity is peripheral to the plasma membrane and is associated with the cytoskeleton. *Plant Cell*, **6**, 1941-1953.
- Darwin, C. and Darwin, F. (1881) *Darwins Gesammelte Werke*. Schweizerbart'sche Verlagsbuchhandlung, Stuttgart.
- Davies, P. (1995) Plant hormones: Physiology, biochemistry and molecular biology. *Kluwer Academic Publisher*, **2**.
- Deichsel, H., Friedel, S., Detterbeck, A., Coyne, C., Hamker, U. and MacWilliams, H.K. (1999) Green fluorescent proteins with short half-lives as reporters in *Dictyostelium discoideum*. *Dev. Genes Evol.*, **209**, 63-68.

- Delbarre, A., Muller, P. and Guern, J. (1998) Short-lived and phosphorylated proteins contribute to carrier-mediated efflux, but not to influx, of auxin in suspension-cultured tobacco cells. *Plant Physiol.*, **116**, 833-844.
- Delbarre, A., Muller, P., Imhoff, V. and Guern, J. (1996) Comparison of mechanisms controlling uptake and accumulation of 2,4-Dichlorophenoxy acetic acid, Naphthalene-1-acetic acid, and Indole-3-acetic acid in suspension-cultured tobacco cells. *Planta*, **198**, 532-541.
- Deruere, J., Jackson, K., Garbers, C., Soll, D. and DeLong, A. (1999) The RCN1-encoded A subunit of protein phosphatase 2A increases phosphatase activity in vivo. *Plant J.*, **20**, 389-399.
- Dünnwald, M., Varshavsky, A. and Johnsson, N. (1999) Detection of transient in vivo interactions between substrate and transporter during protein translocation into the endoplasmic reticulum. *Mol. Biol. Cell*, **10**, 329-344.
- Evans, M.L. and Ishikawa, H. (1997) Cellular specificity of the gravitropic motor response in roots. *Planta.*, **203**, S 115-S 122.
- Fasano, J.M., Swanson, S.J., Blancaflor, E.B., Dowd, P.E., Kao, T. and Gilroy, S. (2001) Changes in Root Cap pH Are Required for the Gravity Response of the Arabidopsis Root. *Plant Cell*, **13**, 907-922.
- Firn, R.D., Wagstaff, C. and Digby, J. (2000) The use of mutants to probe models of gravitropism. *J. Exp. Bot.*, **51**, 1323-1340.
- Fitzelle, K.J. and Kiss, J.Z. (2001) Restoration of gravitropic sensitivity in starch-deficient mutants of Arabidopsis by hypergravity. *J. Exp. Bot.*, **52**, 265-275.
- Friml, J., Benkova, E., Bililou, I., Wisniewska, J., Hamann, T., Ljung, K., Woody, S., Sandberg, G., Scheres, B., Jürgens, G. and Palme, K. (2002a) AtPIN4 mediates sink-driven auxin gradients and root patterning in Arabidopsis. *Cell*, **108**, 661-673.
- Friml, J., Wisniewska, J., Benkova, E., Mendgen, K. and Palme, K. (2002b) Lateral relocation of auxin efflux regulator PIN3 mediates tropism in Arabidopsis. *Nature*, **415**, 806-809.
- Fukaki, H., Wysocka-Diller, J., Kato, T., Fujisawa, H., Benfey Philip, N. and Tasaka, M. (1998) Genetic evidence that the endodermis is essential for shoot gravitropism in Arabidopsis thaliana. *Plant J.*, **14**, 425-430.

- Gälweiler, L., Guan, C.H., Müller, A., Wisman, E., Mendgen, K., Yephremov, A. and Palme, K. (1998) Regulation of polar auxin transport by AtPIN1 in Arabidopsis vascular tissue. *Science*, **282**, 2226-2230.
- Geldner, N., Friml, J., Stierhof, Y.-D., Jürgens, G. and Palme, K. (2001) Auxin transport inhibitors block PIN1 cycling and vesicle trafficking. *Nature*, **413**, 425-428.
- Gil, P., Dewey, E., Friml, J., Zhao, Y., Snowden, K.C., Putterill, J., Palme, K., Estelle, M. and Chory, J. (2001) BIG: a calossin-like protein required for polar auxin transport in Arabidopsis. *Genes Dev.*, **15**, 1985-1997.
- Gilroy, S. and Trewavas, A. (2001) Signaling processing and transduction in plant cells: the end of the beginning? *Nat. Rev. Mol. Cell Biol.*, **2**, 307-314.
- Gluck, S., Cannon, C. and Al-Awqati, Q. (1982) Exocytosis regulates urinary acidification in turtle bladder by rapid insertion of H⁺ pumps into the luminal membrane. *Proc. Natl. Acad. Sci. USA*, **79**, 4327-4331.
- Goldsmith, M. (1977) The polar transport of auxin. *Ann. Rev. Plant Physiol.*, **28**, 439-478.
- Hadfi, K., Speth, V. and Neuhaus, G. (1998) Auxin-induced developmental patterns in *Brassica juncea* embryos. *Develop.*, **125**, 879-887.
- Haseloff, J. and Amos, B. (1995) GFP in plants. *Trends Genet.*, **11**, 328-329.
- Haseloff, J., Siemering, K.R., Prasher, D.C. and Hodge, S. (1997) Removal of a cryptic intron and subcellular localization of green fluorescent protein are required to mark transgenic Arabidopsis plants brightly. *Proc. Natl. Acad. Sci. USA*, **94**, 2122-2127.
- Imhoff, V., Muller, P., Guern, J. and Delbarre, A. (2000) Inhibitors of the carrier-mediated influx of auxin in suspension-cultured tobacco cells. *Planta*, **210**, 580-588.
- Ishikawa, H. and Evans, M.L. (1992) Induction of curvature in maize roots by calcium or by thigmostimulation: role of the postmitotic isodiametric growth zone. *Plant Physiol.*, **100**, 762-768.
- Ishikawa, H. and Evans, M.L. (1993) The role of the distal elongation zone in the response of maize roots to auxin and gravity. *Plant Physiol.*, **102**, 1203-1210.
- Johnsson, A. (1997) Circumnutations: results from recent experiments on Earth and in space. *Planta*, **203**, S147-158.
- Johnsson, N. and Varshavsky, A. (1994a) Split ubiquitin as a sensor of protein interactions in vivo. *Proc. Natl. Acad. Sci. USA*, **91**, 10340-10344.
- Johnsson, N. and Varshavsky, A. (1994b) Ubiquitin-assisted dissection of protein transport across membranes. *EMBO*, **13**, 2686-2698.

- Jones, A.M. (1998) Auxin transport: down and out and up again. *Science*, **282**, 2201-2203.
- Juniper, B., Gorves, S., Landau-Schacher, B. and Audus, L. (1966) Root caps and the perception of gravity. *Nature*, **209**, 93-94.
- Kiss, J.Z. (2000) Mechanisms of the early phases of plant gravitropism. *CRC Crit. Rev. Plant Sci.*, **19**, 551-573.
- Kiss, J.Z., Wright, J.B. and Caspar, T. (1996) Gravitropism in roots of intermediate-starch mutants of *Arabidopsis*. *Physiol. Plant*, **97**, 237-244.
- Kodera, Y. and Sato, S. (2001) Recovery of gravitropic response during regeneration of root caps does not require developed columella cells and sedimentation of amyloplasts. *Cytobios.*, **104**, 53-65.
- Koncz, C. and Schell, J. (1986) The promoter of TL-DNA gene 5 controls the tissue-specific expression of chimeric genes carried by a novel type of *Agrobacterium* binary vector. *Mol. and Gen.*, **204**, 383-396.
- Konings, H. (1968) The significance of the root cap for geotropism. *Acta Bot. Neerl.*, **17**, 203-211.
- Kuznetsov, O.A. and Hasenstein, K.H. (1997) Magnetophoretic induction of curvature in coleoptiles and hypocotyls. *J. Exp. Bot.*, **48**, 1951-1957.
- Laser, H., Bongards, C., Schuller, J., Heck, S., Johnsson, N. and Lehming, N. (2000) A new screen for protein interactions reveals that the *Saccharomyces cerevisiae* high mobility group proteins Nhp6A/B are involved in the regulation of the GAL1 promoter. *Proc. Natl. Acad. Sci. USA*, **97**, 13732-13737.
- Lee, J.S. and Evans, M.L. (1985) Polar transport of 45Ca^{2+} across the elongation zone of gravistimulated roots. *Plant Cell Physiol.*, **26**, 1587-1595.
- Legue, V., Blancaflor, E., Wymer, C., Perbal, G., Fantin, D. and Gilroy, S. (1997) Cytoplasmic free Ca^{2+} in *Arabidopsis* roots changes in response to touch but not gravity. *Plant Physiol.*, **114**, 789-800.
- Li, Y., Hagen, G. and Guilfoyle, T.J. (1991) An auxin-responsive promoter is differentially induced by auxin gradients during tropisms. *Plant Cell*, **3**, 1167-1176.
- Lomax, T., Muday, G. and Rubery, P. (1995) Auxin transport. In: *Plant hormones, Physiology, Biochemistry and Molecular Biology*. (Davies, P.J., ed.). 509-530.
- Luschnig, C., Gaxiola Roberto, A., Grisafi, P. and Fink Gerald, R. (1998) EIR1, a root-specific protein involved in auxin transport, is required for gravitropism in *Arabidopsis thaliana*. *Genes. Dev.*, **12**, 2175-2187.

- MacCleery, S.A. and Kiss, J.Z. (1999) Plastid sedimentation kinetics in roots of wild-type and starch-deficient mutants of Arabidopsis. *Plant Physiol.*, **120**, 183-192.
- Marchant, A., Kargul, J., May Sean, T., Muller, P., Delbarre, A., Perrot-Rechenmann, C. and Bennett Malcolm, J. (1999) AUX1 regulates root gravitropism in Arabidopsis by facilitating auxin uptake within root apical tissues. *EMBO*, **18**, 2066-2073.
- Marty, I., Monfort, A., Stiefel, V., Ludevid, D., Delseny, M. and Puigdomenech, P. (1996) Molecular characterization of the gene coding for GPRP, a class of proteins rich in glycine and proline interacting with membranes in Arabidopsis thaliana. *Plant. Mol. Biol.*, **30**, 625-636.
- Mattsson, J., Sung, Z.R. and Berleth, T. (1999) Responses of plant vascular systems to auxin transport inhibition. *Dev.*, **126**, 2979-2991.
- Monshausen, G.B., Zieschang, H.E. and Sievers, A. (1996) Differential proton secretion in the apical elongation zone caused by gravistimulation is induced by a signal from the root cap. *Plant Cell Environ.*, **19**, 1408-1414.
- Morris, D.A. and Robinson, J.S. (1998) Targeting of auxin carriers to the plasma membrane - differential effects of Brefeldin A on the traffic of auxin uptake and efflux carriers. *Planta*, **205**, 606-612.
- Morris, D.A., Rubery, P.H., Jarman, J. and Sabater, M. (1991) Effects of inhibitors of protein synthesis on transmembrane auxin transport in Cucurbita pepo L. hypocotyl segments. *J. Exp. Bot.*, **42**, 773-784.
- Muday, G. (2001) Auxins and tropisms. *J Plant Growth Regul.*, **20**, 226-243.
- Mullen, J.L., Ishikawa, H. and Evans, M.L. (1998) Analysis of changes in relative elemental growth rate patterns in the elongation zone of Arabidopsis roots upon gravistimulation. *Planta*, **206**, 598-603.
- Mullen, J.L., Wolverton, C., Ishikawa, H. and Evans, M.L. (2000) Kinetics of constant gravitropic stimulus responses in arabidopsis roots using a feedback system [In Process Citation]. *Plant Physiol.*, **123**, 665-670.
- Müller, A., Guan, C., Galweiler, L., Tanzler, P., Huijser, P., Marchant, A., Parry, G., Bennett, M., Wisman, E. and Palme, K. (1998) AtPIN2 defines a locus of Arabidopsis for root gravitropism control. *EMBO*, **17**, 6903-6911.
- Okada, K., Ueda, J., Komaki, M.K., Bell, C.J. and Shimura, Y. (1991) Requirement of the auxin polar transport system in early stages of Arabidopsis floral bud formation. *Plant Cell*, **3**, 677-684.

- Palme, K. and Galweiler, L. (1999) PIN-pointing the molecular basis of auxin transport. *Curr. Opin. Plant Biol.*, **2**, 375-381.
- Park, A.R., Cho, S.K., Yun, U.J., Jin, M.Y., Lee, S.H., Sachetto-Martins, G. and Park, O.K. (2001) Interaction of the Arabidopsis receptor protein kinase Wak1 with a glycine-rich protein, AtGRP-3. *J. Biol. Chem.*, **276**, 26688-26693.
- Parry, G., Delbarre, A., Marchant, A., Swarup, R., Napier, R., Perrot-Rechenmann, C. and Bennett, M.J. (2001) Novel auxin transport inhibitors phenocopy the auxin influx carrier mutation aux1. *Plant J.*, **25**, 399-406.
- Pilet, P. and Ney, D. (1981) Differential growth of georeacting maize roots. *Planta*, **151**, 146-150.
- Prasher, D., Eckenrode, V., Ward, W., Prendergast, F and Cormier, M. (1992) Primary structure of the Aequorea victoria green-fluorescent protein. *Gene*. **111**, 229-223.
- Rashotte, A.M., Brady, S.R., Reed, R.C., Ante, S.J. and Muday, G.K. (2000) Basipetal auxin transport is required for gravitropism in roots of Arabidopsis. *Plant Physiol.*, **122**, 481-490.
- Rashotte, A.M., DeLong, A. and Muday, G.K. (2001) Genetic and chemical reductions in protein phosphatase activity alter auxin transport, gravity response, and lateral root growth. *Plant Cell*, **13**, 1683-1697.
- Raven, J. (1975) Transport of indoleacetic acid in plant cells in relation to pH and electric potential gradients, and its significance for polar IAA transport. *New Phytol.*, **74**, 163-172.
- Reed, R.C., Brady, S.R. and Muday, G.K. (1998) Inhibition of auxin movement from the shoot into the root inhibits lateral root development in Arabidopsis. *Plant Physiol.*, **118**, 1369-1378.
- Roman, G., Lubarsky, B., Kieber Joseph, J., Rothenberg, M. and Ecker Joseph, R. (1995) Genetic Analysis of Ethylene Signal Transduction in Arabidopsis thaliana: Five Novel Mutant Loci Integrated into a Stress Response Pathway. *Genetics*, **139**, 1393-1409.
- Rubery, P.H. and Shelldrake, A.R. (1974) Carrier mediated auxin transport. *Planta*, **118**, 101-121.
- Sabatini, S., Beis, D., Wolkenfelt, H., Murfett, J., Guilfoyle, T., Malamy, J., Benfey, P., Leyser, O., Bechtold, N., Weisbeek, P. and Scheres, B. (1999) An auxin-

- dependent distal organizer of pattern and polarity in the Arabidopsis root. *Cell*, **99**, 463-472.
- Sachetto-Martins, G., Franco, O. and Oliveira, D. (2000) Plant glycine-rich proteins: a family or just proteins with a common motif. *Biochim. Biophys. Acta*, **1492**, 1-14.
- Sack, F.D. (1991) Plant gravity sensing. *Int. Rev. Cytol.*, **127**, 193-252.
- Sack, F.D. (1997) Plastids and gravitropic sensing. *Planta*, **203**, S 63-S 68.
- Sambrook, J. and Fritsch, E. (1998) Molecular cloning, a laboratory manual. Second edition. New York, *Cold Spring Harbor Laboratory Press*.
- Scott, A.C. and Allen, N.S. (1999) Changes in cytosolic pH within Arabidopsis root columella cells play a key role in the early signaling pathway for root gravitropism. *Plant Physiol.*, **121**, 1291-1298.
- Sieberer, T., Seifert, G.J., Hauser, M.-T., Grisafi, P., Fink, G.R. and Luschnig, C. (2000) Post-transcriptional control of the *Arabidopsis* auxin efflux carrier EIR1 requires AXR1. *Curr. Biol.*, **10**, 1595-1598.
- Sikorski, R.S. and Hieter, P. (1989) A system of shuttle vectors and yeast host strains designed for efficient manipulation of DNA in *Saccharomyces cerevisiae*. *Genetics*, **122**, 19-27.
- Simmons, C., Soll, D. and Migliaccio, F. (1995) Circumnutation and gravitropism cause root waving in *Arabidopsis*. *J. Exp. Bot.*, **46**, 143-150.
- Sinclair, W. and Trewavas, A.J. (1997) Calcium in gravitropism - A re-examination. *Planta*, **203**, S 85-S 90.
- Stagljar, I., Korostensky, C., Johnsson, N. and Te Heesen, S. (1998) A genetic system based on split-ubiquitin for the analysis of interactions between membrane proteins in vivo. *Proc. Natl. Acad. Sci. USA*, **95**, 5187-5192.
- Staves, M.P. (1997) Cytoplasmic streaming and gravity sensing in *Chara* internodal cells. *Planta*, **203**, S79-84.
- Steinmann, T., Geldner, N., Grebe, M., Mangold, S., Jackson, C.L., Paris, S., Galweiler, L., Palme, K. and Jurgens, G. (1999) Coordinated polar localization of auxin efflux carrier PIN1 by GNOM ARF GEF. *Science*, **286**, 316-318.
- Swarup, R., Friml, J., Marchant, A., Ljung, K., Sandberg, G., Palme, K. and Bennett, M. (2001) Localization of the auxin permease AUX1 suggests two functionally distinct hormone transport pathways operate in the Arabidopsis root apex. *Genes Dev.*, **15**, 2648-2653.

- Tsugeki, R. and Fedoroff, N.V. (1999) Genetic ablation of root cap cells in *Arabidopsis*. *Proc. Natl. Acad. Sci. U S A*, **96**, 12941-12946.
- Ulmasov, T., Hagen, G. and Guilfoyle Tom, J. (1997a) ARF1, a transcription factor that binds to auxin response elements. *Science*, **276**, 1865-1868.
- Ulmasov, T., Murfett, J., Hagen, G. and Guilfoyle Tom, J. (1997b) Aux/IAA proteins repress expression of reporter genes containing natural and highly active synthetic auxin response elements. *Plant Cell*, **9**, 1963-1971.
- Utsuno, K., Shikanai, T., Yamada, Y. and Hashimoto, T. (1998) Agr, an agravitropic locus of *Arabidopsis thaliana*, encodes a novel membrane-protein family member. *Plant & Cell Physiol.*, **39**, 1111-1118.
- Valster, A.H., Hepler, P.K. and Chernoff, J. (2000) Plant GTPases: the Rhos in bloom. *Trends Cell Biol.*, **10**, 141-146.
- Varshavsky, A. (1997) The N-end rule pathway of protein degradation. *Genes.*, **2**, 13-28.
- Went, F. (1928) Wuchsstoff und Wachstum. *Rec. Trav. Bot. Neerl.*, **25**, 1-116.
- Went, F. and Thiemann. (1937) Phytohormones. *MacMillan, New York*.
- Wittke, S., Lewke, N., Müller, S. and Johnsson, N. (1999) Probing the molecular environment of membrane proteins in vivo. *Mol. Biol. Cell.* **10**, 2519-2530.
- Wittke, S., Dünwald, M., Johnsson, N. (2000) Sec62p a component of the ER translocation machinery, contains multiple binding sites for sec-complex. *Mol. Biol. Cell.* **11**, 3859-3871.
- Wu, G., Li, H. and Yang, Z. (2000) *Arabidopsis* RopGAPs are a novel family of Rho GTPase-activating proteins that require the CDC42/Rac-interactive binding motif for Rop-specific GTPase stimulation. *Plant Physiol.*, **124**, 1625-1636.
- Yoder, T., Zheng, H., Todd, P. and Staehelin, L. (2001) Amyloplast sedimentation dynamics in maize columella cells support a new model for the gravity-sensing apparatus of roots. *Plant Physiol.*, **125**, 1045-1060.
- Young, L.M., Evans, M.L. and Hertel, R. (1990) Correlations between gravitropic curvature and auxin movement across gravistimulated roots of *Zea mays*. *Plant Physiol.*, **92**, 792-796.
- Young, L.M., Evans, M.L., Ishikawa, H., Wolverton, C., Simmons, C. and Söll, D. (1996) The gravitropic response of primary roots of the *rgr1* mutant of *Arabidopsis thaliana*. In Suge, H. and Takahashi, H. (eds.), *Plants in space biology*. Tohoku University Press, Tohoku, pp. 73-81.

Younis, A. (1954) Experiments on the growth and geotropism of roots. *Journal of Exp. Bot.*,
5, 357-372.

Zerial, M. and Huber, L. (1995) Guidebook to the small GTPases. *Oxford University Press*.

6 Danksagung

Diese Arbeit wurde am Max-Delbrück-Laboratorium in der Max Planck Gesellschaft und am Max Planck Institut für Züchtungsforschung in Köln-Vogelsang durchgeführt.

Mein besonderer Dank gilt Herrn Prof. Klaus Palme für die Möglichkeit in seiner Arbeitsgruppe arbeiten zu dürfen, für die Vergabe des Themas, die anregenden Diskussionen und die Freiheiten, die er mir während der Durchführung der Arbeit gestattete.

Herrn Priv. Doz. Dr. Klaus Theres danke ich für die Betreuung der Arbeit und Herrn Prof. Martin Hülskamp danke ich für die Übernahme des Co-Referats.

Ganz besonders möchte ich mich bei Herrn Dr. Leo Gälweiler, Frau Filipa Santos und Frau Dr. Patricia Wolff für die große wissenschaftliche und ideelle Unterstützung bei der Durchführung dieser Arbeit, die gute Zusammenarbeit, aber auch die vielen netten Gespräche bedanken.

Bei allen ehemaligen und gegenwärtigen Mitgliedern der Arbeitsgruppe Palme möchte ich mich herzlich für die freundliche Arbeitsatmosphäre und die große Hilfsbereitschaft bedanken: Geraldine Bassac, Friedrich Bischoff, Claudia Gilles, Changhui Guan, Jan Hejatko, Juliette Leymarie, Elisabeth Luley, Violante Medeiros, Andreas Müller, Klaus Nettesheim, Ivan Paponov, Fernando Pessoa, Chadalavada Rajendrakumar, Kaliani Rajendrakumar, David Rouquié, Birgit Reintanz, Mario Schelhaas, Petra Spoomaker, Alexander Szyroki, Thomas Teichmann, Martina Trebar und Lars Vahlkamp. Frau Dr. Tinka Eneva danke ich für die gute „Starthilfe“. Bei Frau Dr. Tinka Eneva, Frau Dr. Deborah Grosskopf, Frau Michaela Lehnen, Herrn Dr. Arthur Molendijk und Frau Petra Tänzler möchte ich mich für die fachliche Unterstützung bedanken. Herrn Dr. Leo Gälweiler, Herrn Dr. Matthias Godde, Herrn Dr. Arthur Molendijk, Frau Maria Piques, Frau Filipa Santos und Frau Dr. Patricia Wolff danke ich für die Korrekturvorschläge beim Schreiben dieser Arbeit.

Herrn Prof. Mike Evans und Herrn Dr. Chris Wolverson (Ohio, USA) möchte ich für die Durchführung der Wurzelkrümmungskinetik danken.

Herrn Prof. Goran Sandberg und Frau Dr. Karin Ljung (Umea, Schweden) danke ich für die Durchführung der GC-MS Bestimmung der IAA Konzentrationen.

Herrn Dr. Guido Jach danke ich für die Unterstützung bei der Wahl des geeigneten GFP Konstruktes und für das Überlassen der *GFP-LT* DNA Sequenz.

Herrn Dr. Nils Johnsson, Herrn Dr. Martin Dünnwald und Herrn Dr. Jörg Eckert danke für die fachliche Unterstützung bei der Etablierung des Split-Ubiquitin-Systems.

Herrn Dr. Claudio Moser, Herrn Dr. Benedetto Ruperti, Herrn Dr. Tim Soellick und Herrn Dr. Ralph Stracke danke ich für die Ratschläge bei der Erstellung der cDNA Bank.

Mein besonderer Dank gilt Herrn Dr. Leo Gälweiler, Herrn Dr. Stefan Jakobs, Frau Dr. Cristina Roig, Herrn Dr. Christian Feckler, Herrn Dr. Gabino Rios, Frau Petra Tänzler, Herrn Olaf Tietz, Frau Dr. Patricia Wolff und den Damen des „Chicken Club“, Frau Rossana Henriques, Frau Maria Piques und Frau Filipa Santos, mit denen ich auch außerhalb des Institutes viele nette Stunden verbracht habe. Des weiteren danke ich allen Mitgliedern der Fleischerei Krings, sowie Karlchen, für die moralische Unterstützung während des Schreibens dieser Arbeit.

Nicht zuletzt gilt mein herzliches Dankeschön meinen Eltern, die mir diese lange Ausbildung ermöglicht haben und meinem Freund Theo, der mich in dieser Zeit immer unterstützt hat.

7 Erklärung

Ich versichere, dass ich die von mir vorgelegte Dissertation selbständig angefertigt, die benutzten Quellen und Hilfsmittel vollständig angegeben und die Stellen der Arbeit - einschließlich Tabellen, Karten und Abbildungen -, die anderen Werken im Wortlaut oder dem Sinn nach entnommen sind, in jedem Einzelfall als Entlehnung kenntlich gemacht habe; dass diese Dissertation noch keiner anderen Fakultät oder Universität zur Prüfung vorgelegen hat; dass sie- abgesehen von unten angegebenen Teilpublikationen -noch nicht veröffentlicht worden ist sowie, dass ich eine solche Veröffentlichung vor Abschluß des Promotionsverfahrens nicht vornehmen werde. Die Bestimmung der Promotionsordnung sind mir bekannt. Die von mir vorgelegte Dissertation ist in der Arbeitsgruppe von Prof. Klaus Palme durchgeführt, und von Priv. Doz. Dr. Klaus Theres betreut worden.

Köln, am 16. April 2002

(Iris Ottenschläger)

8 Abstract

Gravitropism plays a major role in orienting plant organs. Root growth corresponding to the gravity vector is the result of gravity perception, signal formation and transmission from sensory cells to the growth response zone. Differential cell elongation at the site of root growth has been proposed to be controlled by the plant hormone auxin. The auxin transporting cells, however, were not identified. Here, the generation of *DR5-GFP-LT-ER*, an *in vivo* auxin response reporter is described. Relative auxin levels, as depicted by *GFP-LT-ER* fluorescence, were monitored at cellular resolution in the Arabidopsis root apex. The symmetric auxin signal in quiescent center, columella initial and columella cells, was shown to asymmetrically redistribute to the lateral root cap following change of gravity vector orientation. The lateral transport of auxin from columella to lateral root cap cells depends on auxin efflux carrier activity, while the basipetal transport of auxin from lateral root cap to the elongation zone requires both, efflux and influx carrier activity. The efflux activity depends in part on the regulation of AtPIN proteins, putative auxin efflux carriers. The split-ubiquitin-system was used for the screening of interaction partners of AtPIN1. After validation of the split-ubiquitin-system, a cDNA library of plant tissues was cloned into a split-ubiquitin prey vector. AtPIN1 was used to screen an aliquot of the cDNA library for putative interaction partners. An Arabidopsis protein of unknown function and an Arabidopsis glycine rich protein were isolated from this screen. Specific interaction of these proteins with AtPIN1 has yet to be confirmed.

9 Zusammenfassung

Pflanzen können durch Wachstumskrümmung ihre Organe in eine bestimmte Richtung zur Erdbeschleunigung ausrichten (Gravitropismus). Die Signalkette, die von der Aufnahme des Schwerkraftreizes in Columellazellen der Wurzelspitze bis zur Umsetzung der Wachstumsbewegung in der Elongationszone stattfindet, ist erst in Ansätzen bekannt. Es wird vermutet, dass die endogene und gerichtete Verteilung des Pflanzenhormons Auxin das differenzielle Wachstum in der Elongationszone steuert. Die Auxin-transportierenden Zellen sind jedoch nicht bekannt. In dieser Arbeit wurden relative Mengen an endogenem Auxin in Wurzeln mit Hilfe des *DR5-GFP* Reporterkonstruktes *in vivo* und mit zellulärer Auflösung nachgewiesen. Bei Änderung des Schwerkraftreizes wurde gezeigt, dass ein zuerst symmetrisch verteiltes Auxinsignal in Zellen des ruhenden Zentrums und Columellazellen, nun asymmetrisch zu Zellen der Wurzelhaube entlang der Wurzelunterseite wandert. Es wurde gezeigt, dass der laterale Auxinfluss von Columellazellen zu Zellen der distalen Wurzelhaube Effluxcarrier-vermittelt ist, während der basipetale Auxinfluss von Zellen der distalen Wurzelhaube zu Zellen der proximalen Wurzelhaube und weiter zur Elongationszone Efflux- und Influxcarrier benötigt. Die Regulation des Efflux-gesteuerten Auxintransportes ist zum Teil von der Aktivität der AtPIN Proteine abhängig. Das Split-Ubiquitin-System wurde daher eingesetzt um Interaktionspartner von AtPIN1 in einer cDNA Expressionsbibliothek zu finden. Nachdem die Interaktion zwischen Pflanzenproteinen mit Hilfe des Split-Ubiquitin-Systems bestätigt wurde, wurde eine cDNA Bank aus pflanzlichem Gewebe in einen Split-Ubiquitin-Vektor kloniert. Ein Teil dieser cDNA Bank wurde verwendet um mit einer AtPIN1 Sonde mögliche Interaktionspartner zu identifizieren. Dabei konnten ein Arabidopsis Protein mit unbekannter Funktion und ein Glycin-reiches Protein isoliert werden. Die spezifische Interaktion dieser Proteine mit AtPIN1 wird überprüft werden müssen.

10 Ausführliche Zusammenfassung

Pflanzen können durch Wachstumskrümmung ihre Organe in eine bestimmte Richtung zur Erdbeschleunigung ausrichten (Gravitropismus). Wenn die Lage von Wurzeln in Richtung des Schwerkraftvektors verändert wird, erfolgt eine Krümmung der Wurzel. Die zugrunde liegende Signalkette ist erst in Ansätzen bekannt. Sie beginnt mit der Aufnahme des Schwerkraftreizes in den statholitenhaltigen Zellen der Wurzelhaube (Calyptra) und endet in einer Wachstumsbewegung, die in der Elongationszone der Wurzel stattfindet. Seit langem wird das Pflanzenhormon Auxin als Botenstoff für das differentielle Wachstum im Bereich der Wurzelkrümmung vermutet. Die genaue Richtung des Auxinflusses und die Identität der Zellen, durch welche dieser Fluß stattfindet, sind jedoch nicht bekannt.

In dieser Arbeit wurden transgene Arabidopsis Pflanzenlinien hergestellt, die ein Reporterkonstrukt enthalten, das aus dem durch Auxin indizierbaren Promotor *DR5* und dem Gen des grün fluoreszierenden Proteins, GFP, besteht (*DR5-GFP*). Aufgrund seiner Fluoreszenz ist eine Detektion von GFP in lebenden Zellen möglich. GFP wurde mit einer Signalsequenz versehen, welche für die Akkumulation von GFP-Molekülen im Endoplasmatischen Retikulum der Zelle sorgt und so die Intensität des Fluoreszenzsignals verstärkt. Es wurde gezeigt, dass *DR5-GFP* durch Zugabe von aktiven Auxinen ab einer Konzentration von 0,1 μM in fast allen Geweben des Arabidopsiskeimlings induzierbar ist und dass diese Induktion 90 Minuten nach Auxinzugabe erstmals mikroskopisch nachgewiesen werden kann. Des weiteren zeigten Auxin-unbehandelte Keimlinge und adulte Pflanzen GFP Signale an Stellen, für welche endogen erhöhte Auxinkonzentrationen entweder schon gemessen wurden oder aufgrund von Wachstumsversuchen postuliert wurden.

DR5-GFP Pflanzen wurden verwendet, um relative Konzentrationen von endogenem Auxin während des gravitropen Wurzelwachstums von Arabidopsis Keimlingen *in vivo* und mit zellulärer Auflösung zu bestimmen. In vertikal gewachsenen Wurzeln wurden GFP-Signale in Zellen des ruhenden Zentrums, in Columella-Initialen und in adulten Columellazellen der Wurzelspitze nachgewiesen. Nach veränderter Gravistimulierung der Wurzeln durch Rotation der Keimlinge in einem Winkel von 135° zum Schwerkraftvektor, konnte eine Änderung der GFP-Verteilung festgestellt werden. GFP-Signale begannen zuerst in an der Wurzelunterseite aufzutauchen und zwar in an Columellazellen angrenzenden Zellen der Wurzelhaube. Schließlich waren Signale in der gesamten Wurzelhaube an der Wurzelunterseite zu sehen.

Das chronologische Erscheinen von GFP-Signalen war ein Hinweis auf das Schwerkraft-induzierte Entstehen eines Auxinflusses an der Wurzelunterseite.

Um die Beteiligung von Influx- und Efflux-gesteuertem Auxintransport an dem Schwerkraft-induzierten Auxintransport zu untersuchen, wurden pharmakologische und genetische Studien durchgeführt. Dabei wurden *DR5-GFP* Pflanzen mit Inhibitoren, welche spezifisch den Influx- oder Efflux-gesteuerten Auxintransport inhibieren, behandelt. Des Weiteren wurden synthetische Auxine, die ausschließlich von Auxin Influx- oder Auxinefflux Carriern transportiert werden, zu *DR5-GFP* Pflanzen zugegeben. Die Wirkung dieser Substanzen auf die Kinetik der Wurzelkrümmung sowie auf die Verteilung des GFP Signals vor und während der Wurzelkrümmung wurde untersucht. In einem weiteren Versuch wurde die agravitrope Auxintransportmutante *Atpin2/eir1-1* mit dem *DR5-GFP* Konstrukt transformiert. Die GFP-Verteilung in Keimlingen der *Atpin2/eir1-1* Mutante wurde analysiert. Diese Versuche zeigten, dass die Wurzelkrümmung immer mit einem Auxintransport von Columellazellen zu Zellen der Wurzelhaube und Elongationszone an der Wurzelunterseite einhergeht. Der laterale Auxintransport von Columellazellen zu Zellen der distalen Wurzelhaube ist dabei ausschließlich Effluxcarrier vermittelt. Der basipetale Auxintransport von Zellen der distalen Wurzelhaube zu Zellen der proximalen Wurzelhaube und weiter zu Zellen der Elongationszone ist dagegen sowohl Efflux- als auch Influxcarrier vermittelt.

Die Kontrolle des Efflux-gesteuerten Auxintransportes ist noch weitgehend unbekannt. Es ist aber wahrscheinlich, dass eine Regulation von AtPIN Proteinen, putativen Effluxcarriern, einen Einfluss auf den Efflux von Auxin hat. Die Identifizierung von Proteinen, die mit AtPIN Proteinen interagieren, ist daher von besonderem Interesse. Das Split-Ubiquitin-System wurde eingesetzt, um Interaktionspartner des AtPIN1 Proteins in einer Expressions-cDNA Bibliothek zu finden. Ein Teil dieser Bibliothek wurde verwendet um mit einer AtPIN1 Sonde mögliche Proteininteraktionspartner zu identifizieren. Dabei wurden zwei Proteine, die möglicherweise mit AtPIN1 interagieren, isoliert. Es handelt sich dabei um ein Protein von unbekannter Funktion und ein Protein der Familie von Glycin-reichen-Proteinen. Die spezifische Interaktion dieser Proteine mit AtPIN1 wird überprüft werden müssen.

11 Lebenslauf

Persönliche Daten

Name: Iris Ottenschläger
Geburtsdatum: 22. Mai 1972
Geburtsort: Linz an der Donau, Österreich
Staatsangehörigkeit: Österreich

Ausbildung

09/1978-09/1982 Grundschule Traun, Österreich

09/1982-02/1988 Bundesrealgymnasium Traun, Österreich

02/1988-05/1990 American Embassy School, Neu Delhi, Indien

05/1990 Abitur in Form des Internationalen Baccalaureates, Neu Delhi, Indien

10/1990-01/1998 Studium der Biologie an der Universität Wien

10/1993 Diplom Vorprüfung

02/1996-01/1998 Diplomarbeit an der Universität Wien in der Abt. Pflanzengenetik bei Prof. E. Heberle-Bors, Thema: "Green fluorescent protein as a marker during pollen development."
Veröffentlichung: Ottenschläger *et al.*, 1999, Green fluorescent protein (GFP) as a marker during pollen development. *Transgenic Res.* 8 (4), 279-294.

01/1998 Diplom Biologie

04/1998-06/2002 Promotionsstudium an der Universität zu Köln. Anfertigung der Dissertation am Max Delbrück Laboratorium in der Max Planck Gesellschaft und am Max Planck Institut für Züchtungsforschung in Köln in der Arbeitsgruppe von Prof. K. Palme und der Betreuung von Priv. Doz. Dr. K. Theres, Thema: "Gravity regulated differential auxin transport in Arabidopsis roots and the search for interaction partners of AtPIN1."
Veröffentlichung: Ottenschläger *et al.*, 2002, Gravity regulated differential auxin transport from Arabidopsis columella to lateral root cap cells, 2002, *Letters to Nature*, subm.